Fertile Free Fuels for Plutonium and Minor Actinides Burning in LWRs

By

Yi Zhang

Bachelor of Engineering, Engineering Physics Department,
Tsinghua University, P.R.China (2001)

Submitted to the Department of Nuclear Engineering
in partial fulfillment of the requirements for the degree of

MASTER OF SCIENCE

at the
MASSACHUSETTS INSTITUTE OF TECHNOLOGY

August 2003

Signature of Author _____
Department of Nuclear Engineering
August 20, 2003

Certified by _____
Mujid S. Kazimi (thesis supervisor)
TEPCO Professor of Nuclear Engineering

Certified by _____
Pavel Hejzlar (thesis reader)
Principal Research Scientist

Accepted by _____
Jeffrey A. Coderre
Chairman, Department Committee on Graduate Students

Fertile Free Fuels for Plutonium and Minor Actinides Burning in LWRs

By

Yi Zhang

Submitted to the Department of Nuclear Engineering
in partial fulfillment of the requirements
for the degree of
Master of Science

Abstract

The feasibility of using various uranium-free fuels for plutonium incineration in present light water reactors is investigated. Two major categories of inert matrix fuels are studied: composite ceramic fuel particles dispersed in another ceramic matrix (CERCER) and ceramic fuel particles dispersed into a metallic matrix (CERMET). In the category of CERCER, the current world wide research effort has been focused on three matrix candidates: (1) Spinel ($MgAl_2O_4$); (2) CeO_2, and (3) MgO. In contrast, there are still no emerging commonly accepted matrix candidates for a CERMET.

The fuel may consist of plutonium, minor actinides (MA), or both which are termed trans-uranium (TRU) fuel. The transmutation rate and the transmuted fraction of initial loadings are calculated using CASMO-4. Different inert matrix fuels have similar burning abilities in terms of how much and how fast the Pu, MA or TRU can be burned, and they are all superior to the mixed UO_2-PuO_2 (MOX) fuel. From this point of view, there is no good reason to favor one inert matrix over another. The burning rates in terms of kg/(GWe-Year) of different inert matrix fuels are quite stable with regard to changing the moderation level (or H/HM ratio) in the core. Changing initial loadings and changing power densities can not result in large change in the burned percentage of initial loadings and burning rate.

Lack of U-238 and the neutronic characteristics of plutonium lead to degradation of safety related kinetic parameters. It is found that various inert matrix fuels have similar values for the Doppler coefficient, moderator temperature coefficient, void coefficient, boron worth and effective delayed

neutron fraction β_{eff}. But their Doppler coefficients are much smaller than those of MOX and UO_2 fuels. Both inert matrix fuels and MOX fuel have a much smaller effective delayed neutron fraction than UO_2 fuel. IMF fuel's value is smaller than that of UO_2 fuel, but close to that of MOX.

The void coefficient is also a potential problem. The coolant void reactivity worth becomes positive if the void fraction reaches 80 percent at beginning of life for boron concentration of 1500 ppm. This is confirmed by MCNP-4C and modified CASMO-4 calculations. The situation is generally much worse at BOL than at EOL. This is of concern during loss of coolant accidents.

Two options are explored in order to improve safety coefficients: 1. Adding fertile materials into IMF fuel pins; 2. Adding fertile fuel pins into IMF fuel assemblies. UO_2 and ThO_2 are used as fertile additives. In option 1 it is found that adding UO_2 will result in a worse degradation of burning ability. However, adding UO_2 provides a better Doppler coefficient than adding ThO_2. Adding about 20 w/o of UO_2 achieves a BOL Doppler coefficient and other safety coefficients comparable to the traditional UO_2 fuel. Yet, the fuel still has a much better burning percentage than MOX fuel for Pu (47.5% versus 13.2%) and for MA (36.1% versus 19.0%), and a much better burning rate for Pu (834 versus 285 kg/GWe-Year) and for MA (98 versus 63 kg/GWe-Year). In option 2 it is found that in order to reach the same level of safety coefficients, the burning rate of the minor actinides becomes comparable to that of MOX: 68.7 versus 63.3 kg/GWe-Year. Thus the option of adding fertile material into the fuel pins is preferable over a heterogeneous assembly option if fast burning of minor actinides is favored.

Table of Contents

List of Figures

List of Tables

Chapter 1: Motivation and Scope of Work

The technology of using UO_2 fuel in light water reactors (LWRs) is pretty mature. UO_2 has been used as fuel for LWRs since the very beginning of peaceful utilization of nuclear energy. Because UO_2 fuel contains mostly the isotope U-238 (>95% weight percent in a typical LWR fuel), which is converted to plutonium by interacting with neutrons under irradiation in the reactors, a large amount of plutonium has been produced during the last few decades, and currently resides in the spent fuel. In a few countries, such as France and Britain, this plutonium has been extracted by reprocessing the spent fuel and is mixed into new LWR fuels (the MOX fuel). But even in those countries, plutonium is to be recycled once, and no plans exist for further recycling.

Another major source of plutonium is from military weapons. As the cold war ended, a large number of nuclear warheads has been disassembled. It is now intended to burn this surplus plutonium as MOX in LWRs or other existing reactors.

A worldwide concern about the large stockpile of plutonium from either disassembled nuclear warheads or civilian source has existed for many years because plutonium is a hazardous material and it takes long time for plutonium to decay. For example, Pu-239 has a 24,000 year half life and it decays to U-235 which is very stable (700,000,000 year half life). Moreover, both Pu-239 and U-235 are excellent materials for building nuclear weapons. The plutonium inventories in the world are shown in Table 1.1.

Table 1.1: Plutonium Stockpiles, 1999 [from the Bulletin of the Atomic Scientists, September/October 1999].

Country of Origin	Weapon-Grade Plutonium	Commercial-Grade Plutonium
Argentina	0	6 metric tons (t)
Belgium	0	23-31 t
Brazil	0	0.6 t
Britain	7.6 t	98.4 t (~51 t separated)
China	1.7-2.8 t	1.2 t
France	6-7 t	151-205 t (~70 t separated)
Germany	0	75-105 t (~17 t separated)
India	150-250 kg	6 t (<1 t separated)
Israel	300-500 kg	0
Japan	0	119-262 t (~21 t separated)
Kazakhstan	2-3 t	0
North Korea	25-35 kg	0
Pakistan	0	0.5 t (0 separated)
Russia	140-162 t	65 t (~30 t separated)
United States	85 t	257.2 t (14.5 t separated)

(t = metric ton (2,200 pounds); kg = kilogram)

Because of its radioactivity, plutonium is hazardous like other radioactive materials. What makes it unique is its ability to constitute a small critical mass with only a few kilograms. Because the basic information needed to assemble a nuclear weapon has been public for many years and the necessary equipments are accessible worldwide, it is considered very dangerous if sufficient plutonium is acquired by unscrupulous persons or organizations. This is the concern in the aftermath of the proliferation of plutonium.

In order to avoid plutonium proliferation, safeguarding measures with continuous surveillance are needed. About 80 percent of the world plutonium inventory is from commercial power plants and is continuously being produced. Plutonium produced from this source is called Reactor Grade Plutonium (RGPu), it has a different isotopic mix from Weapon Grade Plutonium (WGPu) (see Table 1.2). Spent fuel RGPu is produced by, and is in the custody of, more than two hundred private electric utilities all over the world. Responsibility for the security falls predominantly on the individual custodians. It's costly to manage these plutonium inventories to prevent nuclear material diversion. In a few countries, the plutonium is separated for use in mixed oxide fuel to be fed to the LWRs. However, this method cannot decrease the worldwide plutonium stockpile effectively. Other long term reprocessing, storage or transmutation methods are needed.

Table 1.2: Approximate isotopic composition of various grades of plutonium

Grade	Isotope				
	Pu-238	Pu-239	Pu-240	Pu-241[a]	Pu-242
Weapons-grade[b]	.00012	.938	.058	.0035	.00022
Reactor-grade[c]	.013	.603	.243	.091	.050

a. Pu-241 plus Am-241.
b. [Micholas 1992]
c. Plutonium recovered from low-enriched uranium pressurized-water reactor fuel that has released 33 megawatt-days/kg fission energy and has been stored for ten years prior to reprocessing (Plutonium Fuel: An Assessment (Paris:OECD/NEA, 1989) Table 12A).

Spent fuel reprocessing is carried out in France, Britain and Russia, and is being planned in Japan; it is not done in the US and will probably not be considered in the near future. The practice in Europe and Japan shows that it's uneconomic. Central interim storage is a possible choice:

Department of Energy (DOE)'s submission of Yucca Mountain application has been allowed by congress in 2002. But this is only suitable as a middle-term solution, and transportation of the nuclear material is a common public concern.

To reduce the growing amount of plutonium inventory in the long term, nuclear transmutation is the preferred way. Fast and thermal reactors can use plutonium fuel, thus they can be used to reduce the plutonium inventory. However, fast reactor programs have been delayed in response to public concerns, technical problems, large cost and the lower growth of nuclear energy demand than expected in 1970's.

Thermal reactors, especially light water reactors, appear to be a good choice for transmuting plutonium because a large number of LWRs are operating worldwide. Pressurized Water Reactors (PWRs) are the dominant type of LWRs available worldwide as well as in US, thus plutonium inventories can be reduced quickly if an efficient way to burn plutonium in PWRs is proved feasible.

Four generic fuel types can be used for burning weapons-grade or reactor-grade plutonium in LWRs:

1. Uranium-based mixed oxides (MOX): $(U, Pu)O_2$.
2. Inert matrix fuels (IMF), in which PuO_2 is dispersed in a neutron transparent ceramic or metallic inert carrier.
3. Thoria-doped inert matrix fuels (TD), in which a small amount of thorium oxide is added to the inert matrix in order to improve the dynamic coefficients. To denature U-233 which will be produced during fuel lifetime, an amount of U-238 may also be included as natural, depleted or

low-enriched uranium.

4. Thorium-based mixed oxides (Th, Pu)O_2. Again, natural uranium is possibly necessary to be added for denaturing U-233.

Mixed uranium-plutonium dioxide (MOX) fuels are already used to burn plutonium in the LWRs in several nations, for example, France. However, at the same time when the old plutonium is being incinerated in a reactor, new plutonium is being produced because of the existence of U-238, which makes net plutonium destruction difficult. In fact, a 1/3 MOX core generally results in net plutonium production in current light water reactors [Chodak, et al., 1997.]. 100% MOX fuel core can be used, but that may require reactor modifications to accommodate the smaller delayed neutron fraction, which reduces the control materials' worth. Also, the enrichments are likely to be limited, thereby reducing the overall burn rate.

As indicated by the last row of Table 1.3, only for relatively low plutonium "enrichment" (4.0%) and for plutonium originating from dismantled nuclear weapons, the current general maximum of about 30% MOX in the reactor core can give a net reactor plutonium production of zero -- there is still no net consumption by the system then. The column with 5% fissile Pu probably represents the general majority of current MOX fuels. For today's MOX loading possibilities, such MOX systems will not reach the break-even point.

Table 1.3: Some parameters of MOX as plutonium burning is concerned

Pu in MOX, quality	LWR	LWR	LWR	Weapon
Pu-fis in MOX, start	4.0%	5.0%	6.0%	4.0% (assumed)
Pu-tot in MOX, start	6.2%	7.7%	9.2%	4.3% (assumed)
U-235 in UOX, start	3.4%	4.2%	5.0%	3.4%
UOX burn-up (MWd/kg)	34	42	50	34
MOX burn-up (MWd/kg)	43	53	63	43
Pu-tot in MOX, end	~4%	~6%	~7%	~2%
Pu-tot in UOX, end	0.9%	1.3%	2.0%	0.9%
Break-even MOX share	~30%	~43%	~50%	~25%

Assumptions: 1) 65% fissile part in LWR-Pu (1st recycle).
2) 93% fissile part in weapon-Pu.
Burn-up rates are all equivalent in terms of total energy.

(source http://www.ricin.com/nuke/bg/puinlwrs.html)

Due to the reasons mentioned above, MOX fuel is acceptable for the Weapon Grade Plutonium transmutation mission where the conversion of the plutonium isotopic composition to the “spent fuel standard” is a key, but it doesn’t offer the potential to substantially eliminate plutonium because of the breeding effect from uranium.

Since the use of MOX fuel in LWRs does not allow rapid reduction of plutonium stockpiles, the replacement of uranium dioxide by an inert matrix has been recommended.

Elimination of plutonium in current LWRs can be achieved either in a once-through deep burning fuel cycle or in a multi-recycling option. The once-through cycle scheme means that the spent fuel is supposed to be sent directly to final disposal in deep geological formations without requiring any further reprocessing treatment. Japan Atomic Energy Research Institute (JAERI) is active in a once-through cycle scenario with Spinel as inter matrix material. ([Akie 1997], [Yamashita 2001].)

We can also burn plutonium with multi-recycling strategy to achieve a sustainable system. Each cycle can be divided into three stages:

1. Reprocessing and fabrication.
2. Irradiation.
3. Cooling.

For example, CEA's Advanced Plutonium Assemblies (APA) is a multi-recycling design [Puill 1997]. MIT's Combined Non-fertile and Uranium (CONFU) assembly design also deals with multi-recycling scenario [Shwageraus, et al., 2002].

For both the once-through and multi-recycling options, a novel fuel needs to be designed to maximize plutonium destruction. Non-uranium or inert fuel can enhance the destruction capability and it is suitable for both WGPu and RGPu disposition.

Since inert matrix fuels are free of fertile materials such as U-238, they have high plutonium transmutation capability. However, the lack of fertile material U-238 also increases the reactivity swing, degrades the kinetic coefficients, which raises concerns about safety and controllability of the reactors operating with inert matrix fuels.

The scope of this work is to investigate the feasibility of using various inert matrix fuel types, primarily from the reactor physics viewpoint. First a discussion of how to choose inert matrix material is presented in Chapter 2. Next the properties of various materials are compared against the material choice criteria. Plutonium and minor actinides burning rates of various inert fuels and of MOX are compared in Chapter 3. The safety issues are studied and possible methods to improve them are conducted in Chapter 4. Spent

fuel radioactivity and fissile material content characteristics are compared in Chapter 5.

Chapter 2: Choosing Inert Matrix Materials

2.1 Selection criteria for inert matrix materials

As discussed before, the absence of uranium in the inert matrix fuel reduces the fuel temperature coefficient, which is disadvantageous from the viewpoint of reactivity induced accidents. It also significantly influences the burnup reactivity swing. Whether inert matrix fuels are acceptable depends mainly on their irradiation performance in reactors, and on other criteria such as the thermal properties of the matrix, like the thermal conductivity and the melting point. It also depends to a large extend on the possibilities to increase the magnitude of the safety coefficients which deteriorate due to the absence of U-238.

The ideal fuel and fuel cycle design would result in spent fuel with reduced plutonium content, and residual plutonium should be richer in the non-fissile isotopes. For use in a once-through scenario, the spent fuel should also be acceptable for geologic disposal. Table 2.1 shows the general requirements.

Table 2.1: General fuel performance requirements (expanded from [Chodak, et al., 1997].

Requirements	Operating conditions	Accident conditions
Chemical stability	Compatible with cladding.	Compatible with water. No autocatalytic exothermic reactions with H_2O or air at temperatures less than 1200℃.
Irradiation stability	No degradation of properties below limits over expected residence time, fluence. Swelling less than UO_2.	No significant release of energy stored in crystalline lattice.
Thermal conductivity	Greater than that of UO_2 over service life.	Not degraded below that of UO_2 for peak transient temperatures.
Specific heat	No specific requirement	Comparable to or less than UO_2
Fission gas release and thermal expansion	Less than UO_2	Comparable to or better than UO_2
Neutronic	High density of fissile materials Low neutron absorption	Feedback coefficients comparable to or better than UO_2: Doppler, moderator temperature, and void coefficient.

The materials should have high thermal neutron transparency: The matrix materials must be constituted of elements with small neutron capture cross-sections to save as many neutrons as possible for fissioning plutonium, to keep neutron activation low and to avoid changes in materials properties. Neutronic considerations also include radial power peaking, reactivity vs. burnup profiles and depletion composition.

The matrix should have high chemical stability and be compatible

with the cladding. The matrix should also form preferred crystalline structures which will be stable and compatible with the cladding. Satisfactory performance can be defined as the maintenance of cladding integrity without any need for a reduction in reactor plant operational status. High chemical stability with coolant (water) is also a requirement.

The material should have good resistance to irradiation damage. Inert matrix fuels for transmutation of burning excess plutonium (or for minor actinides) are subjected to and should be stable under four different irradiation damage sources [Matzke, 1998]:

- Thermal or fast neutrons.
- α-decay (5-6 MeV He-ions, ~100keV daughter recoil atoms).
- Fission fragment impact (70-100 MeV heavy ions of elements between Ga and Dy).
- Intense β and γ radiation.

These damage processes should not render the matrix amorphous.

The requirement that the matrix should be stable under fission fragment impact can be relaxed if the hybrid fuel concept, as will be discussed in Section 2.4, is used. By limiting the contact area of fissile phase with the matrix, the integrity of matrix can be preserved even if it is not quite stable under fission product impact.

Though the cost of new fuel does not have to be lower than, or even the same as, that of UO_2 because the government may give reimbursement for the benefit of reduction of plutonium stockpile, it should not be economically unreasonable.

Good thermal conductivity is also required. The benefits of higher conductivity include:

- Higher allowable linear heat generation rate.
- Larger melting margin.
- Lower fuel centerline temperature and thus lower stored energy.
- Smaller thermal gradient in the fuel, therefore less severe fuel cracking and better passive heat conduction in an accident scenario.

Other favorable thermal properties are: Good heat capacity, high melting or phase transformation temperature, and low thermal expansion.

For choosing an inert matrix, easy availability of the material and simple fabrication and processing are very important because of their strong impacts on fuel cost. Use of conventional technologies is economical and reliable thus it is desirable that the fuels can be produced by using the conventional MOX fuel technological experience. Much technological experience has been accumulated in the fabrication of oxide fuels, thus an oxide matrix is preferred over others in this regard.

The fuels also should have good mechanical properties such as suitable plastic constant and high hardness.

For the purpose of increasing the plutonium transmutation throughput, high burnup ability is favorable. The fuel should ensure that the Doppler, temperature, and moderator void coefficients of reactivity remain negative over the fuel burnup life time. For fuels containing uranium or thorium dioxide, a large contribution to fuel temperature coefficient (FTC) is due to

U-238 or Th-232 (about -2.2 pcm/K). In addition, quite a large contribution is present due to Pu-240 (about -1pcm/K) [Kloosterman & Konings, 1998.]. When the fuel matrix is made of a neutron inert material, only the plutonium isotopes contribute to FTC. For this reason, for the IMF fuel types attention should be paid to make sure that the FTC is negative and acceptably large in magnitude.

The fuel's overall performance in the core must support its integration into the current LWR fuel cycle with minimum perturbation.

If using the once-through scenario, because the spent fuel is to be sent to a permanent disposal site without further processing, it should be geologically suitable for environmental safety consideration. In the reprocessing scenario this requirement is less strict, but on the other hand the processing difficulties and byproducts should be acceptable.

Regarding the fuel properties requirements mentioned above, UO_2 fuel characteristics are used as the baseline minimum performance standards. Table 2.2 gives some property values of UO_2 for reference.

Table 2.2: Reference UO_2 Properties [Chodak, et al., 1997].

Fresh fuel property	Value	Associated design limit(s)
Thermal conductivity(200-1000℃)	3.6W/m-℃	Steady state and transient fuel peak centerline temperature: no incipient melt.
Melting point	2800℃	Steady state and transient fuel peak centerline temperature: no incipient melt.
Specific heat@100℃	247J/kg-℃	Transient Peak centerline temperature: no incipient melt
Linear expansion coefficient(400-1400℃)	$1.01 * 10^{-5}$ /℃	<1% clad strain
Stability range	No phase change from 20℃ up to melting point	<1% clad strain
Theoretical density	10.97 gm/cm^3	Minimum porosity for swelling (~5%)

Furthermore, "from past experience with MOX fuel, it must be assumed that an eventual utilization of IMF assemblies in present-day LWRs will be gradual. Therefore, from a practical point of view, although asymptotic 100% IMF fuel cycles are feasible, core design efforts must be concentrated on studies dealing with mixed UO_2-IMF loadings" [Stanculescu, et al., 1999].

2.2 Inert material selection process

RGPu and WGPu are composed mostly of fissile isotopes. Higher actinides contain both fissile and fertile materials. In contrast, conventional UO_2 fuel typically has less than 5% weight percent fissile isotopes U-235. PuO_2 must be diluted before use. The host fuel matrices can be UO_2, ThO_2

or inert materials.

Using UO_2, as stated before, the plutonium consumption in the MOX $(U,Pu)O_2$ fuel is limited, hence some uranium-free designs have been examined, with or without inert matrix, and among them, the use of Th/Pu fuels. Thorium could be a good matrix to support plutonium, with a high melting point allowing for large burn-ups and providing some extra Doppler effect due to the resonances of Th-232. But the plutonium consumption rate in a Th/Pu fuel would be somewhat less than in a (Pu + inert matrix) fuel, as the U-233 bred from Th-232 will contribute to fission power. In addition, to prevent misuse of relatively pure U-233 for weapons, denaturing of thorium with natural uranium fuel is required.

IMF tests were performed as early as in the 1960's when plutonium was thought of usable to produce energy. Irradiations of ZrO_2-UO_2 were successfully performed in various reactors followed by some tests with ZrO_2-PuO_2 [Degueldre & Paratte, 1999]. Clearly, the current rebirth of such programs worldwide has taken place in a new context.

The following steps can be used to choose a proper inert matrix material [Chodak, et al., 1997]:

1. From the periodic table of elements, choose the proper ones.
2. For these elements, choose a proper form: metallic, silicide, nitride, carbide, or oxide.
3. Choose a stable crystalline structure under irradiation.

In step 1, according to the material property requirements described before, the elements with small thermal absorption cross sections are

identified first. The viable elements include H, He, Be, C, N, O, F, Ne, Na, Al, Si, P, S, Ar, Ca, Y, Zr, Ce, Pb [Chodak, et al., 1997].

In step 2, emphasis in available literature has been given to various oxides. The metals are less investigated, and silicides, nitrides and carbides are investigated the least. Carbides or nitrides have been found to be acceptable in some specific cases. Silicon carbide (SiC) has been proposed as IMF for CANDU reactors [Verrall, et al., 1998]; nitrides have better thermal conductivity and have been identified as candidate fuels for fast reactors [Tommasi, Beaumont & Newton, 1998]. But the carbide and nitride fuels are less acceptable for LWRs because of their chemical interaction with water.

The large existing fabrication and operating experience with oxide fuels gives them a significant advantage: their fabrication would require less modification of existing technology than others. Moreover using oxide compounds is favorable for spent fuel direct disposal because many oxide compounds are stable in nature.

In step 3 of choosing crystalline structure, one requirement is that the crystalline structure of the oxide matrix be able to incorporate plutonium, burnable poisons and fission products.

Peroskovites, fluorites, yag and rutile crystalline structures are capable of incorporating actinides and rare earths. The vacancies in a fluorite structure make it particularly suitable to the incorporation of fission products. Fluorite is also known to readily incorporate fission products without phase change. Furthermore, fluorite oxides have the largest experience base and the most mature manufacturing infrastructure. Thus, the

fluorite structure is selected as preferred for containing plutonium.

In many cases rare earth burnable poisons are necessary. Burnable poisons are used to serve three purposes:

- To provide beginning of cycle excess reactivity control, allow increased fissile material loading.
- To shape the reactivity vs. burnup curve.
- To provide negative contributions to FTC and MTC through resonance absorption.

In choosing rare earth oxide burnable poisons, the five leading candidates are: gadolinia, europia, erbia, samaria, hafnia. Erbia is superior, followed by gadolinia. Erbia (Er_2O_3) is often chosen as additive burnable poison.

Three forms of inert matrix fuels have been selected in the past [Porta & Puill, 1998]:

1. Ceramic-Ceramic (CERCER): The fuel in the form of particles of a kind of ceramic is dispersed in another ceramic which acts as a matrix for filling the fuel rod.
2. Ceramic-Metal (CERMET): The ceramic fuel is dispersed into a metallic matrix.
3. Solid Solution (Solid Solution Pellet, SSP): The fuel and the matrix form a solid solution in order to obtain very precise characteristics for highly specific objectives. This can be a metallic or oxidic solution.

CERCER and CERMET are both two-phase heterogeneous materials.

By using two-phase plutonium materials the integrity of the inert matrix is better preserved during irradiation. The drawbacks are: more complicated manufacturing, potential hot spots and absence of thermodynamic stabilization.

A ceramic can be transparent to neutrons. However, R&D is needed to investigate and develop CERCERs with resistance to irradiation and with high thermal conductivity and viscoplasticity.

CERMET uses metal as matrix. Metals have four essential advantages:

1. Metals are potential barriers against gas diffusion and therefore ensure better fission gas retention. This also relieves mechanical stress on the cladding and thus the matrix becomes the first safety-related barrier. [Porta & Doriath, 1999.]

2. Due to metals' high thermal conductivity, using them will result in a decrease in the fuel temperature and thus decreases in fission gas release and thermal-mechanical stresses.

3. Safety is increased because metals decrease stored potential energy, which is a favorable factor in the event of a loss of coolant accident.

4. Metals form a metal-to-metal contact for the cladding and the matrix, which limit, or even avoid, the occurrence of pellet-cladding interaction (PCI).

There can be drawbacks to metals at high burnup, such as swelling and embrittlement. Furthermore, some metals are a source of hazard during severe accidents due to chemical reactions with steam leading to hydrogen production. Referring to the requirements addressed before, the chosen metals should be transparent to neutrons. But sometimes absorbent metals

are also considered because they permit higher initial fissile material loading, and therefore greater in-vessel plutonium storage, which is interesting from the standpoint of strategies aiming to reduce plutonium stockpiles.

Two candidates are potentially of interest among the "transparent metals": Zr, as it is the metal used for the cladding, and silumin (88%Al, 12%Si), which has particularly interesting thermal conductivity [Porta, Aillaud & Baldi, 1999]. Zr in particular is a source of concern in LWR accident analysis. Table 2.3 shows some characteristics of metallic inert matrix candidates.

Table 2.3: Some characteristics of metallic inert matrix candidates [Porta, Aillaud & Baldi, 1999]

	T Melt. (K)	Density (kg/m3)	Thermal Conductivity (W m-1 K-1)				Heat Capacity (J kg-1 K-1)
		293K	293K	373K	673K	873K	293K
Mo	2850	9590	138	135	123	116	225
Al	940	2710	236	240	228	215	902
SiAl	-	2260	162	173	180	-	871
Zr_4	2120	6570	23	21.8	21.4	22.3	276
Inox (304)	1680	7820	15.2	16.6	20.8	23.5	460
UO_2	3100	1100	5	-	-	-	235

Others metallic candidates include Cr, V, W and Steel(EM10) [Cocuaud, et al., 1997], as shown in Table 2.4.

Table 2.4: Evaluation of metals as inert matrices [Cocuaud et al, 1997]

	Cr	V	W	Steel(EM10)
Neutron activation	+	+	+	+
Fabrication	+	+	+	+
Cladding compatibility	+	+	+	+
Sodium compatibility	+	+	+	+
Basic properties	+	+	+	+
Ability to be dissolved	-	+	-	+

Although they showed good potential for use as inert matrix, they are nonetheless not well studied in the literature.

One other possible structure of the fuel is to form solid solution pellets of PuO_2 in inert ceramic oxides and/or thoria. This is a kind of homogeneous material. The advantages of solid solutions are [Cocuaud, et al., 1997]:

1. Hot spots are not likely to occur.
2. Additions of elements can stabilize the actinide compound.

Its disadvantages include:

1. Its ability to be dissolved.
2. Its thermal conductivity is lower than that of its constituents.

2.3 Properties of inert material candidates

2.3.1 Zr based materials

Zircon, (Zr,Hf,Pu,…)SiO_4, and zirconia, (Zr, Hf, Pu,…)O_2, have been proposed as durable actinide host phases for the immobilization of weapons grade plutonium and other actinides. Both proposed host phases have durable natural analogues: zircon of monoclinic baddeleyite, and zirconia of cubic tazheranite, (Zr, Hf, Ca, Ti)O_2. Waste forms based on zircon and zirconia are geo-chemically compatible analogues of accessory minerals of natural rocks. [Burakov, et al., 2001.]

Zircon ($ZrSiO_4$) is rejected because of its dissociation upon high temperatures and its poor stability against radiation. [Matzke, Rondinella & Wiss, 1999.]

Promising reactor physics characteristics have been achieved for ZrO_2-based solid solution IMF assemblies [Pillon, et al. 1998.]. IMF cores have been shown to be at least as effective as MOX fuel to reduce plutonium. One major concern is the low thermal conductivity as shown in Table 2.5.

Table 2.5: Thermal conductivity: Values for normal porosities(~5%) and impurity contents (~10^2 ppm) in $Wm^{-1}K^{-1}$ [Chauvin, Konings & Matzke, 1999].

	$MgAl_2O_4$	MgO	ZrO_2	UO_2
600K	8	23	1.8	5.5
1000K	6	10	1.8	4

From Table 2.5, it can be seen that MgO and $MgAl_2O_4$ show superior conductivities to those of UO_2 whereas ZrO_2, in any form and degree of stabilization, has much lower conductivity, which is the greatest challenge confronting the application of ZrO_2-based fuels.

To overcome ZrO_2-based fuels' poor thermal conductivity, a hybrid fuel concept can be used. By adding Spinel and selecting an appropriate zirconia/Spinel ratio, it is possible to overcome the low thermal conductivity of zirconia. Also the feasibility of a CERMET consisting of fine particles bearing plutonium in a cubic zirconia dispersed in a metallic matrix is being investigated as an option to overcome the low thermal conductivity of zirconia [Burghartz, et al., 1998].

Despite the bad sides, Zr related materials are attractive because of many advantages:

1. Spent fuel is a large potential source of Zr for the synthesis of zirconia based ceramic forms because Zr is widely used as fuel cladding in the nuclear industry, which makes zirconia relatively inexpensive to produce.
2. Double-phase crystalline ceramics based on zirconia are chemically durable and resistant to radiation damage. ZrO_2 is very stable against irradiation.
3. ZrO_2 has a melting point comparable to UO_2.

Zirconia forms a distorted monoclinic fluorite which is not suitable for incorporating plutonium. However, it can be stabilized by the addition of a third oxide to form a stable face centered cubic fluorite. The inert matrix of stabilized zirconia is investigated widely in literature. The Rare Earths (REs) added for neutronic performance reasons can also serve to stabilize

the zirconia. Erbium was found effective [Chodak, et al., 1997].

CaO can be used to stabilize zirconia. The advantages of calcia stabilized zirconia include:

- Relatively low thermal absorption.
- Good thermo mechanical properties.
- Substantial existing developmental and experimental database for both calcia and zirconia.

Yttria stabilized zirconia (YSZ) is an alternative to calcia stabilized zirconia. YSZ in the fluorite phase helps to localize irradiation damage and to contain the actinides and fission products to achieve good physico-chemical stability.

The advantages of YSZ include:

- High chemical stability.
- High melting temperature (about 2600K).
- High irradiation stability. Stable against radiation-induced swelling or amorphisation.
- Excellent actinides host phase.
- Not redox sensitive, a good geological behavior.

The drawback is also low thermal conductivity which will raise the average fuel temperature and reduce the safety margin significantly.

[Kasemeyer, et. al. 1998] investigated the physical and engineering

properties of a core with fuels consisting of 80-90% ZrO_2, 7-14% PuO_2, 3-6%Er_2O_3, with a potential addition of Y_2O_3 as stabilizer. This fuel has a melting point of ~3000K, and it does not have any phase change between room temperature and its melting point. It is chemically inert with clad material (Zircaloy), and its solubility in hot water (at ~500K) is below 10 mol/l. The material is not affected by the transmutations. The fission products are relatively soluble in this solid solution and effects of irradiation would not affect the crystal structure. Gas evolution is very restricted during irradiation. The material behavior during plutonium burning is expected to be quite satisfactory.

2.3.2 Al_2O_3 based materials

Al_2O_3 based materials are considered as possible inert matrices because of the following positive aspects:

1. Al_2O_3's ability to retain the semi-volatile alkali metals by forming alkali aluminates [Yuan, et al., 2001.].
2. Alumina is able to incorporate fission products.
3. Alumina's good thermal metric performance including high thermal conductivity, which is the major advantage of an alumina dispersion fuel.
4. Alumina's chemical stability as a spent fuel form.

When using Al_2O_3 as an inert ceramic matrix, two fluorite-structure ceramics could be used:

PuO_2-ThO_2-Al_2O_3

PuO_2-ZrO_2(Y_2O_3, Gd_2O_3)-Al_2O_3

PuO_2 is combined with zirconia and/or ceria to form a fluorite crystalline structure, and accommodated by alumina matrix. As described before, Y_2O_3, Gd_2O_3 can be added to stabilize zirconium oxide, and rare earths such as Gd and Er can be added as burnable poisons.

The major drawbacks of Al_2O_3 related materials are:

1. They become amorphous and have significant swelling under irradiation; the resulting pellet-cladding interaction will make them inappropriate for use in LWRs.
2. Hibonite type phase formation under low oxygen potential.
3. Low melting temperature of 2020℃
4. Alumina matrix absorbs and combines with fission products to form new crystals which add to the strain.

These drawbacks make Al_2O_3 based materials basically not suitable for use as inert matrix materials. Just as the experiment by [Matzke 1998] showed, Al_2O_3 is unstable against fast neutrons. Al_2O_3 was shown to be amorphised by the impact of heavy ions (Xe, 40keV), and to recrystallise at ~970K, with the moving boundary crystalline/amorphous sweeping the rare gas out of the crystal. Al_2O_3 is also unstable against fission product impact with swelling of up to 30%. It should be discarded as a potential inert matrix.

2.3.3 MgO & Spinel ($MgAl_2O_4$)

MgO and $MgAl_2O_4$ show superior thermal conductivities. They can be added to improve the poor conductivity of ZrO_2. MgO is also a good matrix candidate for fast reactors.

A 40% volume Spinel($MgAl_2O_4$) matrix using fuel spheres of about 120um in diameter was favored by [Porta & Puill 1998]. The spheres are to be pre-cracked for better resistance under irradiation and a specific patented technique for introducing a gap between the matrix and the sphere during sintering was employed so as to accommodate fission gases without damaging the matrix. Viscoplasticity is significantly improved by the gap, thus reducing the risk of pellet-cladding interaction (PCI). In addition, thermal conductivity of the fuel is slightly improved by Spinel.

Spinel ($MgAl_2O_4$) is quite stable against neutron radiation [Yuan, et al., 2001] and has good thermal conductivity. But it exhibits considerable swelling due to fission products. This problem can be solved by using the hybrid fuel concept discussed in Section 2.4. In hybrid fuel, the fission products are confined within the vicinity of fissile phase of the fuel. By limiting the volume percentage of fissile phase in the fuel, the impact of fission products on matrix can be minimized.

Table 2.6 shows the melting points for different compositions of Spinel and YSZ. The melting point of the mixture is lower than either Spinel or YSZ.

Table 2.6: Melting point for different compositions of $MgAl_2O_4$ and YSZ (Excerpted from Yuan, et al., 2001)

$MgAl_2O_4$	YSZ	Melting point (K)
100	0	2375.0
64.3	35.7	2203.7
40.3	59.7	2201.6
0	100	2996.6

We can use Spinel as a matrix, and YSZ to contain the fissile material PuO_2. Fission fragments can be localized in the fissile phase by YSZ particles of adequately large diameters (150-200 μm) thus the instability problem of Spinel under impacts of fission products can be overcome. The ability of this hybrid fuel concept to solve the poor Spinel performance under irradiation is still subject to verification.

2.3.4 Other materials

Silicides, nitrides and carbides are also candidates for inert matrix materials. However, they are less preferred for use in LWRs than oxides.

In the CERMET concept, Cr, V, W and steel are also considered along with Zr. Although they showed good potential for use as inert matrix, they are nonetheless not well studied in the literature. More research work need to be conducted in this area.

Among lanthanides, cerium is unique because it can form a fluorite structure. It can enhance the chemical proliferation barrier of the fuel and can be used to stabilize zirconia. Furthermore, it is transparent to neutrons. Thus CeO_2 and monazite $CePO_4$ are also possible candidates. However, both of them have certain disadvantages. CeO_2 showed swelling and indicated polygonisation, whereas $CePO_4$ was seen to have poor radiation stability during fission product impact (72 MeV iodine). [Matzke, 1998.]

2.4 “Hybrid” fuel concept

We use Spinel ($MgAl_2O_4$) and ZrO_2 to illustrate the hybrid fuel

concept. The basic idea is to exploit the good mechanical and thermal properties of $MgAl_2O_4$ to compensate for the poor conductivity of ZrO_2, and at the same time to utilize the good resistance against fission damage of ZrO_2 while avoiding the poor stability of Spinel under fission product impact.

After the fissile material is solidified in a fluorite phase:

1. It can be homogeneously incorporated into the matrix to form a solid solution.
2. Or it can be contained as particles in YSZ, which is then dispersed into the Spinel matrix homogenously. This is called the ceramic-in-ceramic or CERCER concept. Alternatively, it is called the ceramic dispersion concept.

Method 2 (dispersed) is preferred to method 1 because it can localize the damage to the matrix phase thus it can avoid degradation of its thermal conductivity, which further results in higher achievable burnup.

To minimize the damage of the matrix by the fission product impact, we need to minimize the contact area between the matrix and the fissile phase material. Noticing that a sphere has the lowest surface to volume ratio, it is clear that spherical particles will lead to the least damage within the inert matrix.

Thus a hybrid fuel concept is proposed as consisting of spherical fissile material particles with high resistance against neutron damage and inert matrix with good thermal and mechanical properties.

There are some special considerations to minimize fission product damage (Revised from [Yuan, et al., 2001]):

1. Choice of a proper fissile phase particle size to reduce the region affected by fission products.

As the particle size becomes large, the damage region size in the matrix decreases, since the impact range of the fission products is between 8 and 10 μm. However, the larger the particle size, the larger the thermal gradient between the particle and the matrix, which may result in cracks in the fuel and degrade the thermal conductivity, and aggravate the fission gas release. A proper size should not be smaller than about 50 μm or larger than about 300 μm.

2 Fission phase particles can be coated.

The coating can retain fission products, thus protecting the matrix material from damage by these products. It can also protect the fuel from corrosion by coolant, or matrix materials.

The design of the coating should be careful because the gases accumulated within the coat may produce very high pressure, which may cause the fuel and coating to crack.

3 Gaps are kept between particles and matrix to provide space for irradiation induced expansion of the fuel, to accumulate fission gas, and to limit crack propagation. However, the voids may degrade the thermal properties of the fuel.

2.5 Material properties of inert ceramic and metal matrix candidates

This section presents some key properties of possible ceramic and metal matrix candidates. The candidates of ceramic are MgO, CeO and $MgAl_2O_4$ (Table 2.7); the metallic candidates include metals: Cr, Mo, Fe, W, V and Zr (Table 2.8), and alloys: Zircaloy, inconel, and silumin (Table 2.9).

Regarding the potential candidates for metal matrix, Zr is chosen because it is the metal used for the cladding, and silumin (88%Al, 12%Si) is chosen because it has particularly interesting thermal conductivity [Porta, Aillaud & Baldi, 1999], but its low melting point is a big problem. [Baldi and Porta 2001] chose Molybdenum, Inconel, Zircaloy and Steel as matrix for their study of inert matrix fuel for plutonium incineration and safety coefficients. Other metallic candidates include Cr, V and W [Cocuaud, et al., 1997].

The data in this section comes from different sources. The elements' microscopic thermal neutron absorption cross sections are excerpted from MCNP data library, except for Ce, whose cross section data is from Jef2.2 library. The cross section value of compound is estimated by averaging over their constituents weighted by number percentages. For example, if the cross sections for Al, Mg, and O are σ1, σ2 and σ3, respectively, then

the cross section for $MgAl_2O_4$ is estimated as:

$$\sigma = \frac{\sigma 1 * 2 + \sigma 2 * 1 + \sigma 3 * 4}{7}$$

For alloy candidates, the method used to estimate the cross section is the same. The alloy compositions given as weight percentage in Table 2.9 are first converted to atom percentage, and then the cross sections of the alloys are estimated by averaging over their constituents weighted by atom percentages. The alloys' weight percentage composition data are from an online database: http://www.matweb.com. Other material properties such as thermal conductivity, melting point, etc. are also from this website.

The price data in Table 2.7 are only approximate numbers. The price data in Table 2.8 are from U.S. Geological Survey (http://www.usgs.gov/). There is no cost column in Table 2.9 due to lack of the data.

Table 2.7: Ceramic matrix properties

Candidates	Thermal neutron absorption cross section (barn)	Cost (per metric ton)	Density (g/cc)	CLTE* (μm/m-K)	Thermal conductivity (W/mK)	Melting point (K)
MgO	0.032	~$300	3.58	12.8	42	3037
CeO_2	0.203	-	7.65	-	-	2673
$MgAl_2O_4$	0.076	-	3.60	7.45	15	2403

*CLET: Coefficient of linear thermal expansion, at 293K.

Table 2.8: Metal matrix properties

Candidates	Thermal neutron absorption cross section (barn)	Cost (per metric ton)	Density (g/cc)	CLTE* (μm/m-K)	Thermal conductivity (W/mK)	Melting point (K)	Melting point of oxide (K)
Chromium (Cr)	3.104	~$7600	7.19	6.2	94	2180	CrO_2: 673 (loses 0_2). CrO_3: 463 Cr_2O_3: 2723
Molybdenum (Mo)	2.653	~$5200 (per metric ton of molybdenum contained in molybdic oxide)	10.22	5.35	139	2896	MoO_2: 1373 (decomposes) MoO_3: 1068
Iron $(Fe)^+$	2.562	Not expensive	7.87	11	48	1811	FeO: 1643 Fe_2O_3: 1838 (decomposes) Fe_3O_4: 1873
Tungsten (W)	18.115	$6400 (per metric ton of tungsten contained in WO_3)	19.3	4.4	170	3695	WO_2: 1773 WO_3: 1746
Vanadium (V)	5.049	~$3240 ($V_2O_5$)	6.11	8.33	31	2183	VO: 2063 VO_2: 2240 V_2O_3: 2243 V_2O_5: 958
Zirconium (Zr)	0.186	$350	6.53	5.8	23	2128	ZrO_2: 2950

* Coefficient of linear thermal expansion, at 293K.

+The properties are for steel. One composition AISI 1080 Steel, some what randomly, is chosen.

Table 2.9: Alloy matrix properties

Candidates	Composition (w%)	Thermal neutron absorption cross section (barn)	Density (g/cc)	CLTE* (µm/m-K)	Thermal conductivity (W/mK)	Melting point (K)
Zircaloy-4	Zr: 98 Sn: 1.5 Fe: 0.5	0.210	6.56	6	21.5	2123
Inconel	Ni: 60 Cr: 20 Mo: 10 Fe: 5 Nb: 4 Co: 1	4.252	8.44	12.8	9.8	1570
Siluminum	Al: 88 Si: 12	0.224	2.66	20.4	121	970

* Coefficient of linear thermal expansion, at 293K.

2.6 Summary

Inert matrix fuels are considered for use in current LWRs to reduce the large stockpile of plutonium and minor actinides worldwide. The inert matrix fuel design should be done carefully because the absence of uranium in the fuel significantly influences the burnup reactivity swing, the reactivity coefficients and the kinetic parameters of the fuel.

The chosen material should be thermal neutron transparent, have high

chemical stability with cladding and water, good resistance to irradiation damage, good heat capacity, high melting or phase transformation temperature, low thermal expansion, good thermal conductivity, be economically reasonable, and have good mechanical properties. Fabrication and availability of starting materials are important considerations. Furthermore, the new fuel should be able to maximize the plutonium burnup and be easily incorporated into present LWR fuel cycle.

For the elements meeting the basic neutronic requirements for use as inert matrix materials, several formats are possible among metallic, silicide, nitride, carbide and oxide, and several crystalline structures among peroskovites, fluorites, yag, and rutile.

An oxide form is preferred because of plentiful fabrication and operating experience. The metallic, carbide and nitride fuels are less acceptable for LWRs because of their chemical interaction with water. Fluorite as the crystalline structure is preferred due to its large experience base. Another reason is its ability to incorporate actinides, rare earths and fission products.

The fuel can be in the format of a CERCER, a CERMET, or a SSP. SSP is the result of homogeneous dissolution of fissile isotopes into an inert matrix; the resultant IMF is a single-phase material. Due to the advantages of a “hybrid” fuel described in Section 2.4, the multi-phase CERCER and CERMET provide better performance.

For metals and alloys, Zr, silumin (88% Al, 12% Si), Cr, V, W and steel are possible choices. Using metals has many advantages such as higher thermal conductivity therefore decreased fuel temperature and thermal-

mechanical stresses, decreased stored potential energy thus higher safety. However, both severe accident and waste behavior pose issues that cannot be overcome with present knowledge about CERMETs. Hence more detailed work needs to be done.

Some of the candidates could be rejected: zircon ($ZrSiO_4$) because of its dissociation upon annealing to high temperatures and its high swelling under radiation; Al_2O_3 because of amorphization and large swelling; monazite ($CePO_4$) because of the poor radiation stability due to fission product impact and the poor thermal conductivity. There are known difficulties with CeO_2, because of its polygonizatin and temperature dependent swelling; MgO, because of its disintegration in the event of cladding failure under PWRs condition; and Spinel, because of its instability under fission product impact.

Zirconia can be stabilized by either CaO or yttrium. Y_2O_3 has negligible neutron induced swelling. Yttrium stabilized zirconia (YSZ) has high chemical stability, high melting temperature, high irradiation stability. It is an excellent actinides host phase. CaO is also a good candidate to stabilize zirconia. It has very good thermo-mechanical properties.

The major drawback of the zirconia matrix is the low conductivity of ZrO_2, but Spinel or MgO can be added to compensate this. Spinel has partial amorphization and polygonization and is unstable under fission product impact. We use hybrid fuel format to localize irradiation damage: Plutonium is incorporated with stabilized zirconium to form a fluorite phase, which is subsequently dispersed into inert matrix. Fission fragments can be localized by YSZ in fissile phase.

A burnable poison additive is required to hold down beginning-of-life (BOL) excess reactivity. Also, it helps to improve the reactivity vs. burnup profile, and to improve both the prompt Doppler coefficient and the negative isothermal temperature coefficient. Rare earths such as erbium and gadolinium could be used as burnable poisons. Er (Er_2O_3) is often suggested as burnable poison. Sometimes Gd (Gd_2O_3) is used.

No common strategy for uranium-free fuels has emerged. In the coming chapters we will examine the properties of inert matrix fuels with plutonium dissolved in Y_2O_3 stabilized zirconia as fissile part, and different ceramic materials: Spinel, MgO and CeO_2, and metals: Zr and Fe as supporting matrices.

Chapter 3: Plutonium, Minor Actinides and TRU Burning Abilities of Different Inert Matrix Fuels

Plutonium, minor actinides (MA) and trans-uranium (TRU) burning abilities are measured by how much is burned relative to what is held in the system, in terms of the weight percentage burned as of initial loadings; and by how fast, in terms of Pu, MA, and TRU burned per giga-watts year of electric power generated.

The benefits of compound fuels have been discussed in Chapter 2, so this chapter will use compound formats as the prototype for all calculations. According to the criteria discussed in Chapter 2, five matrices were selected as representatives, including three ceramics: Spinel ($MgAl_2O_4$), MgO, and CeO_2; and two metals: Zr and Fe. These matrices are not yet proven to behave satisfactorily in a reactor, and some of their properties are still under investigation. Siluminum was once thought of as a candidate, but its melting point is too low (970K, Table 2.9) and is thus discarded.

This chapter will compare plutonium, minor actinides and TRU burning abilities of fuels using selected inert matrices. The results are also compared against MOX fuel. The influences of several possible changes in the operating situation on the burning ability are discussed at the end of this chapter. The possible parameter changes investigated include H/HM ratio, initial TRU loading, and increase of power density.

3.1 Methodology

This section gives detailed description of calculating the burning

ability using Spinel inert matrix fuel as representative.

3.1.1 Calculating tool

CASMO-4 is used as the calculation tool for this study. The CASMO-4 code is a multi-group two-dimensional transport code developed by Studsvik, which is entirely written in FORTRAN 77. It is used for burnup calculations on Boiling Water Reactor (BWR) and Pressurized Water Reactor (PWR) assemblies or pin cells. The code can deal with geometries consisting of cylindrical fuel rods of varying composition in a square pitch. It accommodates various rods such as those containing gadolinium, burnable absorber rods, cluster control rods etc. Typical fuel storage rack geometries can also be handled. Detailed information can be obtained from the code user's manual provided by Studsvik [Edenius 1995].

3.1.2 Choosing initial TRU loading

The plutonium and minor actinides are collectively called trans-uranic (TRU) materials. They are all heavier (higher in atomic number) than uranium. However, in this study, small amount of uranium isotopes is also included in addition to TRU because CASMO-4 requires some uranium for calculation to proceed. As will be shown shortly, the uranium isotopes are only a very small part of the fuel.

As discussed in Chapter 2, the fuel is in hybrid form: TRU contained as particles in yttria stabilized zirconium (YSZ), which is then dispersed in the selected matrices homogenously. To limit the damage to and thus preserve the integrity of the matrices, the volume percentage of the fissile phase is limited to about 20 volume percent. This limit applies to those

matrices which are unstable against fission products such as Spinel. To limit the volume percentage of fissile phase material, the volume percentage of the matrix influenced by fission products is also limited, thus the integrity of the matrix can be preserved. Loading too little fissile phase material is also unpractical. Initial TRU loading will range from volume percentage of 10% to 20% in this study. Roughly the same volume of YSZ is needed, so TRU and YSZ together account for 20% to 40% of total volume. The remaining majority, 60%~80%, of the fuel will be the inert matrix. 70 v/o of matrix material will be chosen in the following calculations.

It appears that if we choose 20% TRU, 10% YSZ, and 70% Spinel, as shown in Figure 3.1, the total in-core time of the fuel would be too long since a typical in-core time is about 1500 EFPD:

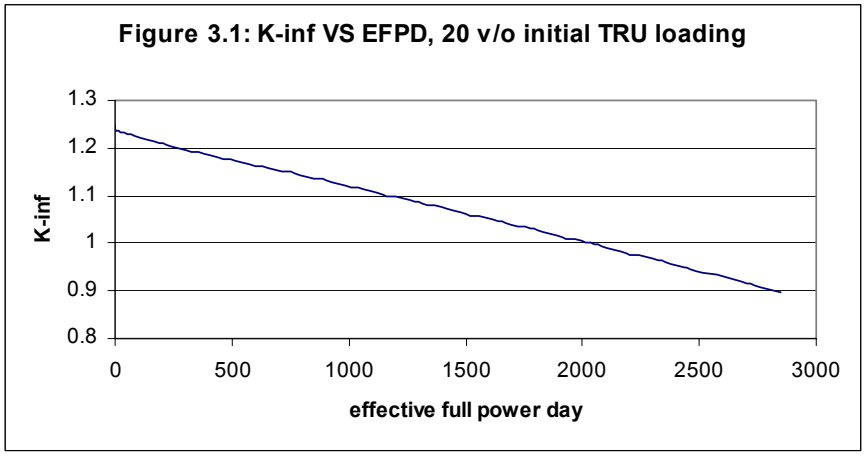

The figure is calculated using the code CASMO-4 and assuming typical geometry and operation parameters, which will be given later. As can be seen, $K_{inf} = 1.0$ occurs after about 2000 effective full power day, which is more than 60 months. This corresponds to reactivity limited burnup BU_1 = 371.1 MWd/kgHM. Assuming a 3-batch fuel management and using the linear reactivity model [Driscoll, et al., 1990], fuel discharge burnup will be:

$BU_3 = BU_1 * 1.5 = 556.6$ MWd/kgHM

This corresponds to approximately 3050 effective full power day, or 102 months, which is too long compared to current practice.

The percentage of initial TRU in the fuel is thus adjusted to obtain realistic cycle length. If the initial TRU volume percentage is 15 percent, repeating the same calculation yield 2370 EFPD for BU_3, which is about 79 month. The cycle length is 79/3 = 26.3, close to a 24 month cycle length. So, initial TRU loading of 15 percent is chosen. Further tuning is needed to achieve the exact cycle length for 12, 18 or 24 month; furthermore, different initial loadings should be chosen for different inert matrices. However, this is not needed for preliminary scoping studies. The fuel composition will be chosen to consist of 15% TRU, 15% YSZ, and 70% inert matrix material (volume percentage) in all the remaining calculations, unless otherwise specified.

3.1.3 Isotope composition

In order for the calculation to proceed, we need to get the detailed compositions of the fuel down to a single isotope level because CASMO-4, and many other commonly used computer code in reactor science, use weight percentage of constituent isotopes as input. This information should be prepared before using the tools.

The chosen fuel is divided into three groups for the purpose of calculating the compositions: the inert matrix (Spinel in this example calculation), the YSZ, and the TRU. The compositions within each group are calculated first, and the results are compiled together to generate the

overall composition data.

Compositions for matrix

For the Spinel matrix, the molecular formula is $MgAl_2O_4$. From this formula, it is clear that the atomic ratio Mg:Al:O is 1:2:4. To change the atomic ratio to weight percentage, the atomic weight values for Mg (24.305), Al (26.981), and O (15.999) are used. The weight percentages are shown in Table 3.1:

Table 3.1: The weight percentages of Mg, Al, and O in Spinel

Element	Mg	Al	O
Weight Percentage	17.1%	37.9%	45.0%

Compositions for YSZ

YSZ is composed of 92% ZrO_2 and 8% Y_2O_3 in molecular percentage. We can convert the molecular percentage to weight percentage using the molecular weight values of ZrO_2 (91.224+15.999*2 = 123.22) and Y_2O_3 (88.906 * 2 + 15.999 * 3 = 225.81) similarly as in calculating weight percentages of Mg, Al, and O in Spinel. We can calculate similarly that ZrO_2 has 74.0 w/o Zr and 26.0 w/o O; Y_2O_3 has 78.7 w/o Y and 21.3 w/o O. Combining these results together yields Table 3.2.

Table 3.2: The weight percentages of Zr, Y, and O in YSZ

Element	Zr	Y	O
Weight Percentage	63.9%	10.7%	25.4%

Composition of TRU

When talking about composition of TRU in this section, we actually mean composition of heavy metal dioxides, or (TRU + U)O_2.

TRU in fuel is in the chemical form of (TRU) O_2. The "atomic" weight of TRU depends on its constituent isotopes, and is calculated from atomic weight of its constituents weighted by number percentage.

The composition of TRU is acquired by assuming the following scenario [Shwageraus, et al, 2002]: Traditional 4.2% enriched UO_2 fuel is burned to burnup of 50 MWd/kg; and then cooled for 10 years. CASMO-4 is used for burning the fuel to 50 MWd/kg, and the ORIGEN-2 code is used for calculating the decay during the 10 years cooling. The resulting composition is shown in Table 3.3.

Table 3.3: Reference TRU isotopic composition

Isotope	Weight Percentage
U-234	0.0001%
U-235	0.0023%
U-236	0.0019%
U-238	0.3247%
Np-237	6.641%
Pu-238	2.7490%
Pu-239	48.6520%
Pu-240	22.9800%
Pu-241	6.9260%
Pu-242	5.0330%
Am-241	4.6540%
Am-242m	0.0190%
Am-243	1.4720%
Cm-242	0.0000%
Cm-243	0.0050%
Cm-244	0.4960%
Cm-245	0.0380%
Cm-246	0.0060%

From the values in Table 3.3, we can calculate the atomic percentage of each isotope in TRU. The results are shown in Table 3.4.

.

Table 3.4: TRU isotopic composition in atomic percentage

Isotope	Atomic Percentage
U-234	0.0001%
U-235	0.0023%
U-236	0.0019%
U-238	0.3268%
Np-237	6.7119%
Pu-238	2.7667%
Pu-239	48.760%
Pu-240	22.935%
Pu-241	6.8837%
Pu-242	4.9816%
Am-241	4.6256%
Am-242m	0.0188%
Am-243	1.4510%
Cm-242	0.0000%
Cm-243	0.0049%
Cm-244	0.4869%
Cm-245	0.0372%
Cm-246	0.0058%

With Table 3.4, the atomic weight value for TRU is:

$$A = \sum_i A_i \text{*(Atomic Percentage)}_i = 239.53$$

Now the weight percentages of TRU and O in $(TRU)O_2$ can be calculated. The result is 88.22% TRU and 11.78% O. From this, the following weight percentage results can be attained:

Table 3.5: Isotopic weight percentages in (TRU) O_2

Isotope	Weight Percentage
U-234	0.00006%
U-235	0.00203%
U-236	0.00170%
U-238	0.28644%
Np-237	5.85838%
Pu-238	2.42504%
Pu-239	42.9185%
Pu-240	20.2718%
Pu-241	6.10979%
Pu-242	4.43988%
Am-241	4.10554%
Am-242m	0.01676%
Am-243	1.29853%
Cm-242	0.00000%
Cm-243	0.00441%
Cm-244	0.43755%
Cm-245	0.03352%
Cm-246	0.00529%
O	11.7847%

Combining the results for $MgAl_2O_4$, YSZ and (TRU)O_2 to calculate the individual weight fractions

Now that we have all the composition results for individual fuel regions, we're ready to calculate the overall isotopic composition for the fuel. This step is not special at all. In fact, it is very straightforward. For example, if 50 w/o of the fuel is YSZ, and 50 w/o of the YSZ is yttria, then we have 50% * 50% = 25% yttria in the fuel. (50% in this example is not

the actual value, nor is the 25%.)

We don't know the weight percentage of each fuel region yet, but we know the volume percentage for of $MgAl_2O_4$, YSZ and $(TRU)O_2$ in the fuel is 70, 15, and 15, respectively. Because volume multiplied by density is weight, if the densities of each region are known, the weight percentages can be easily calculated.

The densities for Spinel and YSZ is 3.7 g/cm^3 and 5.9 g/cm^3, respectively. The density for $(TRU)O_2$ is 10.7 g/cm^3, which is 94% of theoretical result assuming a typical porosity value. The weight percentages of each fuel region are shown in Table 3.6.

Table 3.6: Weight percentages of $MgAl_2O_4$, YSZ and $(TRU)O_2$ in the fuel

	$MgAl_2O_4$	YSZ	$(TRU)O_2$
Weight Percentage	50.88%	17.38%	31.74%

With the results in Tables 3.1, 3.2, 3.5 and 3.6, finally we arrive at the composition of the fuel, as shown in Table 3.7. This is the fuel composition we used for CASMO-4 input file.

Table 3.7: The composition of the sample fuel

Isotop	Weight Percentage
U-234	0.00002%
U-235	0.00065%
U-236	0.00054%
U-238	0.09091%
Np-237	1.85929%
Pu-238	0.76964%
Pu-239	13.6211%
Pu-240	6.43373%
Pu-241	1.93908%
Pu-242	1.40909%
Am-241	1.30298%
Am-242m	0.00532%
Am-243	0.41212%
Cm-242	0%
Cm-243	0.00140%
Cm-244	0.13887%
Cm-245	0.01064%
Cm-246	0.00168%
Y	1.88161%
Zr	11.1013%
Mg	8.69434%
Al	19.3047%
O	31.0209%

3.1.4 Other parameters

The fuel density value is also requested by CASMO-4. Fuel density can be calculated by $\rho = \sum_i (\rho_i * VP_i)$, where ρ_i and VP_i stands for density and volume percentage of region i, respectively. So fuel density is:

$$\rho = 70\% * 3.7 + 15\% * 5.9 + 15\% * 10.7 = 5.08 \ (g/cm^3)$$

With the fuel composition and density results available, the next step is to choose the assembly geometry and operating conditions. Here a typical Westinghouse 4-loop PWR is chosen as the reference. The reference parameters are shown in Table 3.8.

Table 3.8: Reference fuel assembly geometry and operating conditions

Number of Fuel Locations per Assembly	264
Number of Guide Tube Locations	25
Fuel Assembly Pitch, cm	21.5
Fuel Assembly Gap, cm	0.08
Fuel pellet radius, cm	0.4095
Gap thickness, cm	0.0083
Cladding Outer Radius, cm	0.4750
Lattice Pitch, cm	1.26
Active Fuel Height, cm	366
Guide Tube Inner Radius, cm	0.5715
Guide Tube Outer Radius, cm	0.6120
Cladding Material	Zircaloy-4
Cladding Density, g/cm3	6.55
Fuel temperature, K	900
Coolant temperature, K	583
Core Average Power density, kW/l	104
System Pressure, bar	155
Power Plant Thermal Efficiency	0.3311

The CASMO-4 input file can be made from the above data of fuel composition, fuel density, assembly geometry and operating conditions. For each case, typically a first CASMO-4 run is used to determine the reactivity limited burnup. Denote it by BU_1. Then assuming a 3-batch fuel management scheme, the discharge burnup, denoted BU_3, is 1.5 times BU1. The second CASMO-4 run will then burn the fuel to burnup BU_3. The remaining work is to calculate the information we need from CASMO-4 output file.

3.1.5 Calculating plutonium, MA, and TRU burned fraction of initial loading and burning rate

The calculation processes for Pu, MA and TRU burned are essentially the same except for the fact in Pu case we only consider plutonium isotopes,

in MA case, we only consider minor actinide isotopes, and in TRU case we consider all trans-uranic isotopes. Thus burning abilities are calculated for plutonium only as an example in the remaining part of this section.

It is quite easy to calculate the burned fraction of initial loaded plutonium. CASMO-4 output already contains information about the fuel at different burnups such as isotope number densities, masses, et al. For our example fuel, the result is:

(Pu Residual)/(Pu Initial) = 37.7% (Weight percentage)

That is, from beginning of life (burnup = 0) to end of life (burnup = BU3), 63.4 w/o plutonium is burned. Here EOL corresponds to a burnup of 578.4 MWd/kg.

To calculate the burning rate, in unit of kg/(GWe-Year), we need to know how much energy has been produced. This can be calculated from burnup. In this example, the burnup is 578.4 MWd/kg. Here kg is kilogram initial heavy metal, and MWd is thermal energy. Assuming thermal efficiency of 0.33, and 365.25 day per year:

578.4 MWd thermal = 578.4 * 0.33 / (1000*365.25) GWe-Year
= 5.226E-4 (GWe-Year)

The weight percentage of plutonium in heavy metal can be obtained from CASMO-4 output file. The value is Pu/HM = 86.34%. We have already calculated that 63.4% of the initial plutonium is burned, thus 1 kg initial HM corresponds to burned plutonium of:

1 * 86.34% * 63.4% = 0.547 (kg Plutonium burned)

Therefore burning rate can be calculated from burnup 578.4 MWd-thermal/kg HM as:

1 kgHM/578.4 MWd-thermal = 0.547 Pu / 5.225E-4 GWe-Year
= 1046 kg/GWe-Year

The calculations for minor actinides and TRU burning rate are similar.

3.2 Calculation results for fuels with various matrices

The previous section has given detailed information about how to calculate plutonium, MA and TRU burning percentage and burning rate from preparing CASMO-4 input file to extracting and calculating information from CASMO-4 output file. That process is repeated for various inert matrix fuels and MOX fuel, with corresponding data for matrices composition, density, etc. The results are shown in following tables and figures.

Table 3.9: Pu, MA and TRU burned fractions and burning rates of various inert matrix fuels

	CERCER			CERMET		MOX
Matrix	Spinel	MgO	CeO_2	Zr	Fe	MOX
Pu Burned	62.3%	62.7%	62.0%	59.5%	52.7%	13.2%
MA Burned	42.6%	42.8%	42.7%	41.5%	37.9%	19.0%
TRU Burned	59.3%	59.9%	59.1%	56.8%	50.4%	14.0%
Pu burning rate (kg/GWe-Year)	1029	1029	1029	1027	1023	284.9
MA burning rate (kg/GWe-Year)	109	109	109	111	114	63.3
TRU burning rate (kg/GWe-Year)	1136	1136	1136	1135	1135	348.2
EFPD at EOL	2373	2387	2365	2273	2019	881

The EFPDs at which the burning fractions of initial loadings are calculated are also shown in Tables 3.9. As stated before, all the fuels are burned to the burnup of BU_3.

The fractional burnup of Pu, MA, and TRU are shown in Figure 3.2. It's clear that all inert matrices facilitate higher fractional burn than MOX.

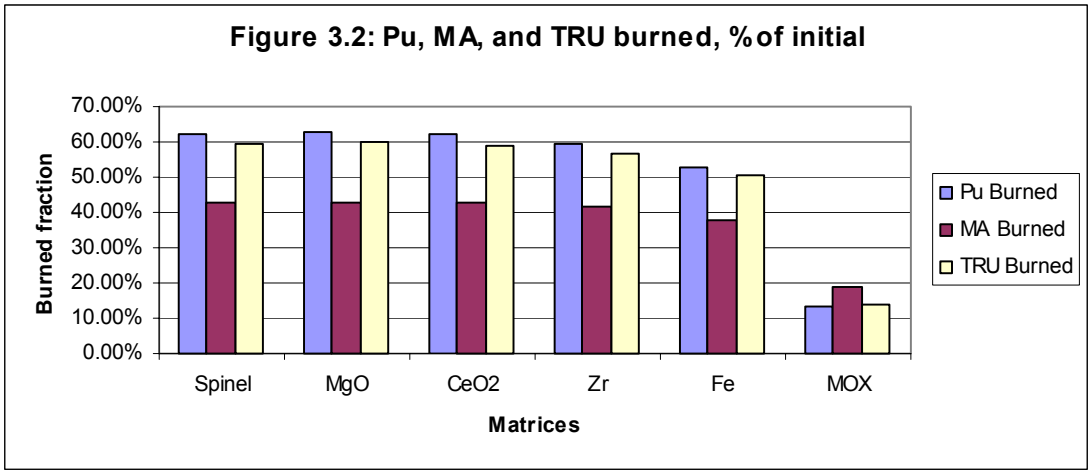

The burning rates of Pu, MA and TRU in terms of kg/(GWe-Year) are

shown in Figure 3.3.

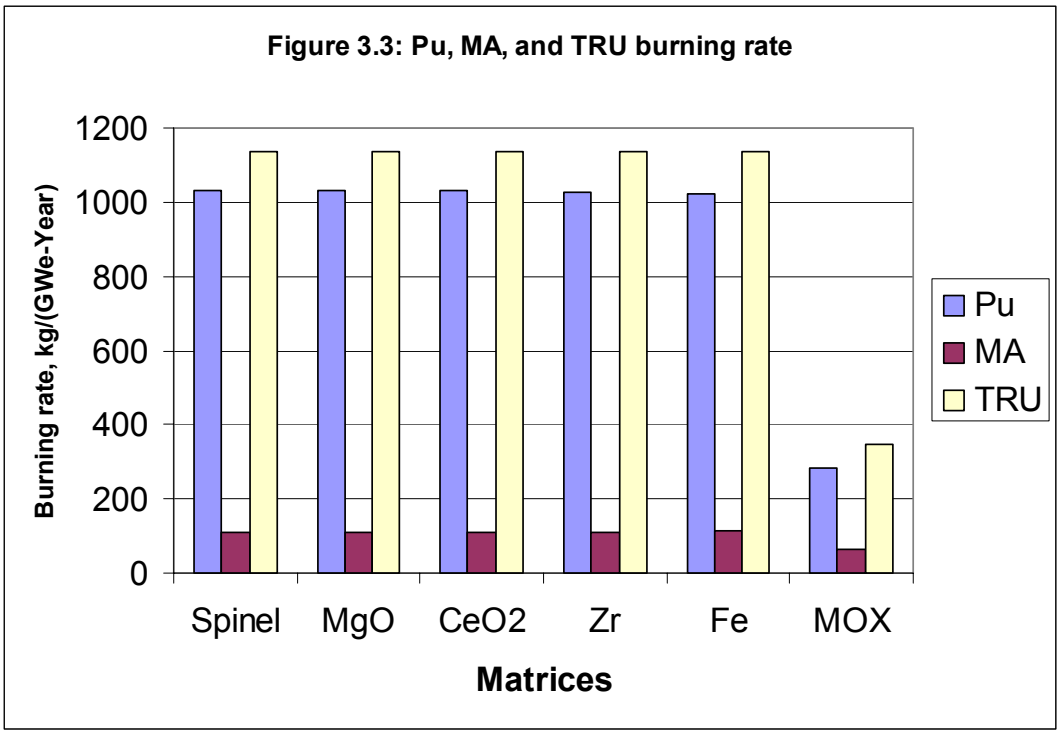

The MA burning rates are already compared in Figure 3.3. However, due to the scaling used, it's hard to detect the difference between different matrices there. So they are redrawn in Figure 3.4.

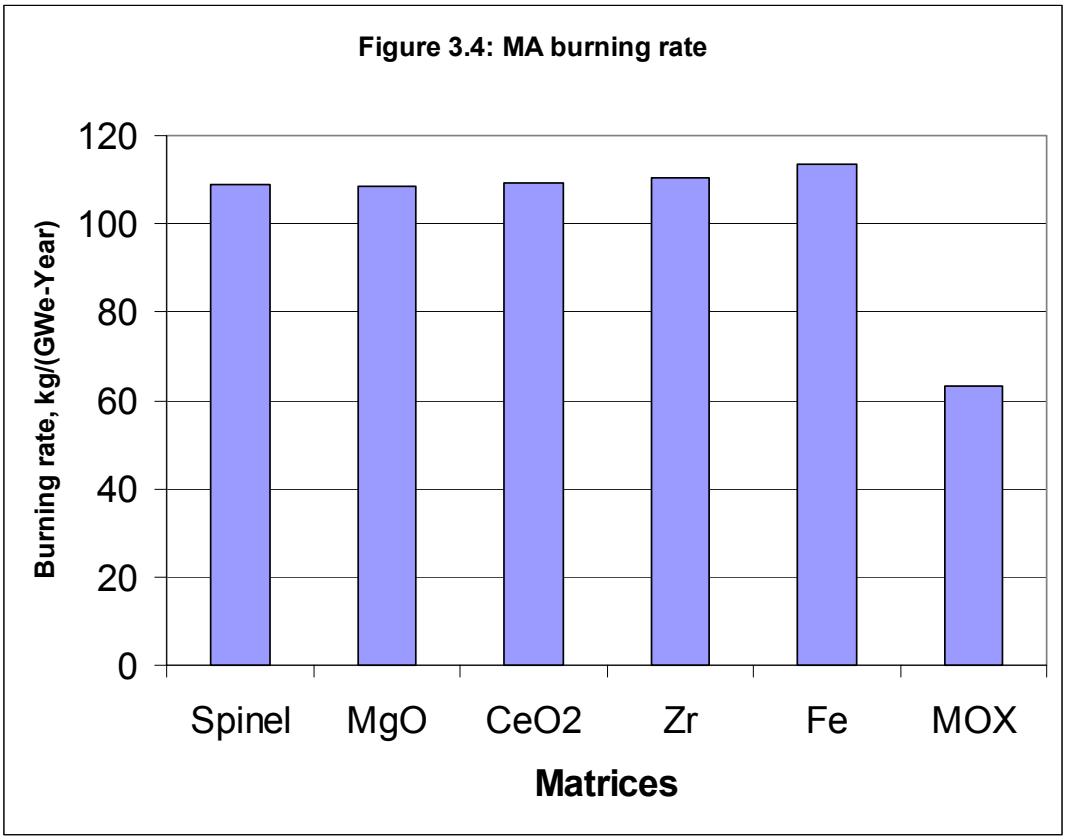

It could be seen from Table 3.9 and Figure 3.3 that the TRU burning rates in terms of kg/(GWe-Year) of various inert matrix fuels are essentially the same. This is expected because the uranium content in these fuels is negligible (Table 3.5) and thus nearly all energy produced comes from the burning of TRU. For MOX, with large amount of uranium present, a large fraction of energy comes from uranium thus the burning rate of TRU is much lower. This can be seen clearly from Figure 3.3. For the plutonium and minor actinides burning rates, the observations are similar: The burning rates are similar among different inert matrix fuels, and they are all superior to that of MOX fuel. From these observations it is confirmed that inert matrix fuels are much better than MOX as Pu, MA or TRU burning rate is concerned.

Comparing inert matrix fuels with each other, from the pure burning

ability point of view, that is, how much and how fast they allow burning plutonium and minor actinides, there is no good reason to favor one inert matrix over another. But if taking into account also the cycle length and achievable burnup, there will be differences among different matrices. The selection should also consider price, availability, experience, safety, and many other criteria discussed in Chapter 2.

3.3 Optimization of Actinide Burning

To achieve high burning ability, we can allow deviations from typical operating conditions, and seek new design that optimizes the burning of plutonium and minor actinides. Three options are investigated in this study. One is changing the hydrogen to heavy metal ratio (H/HM) thus changing the neutron spectrum. The other is changing the initial TRU loading, so 10% and 20% loadings are considered in addition to the 15% loading used previously. The third is increasing the core power density to 1.5 and 2 times the original value. This will require special fuel design such as the internally cooled annular fuel [Hejzlar, et al., 2001].

Because, as mentioned previously, using different matrices will not change plutonium, MA or TRU burning ability much, only one representative matrix, Spinel, is used here to investigate the influences on burning ability of various methods of optimization. The results are calculated for about 50 H/HM points ranging from 0.01 to several hundred. Some cases may not be realistic. For example, at H/HM ratio of 0.01, there is too little coolant (little H compare to HM) and the neutron spectrum is in the fast region, thus a lot of other material and control issues will arise. However, the calculation serves this study well for the sole purpose of investigating the neutronic behavior of the inert matrix fuel. The results are

shown in the Figures 3.5 to 3.10.

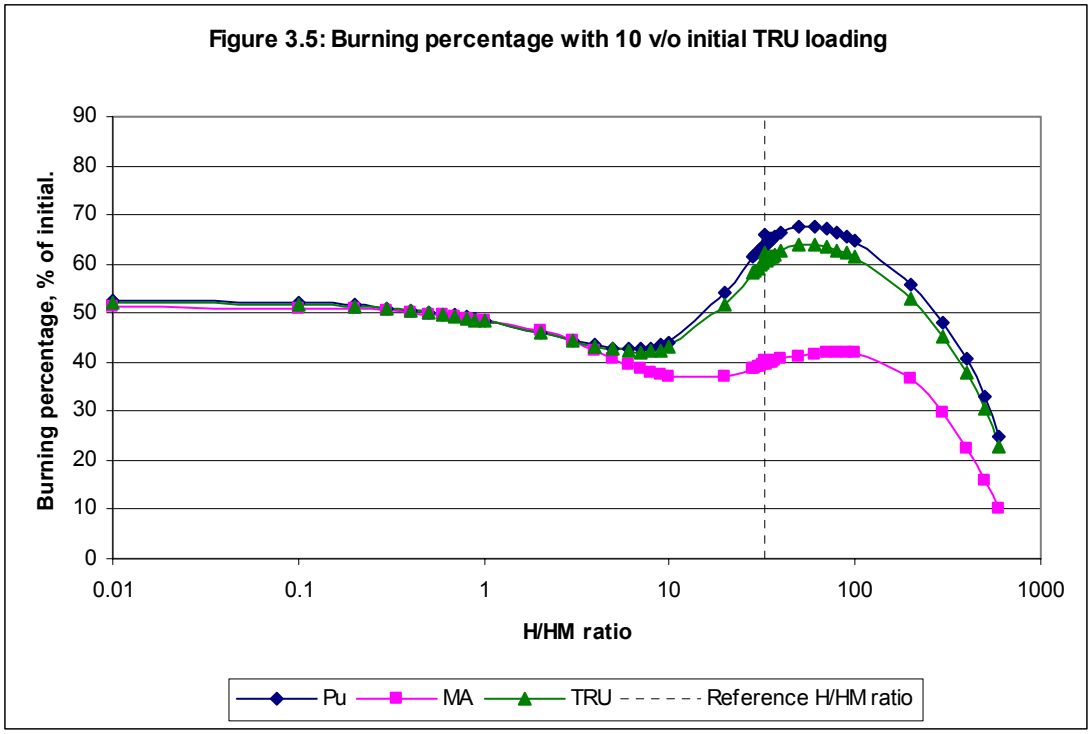

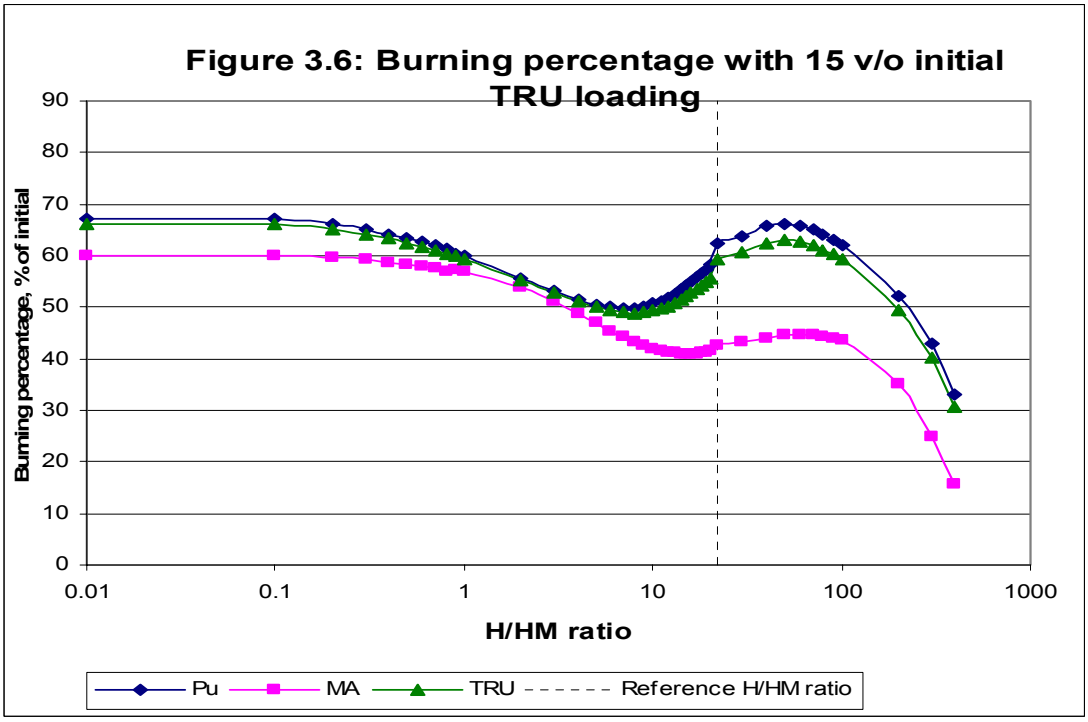

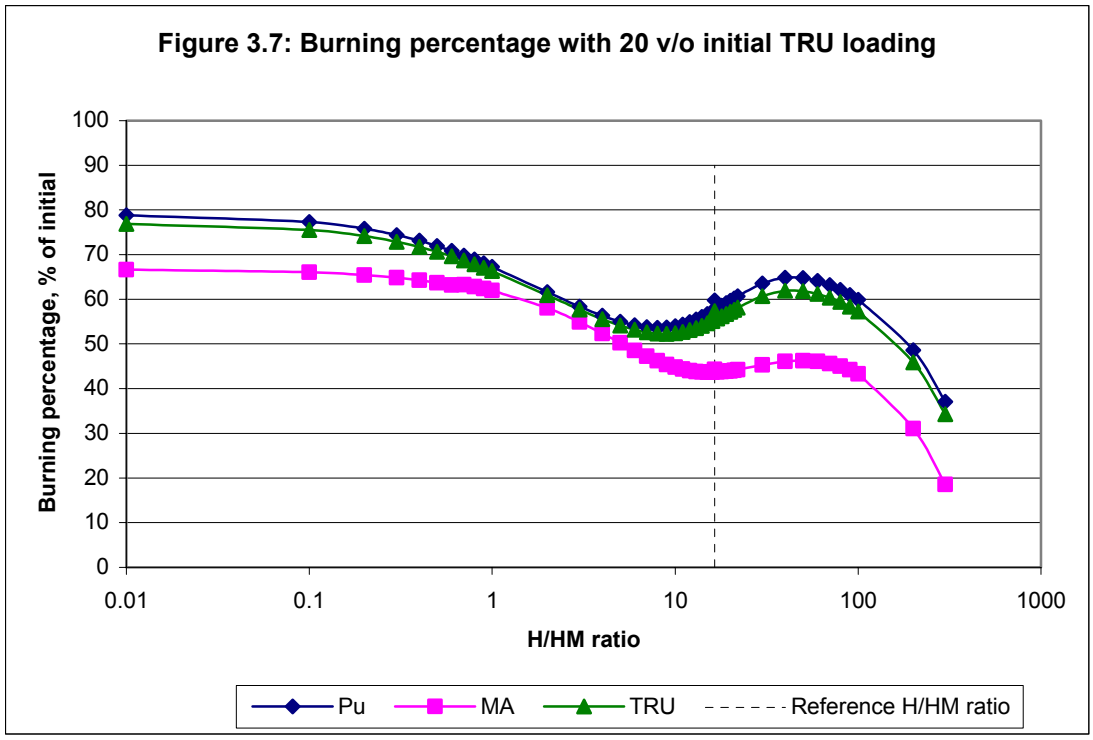
Figure 3.7: Burning percentage with 20 v/o initial TRU loading
Burning percentage, % of initial
100
90
80
70
60
50
40
30
20
10
0
0.01
0.1
1
10
100
1000
H/HM ratio
Pu
MA
TRU
Reference H/HM ratio

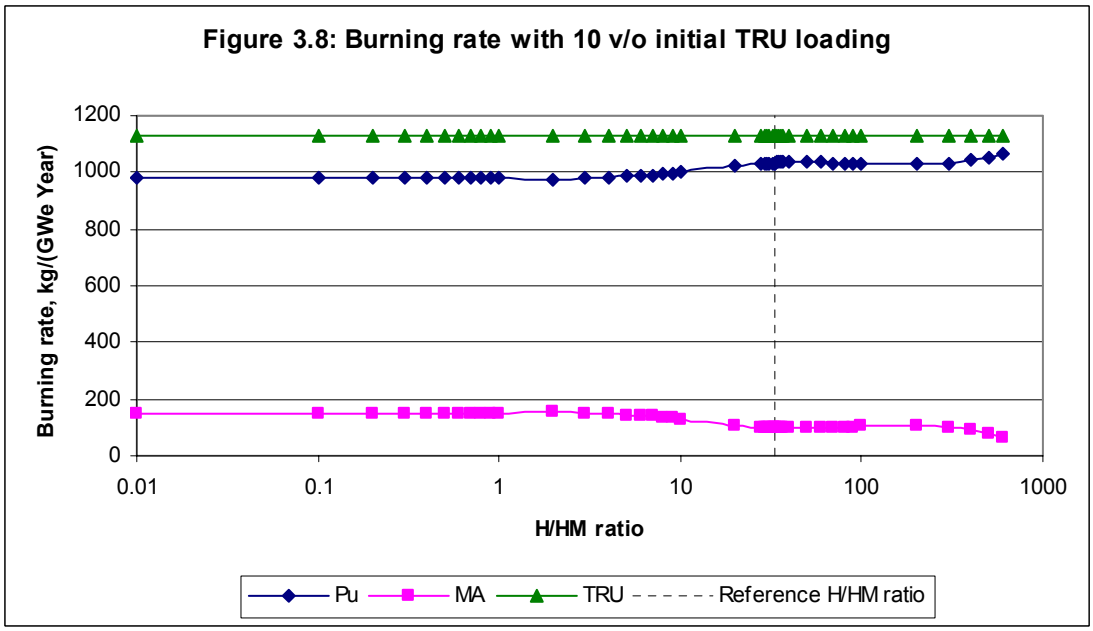
Figure 3.8: Burning rate with 10 v/o initial TRU loading
Burning rate, kg/(GWe Year)
1200
1000
800
600
400
200
0
0.01
0.1
1
10
100
1000
H/HM ratio
Pu
MA
TRU
Reference H/HM ratio

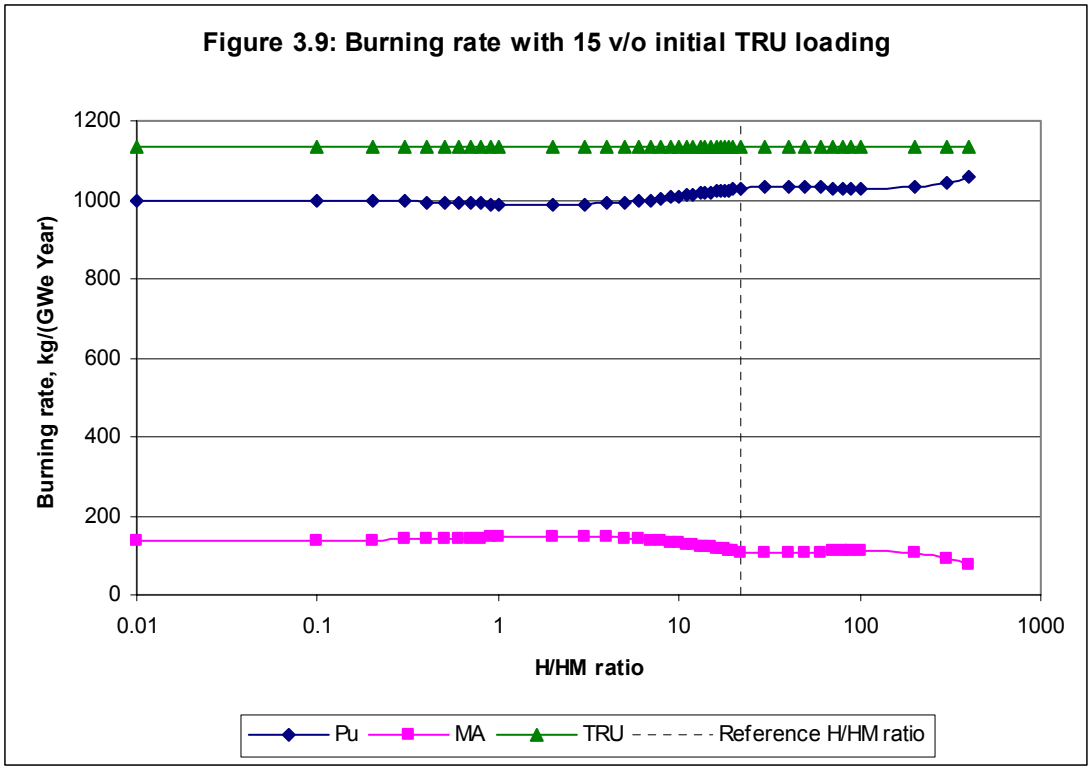

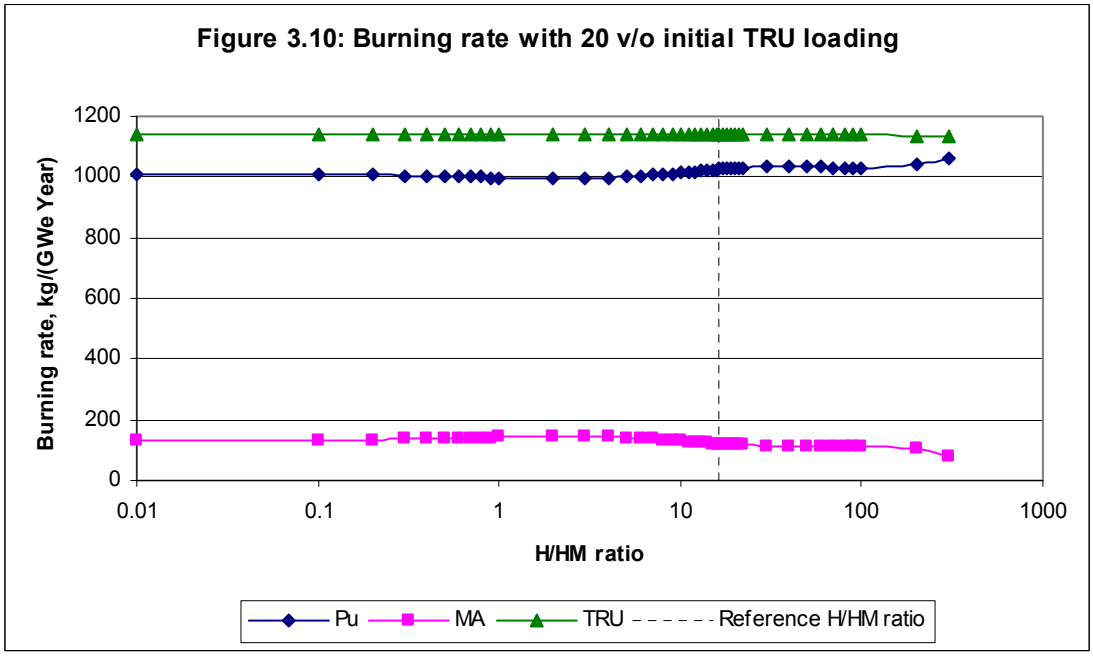

The EFPD at EOL, and k-inf at BOL are shown in Figures 3.11 to 3.12.

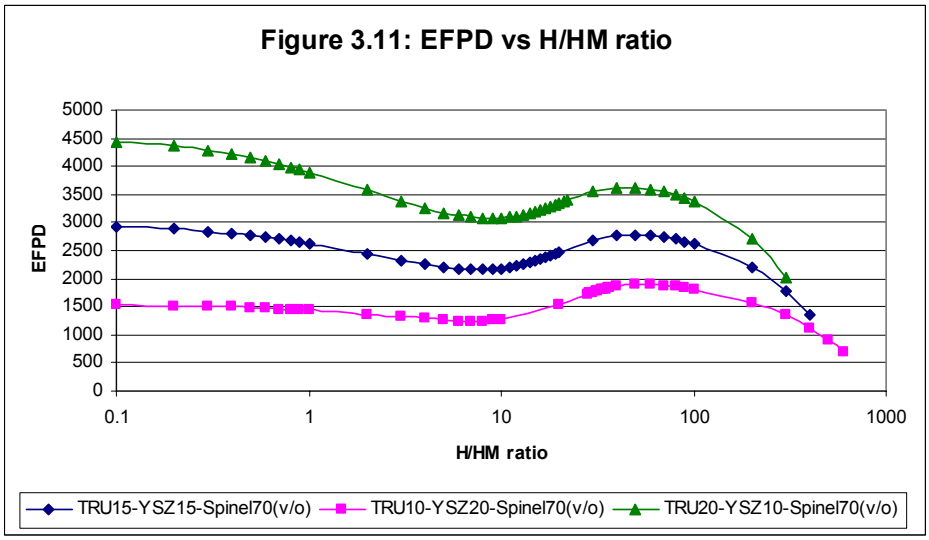

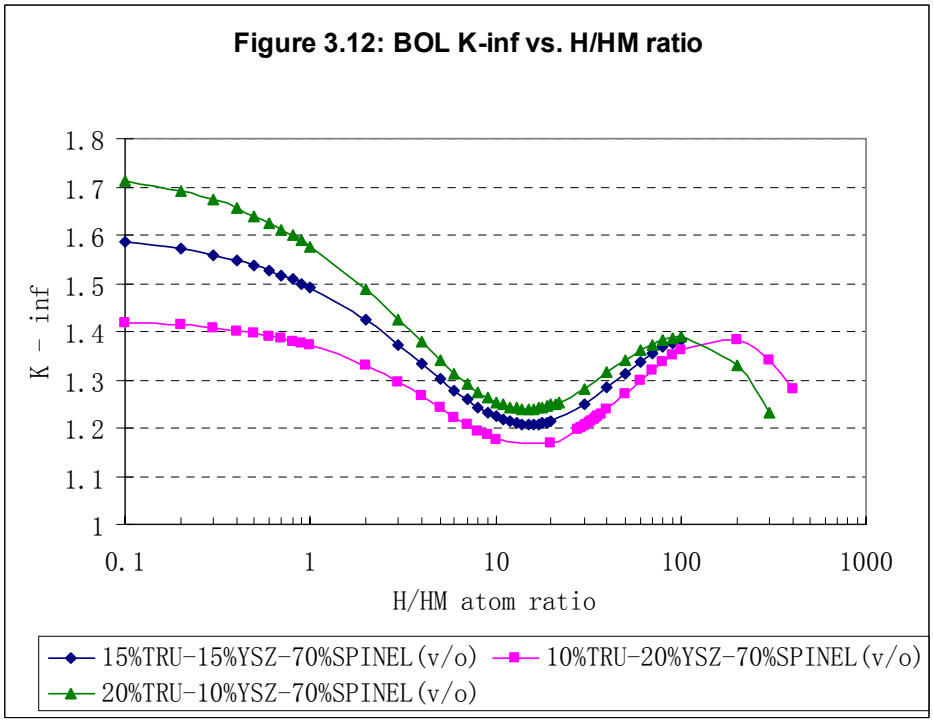

From Figures 3.5 and 3.6, it can be seen that the maximum burning percentages occur at H/HM ratios slightly larger than the reference H/HM ratio in both cases (10% and 15% initial TRU loading). It appears that when the initial loading increases, a lower H/HM ratio is favored with regard to burning percentages. This can be seen in Figure 3.7. With 20% initial loading, the maximum burning percentage occurs at the lowest H/HM ratio,

and 80% of the initial loaded plutonium can be burned. But from Figure 3.5, with 10 v/o initial TRU loading, the maximum burning percentage doesn't occur at the lowest H/HM ratio. The reason for this is probably the achievable cycle length. In Figure 3.11, we can see that for 20% initial loading, the maximum EOL EFPD occurs at the lowest H/HM ratio; with 10% initial loading, the maximum cycle length doesn't occur at the lowest H/HM ratio.

From Figures 3.8, 3.9 and 3.10, it is quite clear that the burning rate in terms of kg/(GWe-Year) is very stable with regard to H/HM ratio. This is expected because a certain amount of heavy metal needs to be burned in order to produce a certain amount of energy, no matter what the H/HM ratio is.

Figures 3.13 and 3.14 are drawn to compare the influence on burning ability of different initial loadings. Both figures are calculated using the reference H/HM ratio for the 10%, 15% and 20% initial loading cases. It can be seen from these two figures that the initial loading doesn't change burning percentage and burning rate much.

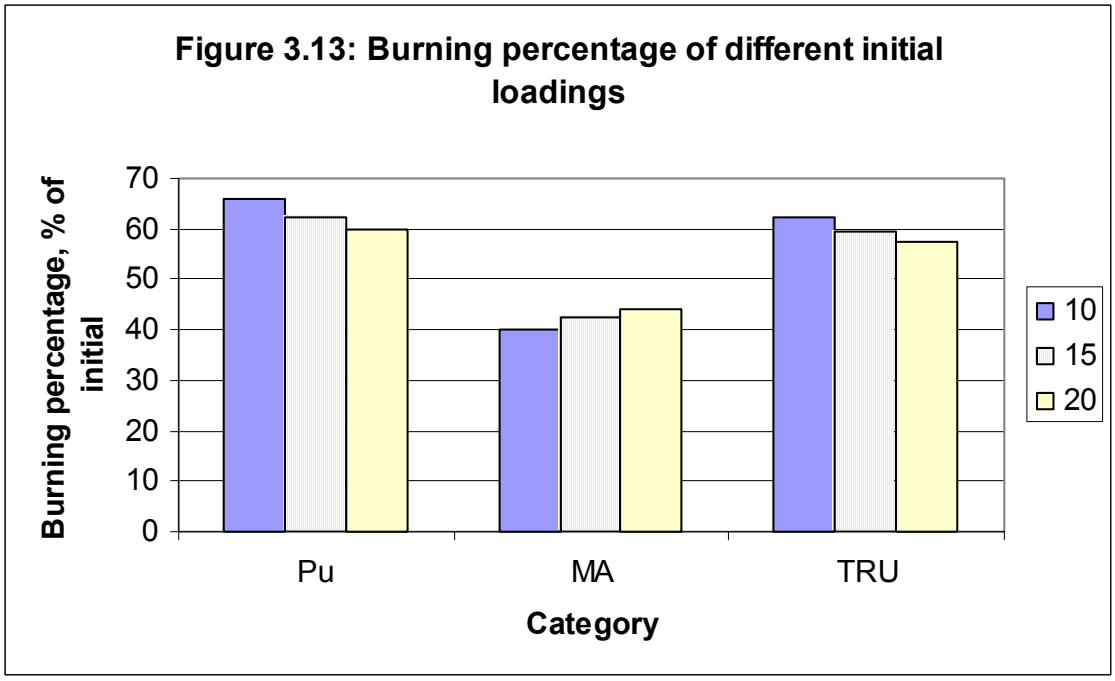

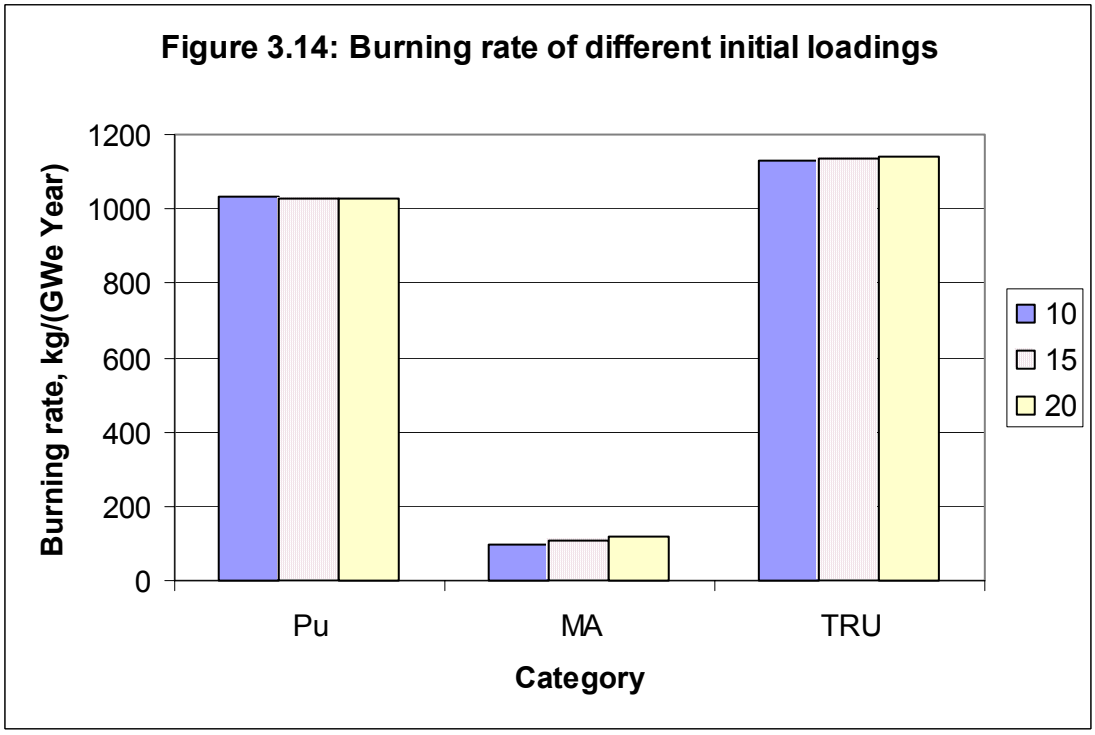

To sum up, from Figures 3.5 through 3.14, it can be concluded that large deviation from the reference design condition by changing the H/HM ratio or the initial TRU loading for the sake of improving the burning ability does not pay off in most cases. Only small improvements are achievable.

But an exception lies in the high initial TRU loading case, i.e., in the 20 volume percent initial TRU loading. In this situation, by moving from the reference H/HM ratio 16.44 to the extreme case H/HM ratio 0.01, the burned fraction of initially loaded Pu, MA and TRU can be improved from 59.8%, 44.3%, and 57.3%, to 78.8%, 66.7%, and 76.9% respectively. These are about 20% improvements for each category.

The effects of increasing power density on burning ability are shown in Figure 3.15 and Figure 3.16.

Figure 3.15: Influence of power density on the burning percentage

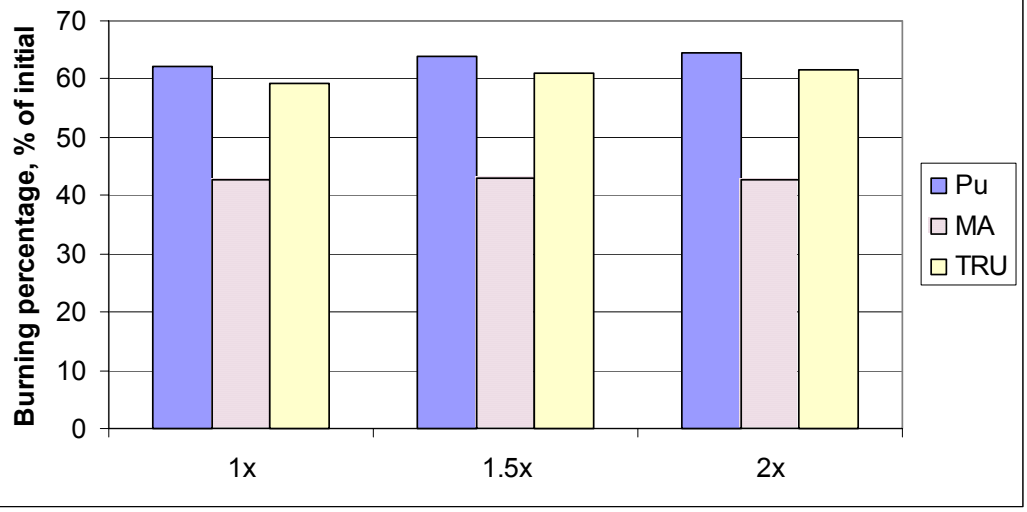

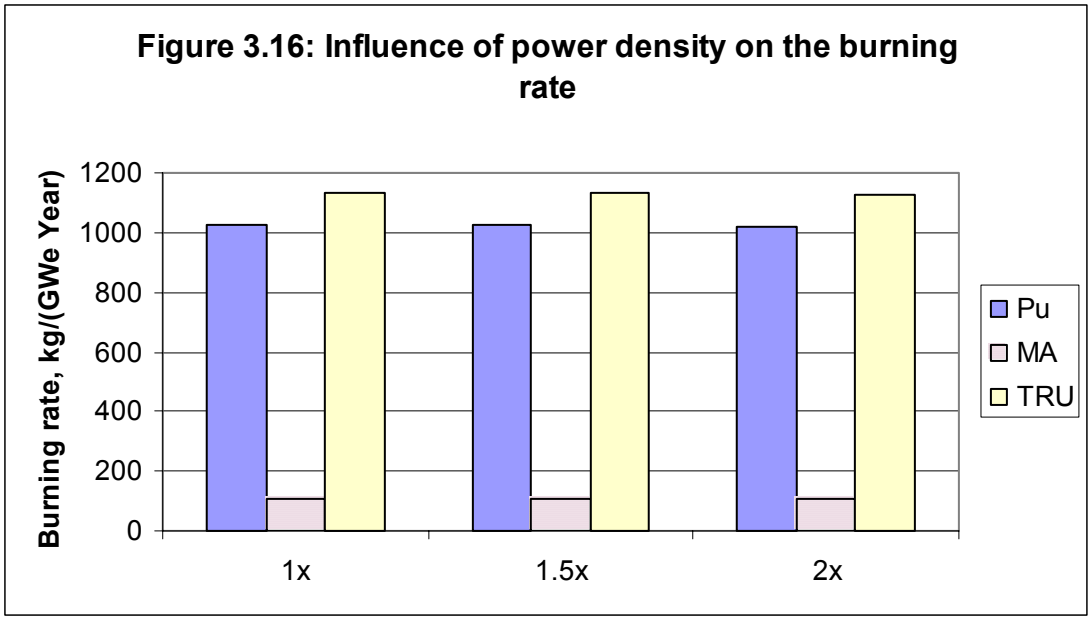

In Figure 3.15 and Figure 3.16, 1x is the case for the original power density; 1.5x and 2x are the cases for power densities of 1.5 times and 2 times the original, respectively.

From the figures, it can be seen that increasing the power density will result in a “tiny” increase of burning percentage and “tiny” decrease of the burning rate. However, the changes are negligible.

Chapter 4: Safety Related Coefficients and Their Improvements

Various safety coefficients such as the Doppler, moderator temperature and void coefficients are very important parameters of reactor design from control and safety points of view. In this chapter the safety coefficient values for the inert matrix fuels of our choice are calculated and compared to those of MOX and traditional UO_2 fuels. The safety coefficients of inert matrix fuels will be degraded due to the absence of the fertile isotope U-238. Some methods for improving the safety coefficients are discussed at the end of this chapter. The improvement is achieved by introducing some fertile material into the system: either adding the material directly into the fuel, or adopting a heterogeneous core with some fertile free fuel rods replaced by UO_2 fuel. As a consequence of adding the fertile materials, the plutonium and MA burning ability will be reduced.

4.1 Methodology

CASMO-4 is used as the calculation tool, as in Chapter 3. The reference operating parameters are in Table 3.8: Fuel temperature 900K, Moderator temperature 583K. Fuel composition is given in Table 3.7. The void fraction is assumed to be 0 at normal operating conditions. The fuel temperature, moderator temperature and void fraction are then changed; their influence on neutron multiplication factor and the corresponding safety coefficients are calculated.

The safety coefficients are calculated at the beginning of life (BOL) as well as at the end of life (EOL). EOL correspondes to burnup BU_3, which

is 1.5 times the single batch reactivity limited burnup BU_1, assuming a 3 batch fuel management scheme. Because soluble boron concentration has a substantial influence on the moderator coefficient and void coefficient, different concentration values are used for calculating the safety coefficients at BOL: 0 ppm, 500 ppm, 1000 ppm and 1500 ppm. At EOL, only the 0 ppm case is considered by assuming no soluble boron left in the moderator at that time.

Doppler coefficient

At reference conditions, the fuel temperature T_1 is 900K, and the neutron multiplication factor K_1 is calculated using CASMO-4. Then the fuel temperature is changed to T_2 = 600K, and the neutron multiplication factor K_2 is recalculated using CASMO-4. The Doppler coefficient (DC) is calculated by:

$$DC = \frac{\Delta\rho}{\Delta T} = \frac{\rho_2 - \rho_1}{T_2 - T_1} = \frac{\frac{K_2 - 1}{K_2} - \frac{K_1 - 1}{K_1}}{T_2 - T_1} = \frac{K_2 - K_1}{K_1 K_2 (T_2 - T_1)} \quad (4.1)$$

Where ρ is reactivity which is by definition equal to (K-1)/K.

An alternative definition of DC is:

$$DC = \frac{\Delta K}{\Delta T} = \frac{K_2 - K_1}{T_2 - T_1} \quad (4.2)$$

Compared to Equation (4.1), the difference is a factor: $1/(K_1K_2)$. At normal operating conditions, the reactor is critical, so K_1 is equal to one.

After changing the fuel temperature for the purpose of calculating the Doppler coefficient, the new neutron multiplication factor K_2 will not be 1 but should be close to that, if the fuel temperature is not changed a lot. So DC values calculated by Equations (4.1) and (4.2) will be close.

Here, the K_{inf} values are used for calculating DC because K_{eff} is not given directly by CASMO-4 for the case of a single pin. However, using K_{inf} will not get a much different DC value compared to using K_{eff} if assuming similar neutron leakage before and after changing the fuel temperature. The difference of K_{eff} and K_{inf} is cancelled out in the numerator (K_2-K_1). The K_{inf} value is also used in calculating the moderator temperature coefficient, void coefficient and boron worth. However, using K_{inf} value is not appropriate in evaluating the void coefficient if we change the void fraction from 0 to a large number, say, 80%, because neutron leakage is surely much larger at such high void fraction. In this situation we should calculate K_{eff} by amending the K_{inf} value calculated by CASMO-4, or using another code such as MCNP-4C or SIMULATE to get the K_{eff} value. The detailed discussion of this issue is given in Section 4.2.

The definition of Equation (4.1) is used in this study to calculate the Doppler coefficient. The moderator temperature coefficient and void coefficient are calculated using the same definition: using $\Delta\rho$ instead of ΔK in the numerator.

Moderator temperature coefficient

The moderator temperature coefficient (MTC) is calculated from:

$$MTC = \frac{\Delta\rho}{\Delta T} = \frac{(K_2 - K_1)}{K_1 K_2 (T_2 - T_1)} \qquad (4.3)$$

Where T_1 is the reference moderator temperature 583K and T_2 is 568K. K_1 and K_2 are the K_{inf} values at the corresponding moderator temperatures.

Void coefficient

The void coefficient (VC) is calculated by observing the difference in K when changing the void fraction (VF). At the reference condition, $VF_1 = 0$, and $K_{inf} = K_1$. Changing the void fraction to $VF_2 = 5$ (5% void), and calculated K_{inf} value is termed K_2. The void coefficient can then be calculated by:

$$VC = \frac{\Delta\rho}{\Delta VF} = \frac{K_2 - K_1}{K_1 K_2 (VF_2 - VF_1)} \qquad (4.4)$$

There is one interesting issue in choosing the VF_2 value. When calculating the void coefficient, we are interested in the void fraction influence on K in the neighborhood of the reference void fraction value. 5 percent is chosen in this study. However, in some severe accident situations such as a loss of coolant accident (LOCA), the void coefficient calculated by using 5% is not representative because the void fraction could be possibly increased to a very high value. The results in the next section will show that using Equation (4.4) to calculate the void coefficient from the K_{inf} values, there are large differences between choosing a small VF_2 such as 5 percent and choosing a large VF_2 such as 90 percent. The VC can even change sign in some cases: from negative for $VF_2 = 5\%$ to positive for VF_2

= 90%. This means that one cannot determine if the reactor is safe by considering only the void coefficient result for small VF_2. However, the case of a high VF_2 may be exaggerated because, as discussed before, at this high void fraction we can not use K_{inf} values in Equation (4.4) for K_1 and K_2. The larger VF_2 will result in larger leakage and thus lower K_{eff} value K_2. This in turn will reduce the value of VC and turn it toward the safer side.

Boron worth

Boron worth (BW) is calculated by increasing boron concentration (BC) by 100 ppm. At BOL, the reference boron concentrations are 0, 500, 1000, and 1500 ppm, so the boron concentrations are increased to 100, 600, 1100, and 1600 ppm respectively to calculate the boron worth.

$$BW = \frac{\Delta\rho}{\Delta BC} = \frac{K_2 - K_1}{K_1 K_2 (BC_2 - BC_1)} \qquad (4.5)$$

Effective delayed neutron fraction

The effective delayed neutron fraction (β_{eff}) is calculated by CASMO-4 directly, and will be given in the tabulated results.

4.2 Calculation results

The results for DC, MTC, VC, BW and β_{eff} are shown in Tables 4.1, 4.2, 4.3, 4.4 and 4.5, respectively. All results are calculated for inert matrix fuels using a 15 volume percent initial TRU loading.

Table 4.1: Doppler coefficient (10^{-5}/K)

		BOL				EOL
	BOR(ppm)	0	500	1000	1500	0
CERCER	Spinel	-0.73	-0.72	-0.70	-0.69	-1.01
	MgO	-0.74	-0.73	-0.71	-0.70	-1.02
	CeO_2	-0.70	-0.69	-0.68	-0.66	-1.02
CERMET	Zr	-0.69	-0.68	-0.67	-0.65	-1.06
	Fe	-0.73	-0.71	-0.70	-0.68	-0.98
MOX		-2.90	-2.91	-2.93	-2.94	-3.06
UO_2		-2.00	-2.11	-2.22	-2.32	-3.34

From Table 4.1 it is seen that all the inert matrix fuels have similar Doppler coefficient values. The difference between the maximum and minimum is less than 10%. For example, at the beginning of life BOR=0 ppm column, the MgO matrix fuel has the most negative DC value of -0.74 pcm among inert matrix fuels, and the Zr matrix fuel has the minimum -0.69 pcm. The difference is (0.74-0.69)/0.74 = 7%.

It can also easily be seen from Table 4.1 that the Doppler coefficients of inert matrix fuels are much worse than either that of the MOX or that of the UO_2 fuels. The situation is generally much worse at the BOL condition than at the EOL condition.

Table 4.2: Moderator temperature coefficient (10^{-5}/K)

		BOL				EOL
	BOR(ppm)	0	500	1000	1500	0
CERCER	Spinel	-19.90	-15.99	-12.14	-8.44	-49.97
	MgO	-19.96	-16.05	-12.17	-8.43	-50.61
	CeO_2	-18.66	-14.77	-10.92	-7.20	-48.64
CERMET	Zr	-21.64	-17.71	-13.90	-10.15	-52.11
	Fe	-19.39	-15.40	-11.54	-7.75	-42.81
MOX		-55.91	-50.18	-44.58	-39.04	-58.72
UO_2		-25.14	-15.34	-5.75	3.79	-49.57

From Table 4.2 it can be concluded that the moderator temperature coefficients of various inert matrix fuels are very close, and they are comparable to MOX and UO_2 fuels. MOX has the most negative MTC values at various boron concentration levels at the beginning of life. At the end of life, there is little difference among the MTC values of inert matrix, MOX, and UO_2 fuels.

A change in moderator density will change the neutron leakage and in an under-moderated core it will also have a major impact on neutron thermalization. Thus, this change will result in a corresponding K_{eff} change. Increasing the void fraction will decrease the moderator density, and increasing the moderator temperature will also decrease its density. This similarity determines the parallel structure of MTC and VC values in Table 4.2 and Table 4.3. As can be seen, the larger the MTC, the larger the corresponding VC. The relative magnitudes among the different fuels are also unchanged.

Table 4.3: Void coefficient (10^{-5}/% void)

		BOL				EOL
	BOR(ppm)	0	500	1000	1500	0
CERCER	Spinel	-52.34	-42.02	-31.90	-21.89	-188.0
	MgO	-52.40	-42.10	-32.00	-22.00	-189.9
	CeO_2	-48.73	-38.37	-28.21	-18.17	-184.0
CERMET	Zr	-57.66	-47.18	-36.90	-26.86	-190.0
	Fe	-52.09	-41.66	-31.17	-21.10	-154.1
MOX		-164.9	-150.0	-135.6	-121.5	-184.8
UO_2		-79.25	-51.78	-24.70	1.74	-202.9

Table 4.4: Boron worth (10^{-5}/ppm)

		BOL				EOL
	BOR(ppm)	0	500	1000	1500	0
CERCER	Spinel	-1.80	-1.77	-1.75	-1.73	-6.38
	MgO	-1.80	-1.77	-1.75	-1.73	-6.51
	CeO_2	-1.78	-1.76	-1.74	-1.71	-6.27
CERMET	Zr	-1.81	-1.79	-1.77	-1.74	-5.81
	Fe	-1.82	-1.79	-1.77	-1.75	-4.49
MOX		-3.00	-2.95	-2.91	-2.88	-3.49
UO_2		-6.74	-6.65	-6.60	-6.47	-10.89

Table 4.5: Effective delayed neutron fraction (10^{-3})

		BOL				EOL
	BOR(ppm)	0	500	1000	1500	0
CERCER	Spinel	2.660	2.659	2.658	2.656	3.867
	MgO	2.660	2.659	2.657	2.656	3.875
	CeO_2	2.653	2.652	2.650	2.649	3.850
CERMET	Zr	2.656	2.654	2.653	2.651	3.820
	Fe	2.656	2.655	2.674	2.652	3.684
MOX		3.696	3.699	3.701	3.704	3.994
UO_2		7.199	7.190	7.181	7.172	4.524

The boron worth values are shown in Table 4.4. It can be seen that various inert matrix fuels have similar boron worth at both BOL and EOL, and at various boron concentration conditions of BOL. They are all negative but the absolute values are smaller than those of UO_2 fuel for all considered cases. The boron worth of MOX fuel is between those of inert matrix fuels and UO_2 fuel at BOL, but is least negative at EOL.

From Table 4.5, it can be seen that both the inert matrix fuels and the MOX fuel have a much smaller effective delayed neutron fraction than UO_2. Also the delayed neutron fraction of inert matrix fuels is smaller than that of MOX. This may raise some concerns for reactor control. Also, it can be seen that UO_2 fuel has a smaller β_{eff} at EOL than at BOL, whereas inert matrix fuel has a larger one at EOL. These observations are actually not surprising given the delayed neutron yields data in Table 4.6. In Table 4.6, it can be seen that plutonium, especially Pu-239, has a small delayed neutron yield. Thus inert matrix fuels have small β_{eff} values at BOL because in these fuels the fissile isotopes are mainly plutonium (Table 3.3, 86 w/o plutonium, 49 w/o Pu-239). As burnup increases, the Pu fraction decreases, and β_{eff}

increases. However, in the case of UO_2 fuel, plutonium actually builds up as burnup increases, thus β_{eff} value decreases toward EOL.

Table 4.6: Total delayed neutron yields (number of delayed neutrons / 100 fission events) for thermal neutron induced fission of different isotopes.

Isotope	Delayed neutron / 100 fissions
U-235	1.621
U-238*	4.39
Pu-239	0.628
Pu-240*	0.95
Pu-241	1.52

*For fast neutron induced fission.

Now we'll address the issue of choosing VF_2 for calculating the void coefficient. As discussed in Section 4.1, to calculate the void coefficient value, a VF_2 value is chosen first. We used 5% for Table 4.3. However, choosing a different VF_2 may result in very different void coefficient values. Strictly speaking, the parameter which will be calculated here should not be called "void coefficient", because by definition the coefficient is the differential coefficient of the K_{eff} vs. void fraction curve at the state point for which we are trying to calculate the coefficient value, i.e., $\frac{dK_{eff}}{dVF}$. 5% is close to the reference void fraction 0%, so it can approximate the differential increase, but >50% void fraction can not. The value calculated this way should be termed coolant void reactivity worth or some other names, but for convenience, we'll still use "void coefficient".

The results are calculated by changing the void fraction from 0 to 5%, 0 to 10%, ... , 0 to 95%. Because as shown in Table 4.3, the void coefficient

values are close for inert matrix fuels using different matrices (However, this conclusion may not be universal, [Baldi & Porta, 2001] got quite different void effects for different metal matrices, but they are using PuO_2 instead of the TRU composition shown in Table 3.4), we'll just use the Spinel matrix fuel as a representative. Results are calculated for BOL with boron concentrations of 0, 500, 1000, and 1500 ppm, and for EOL with 0 boron concentration. MOX and UO_2 cases are also calculated for comparison. The results are shown in Figures 4.1 through 4.5.

Figure 4.1: The void coefficient for various void fraction jumps (BOL, BOR=0)

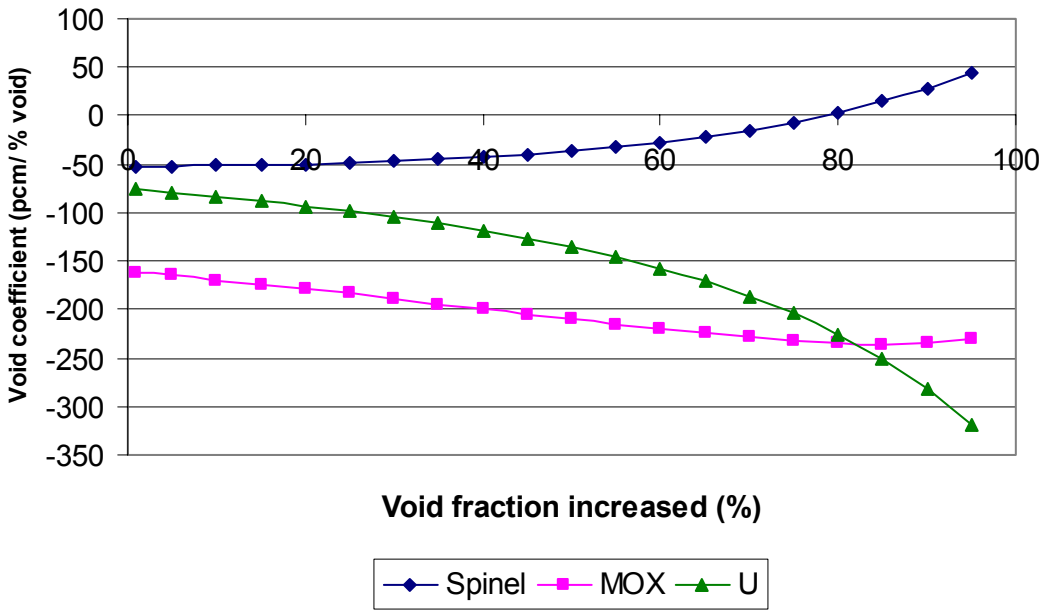

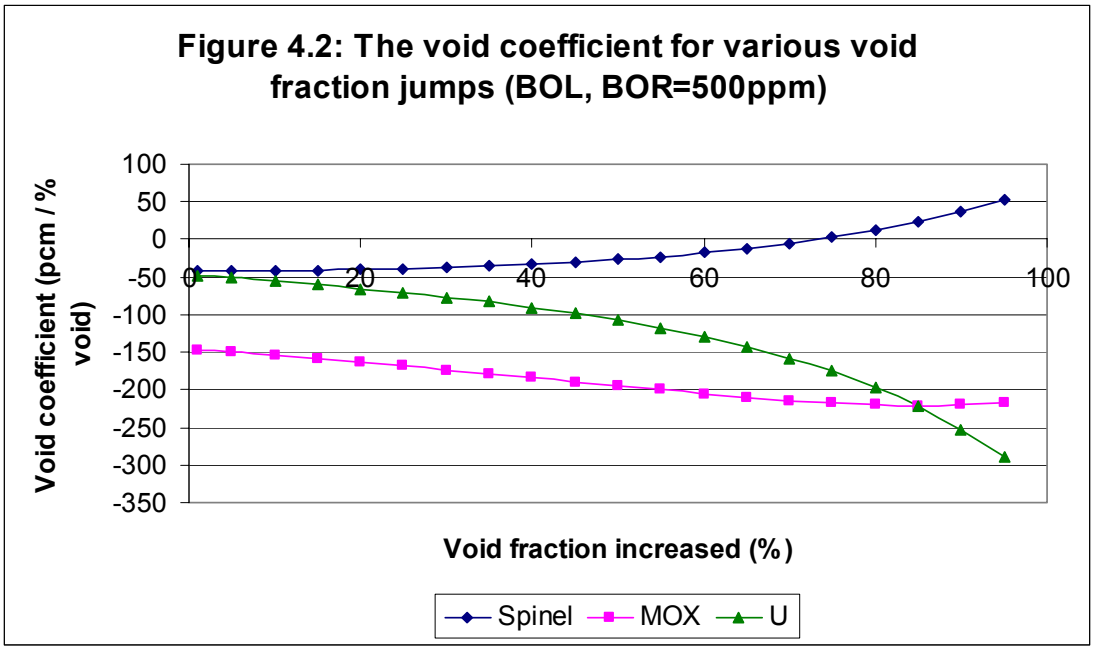
Figure 4.2: The void coefficient for various void fraction jumps (BOL, BOR=500ppm)
Void coefficient (pcm / % void)
100
50
0
-50
-100
-150
-200
-250
-300
-350
0
20
40
60
80
100
Void fraction increased (%)
Spinel
MOX
U

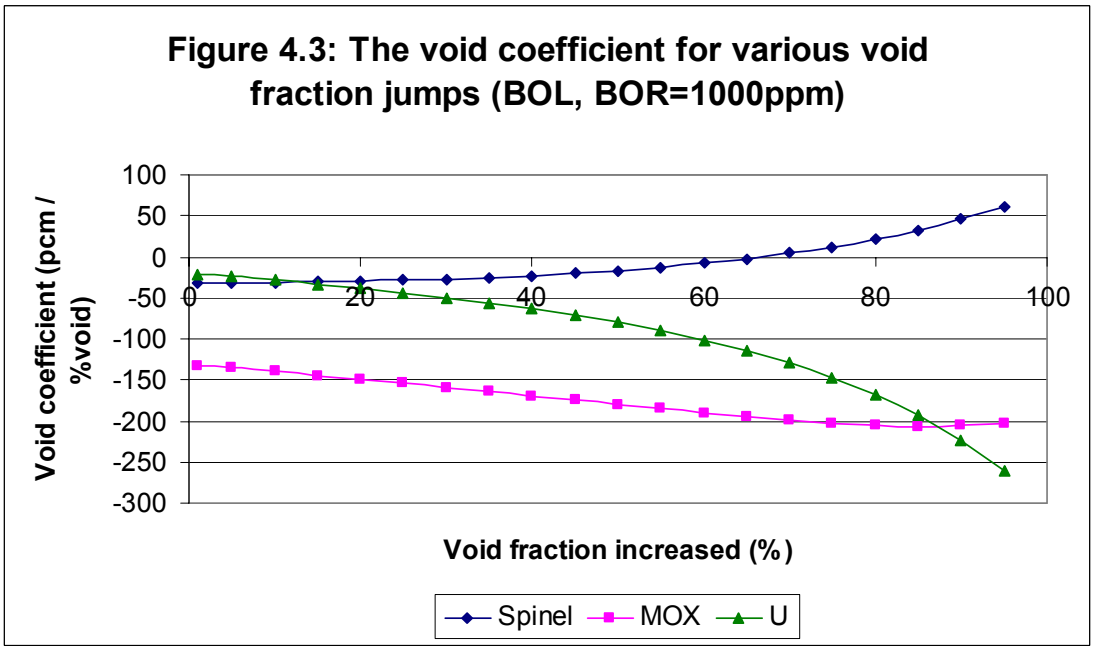
Figure 4.3: The void coefficient for various void fraction jumps (BOL, BOR=1000ppm)
Void coefficient (pcm / %void)
100
50
0
-50
-100
-150
-200
-250
-300
0
20
40
60
80
100
Void fraction increased (%)
Spinel
MOX
U

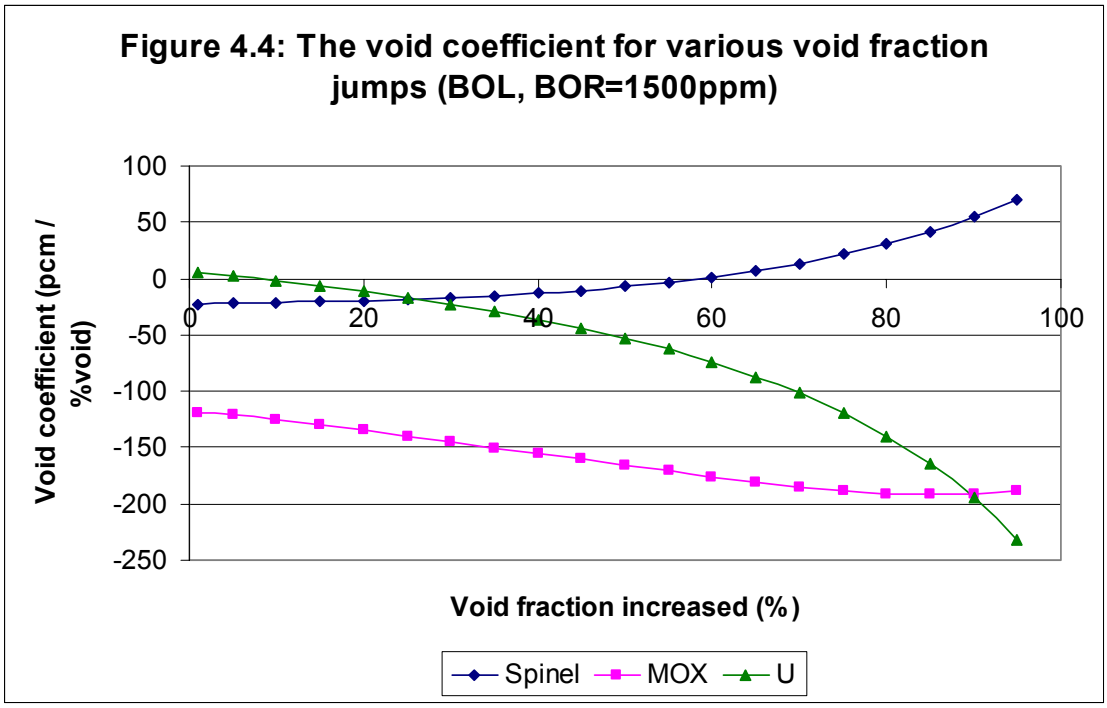

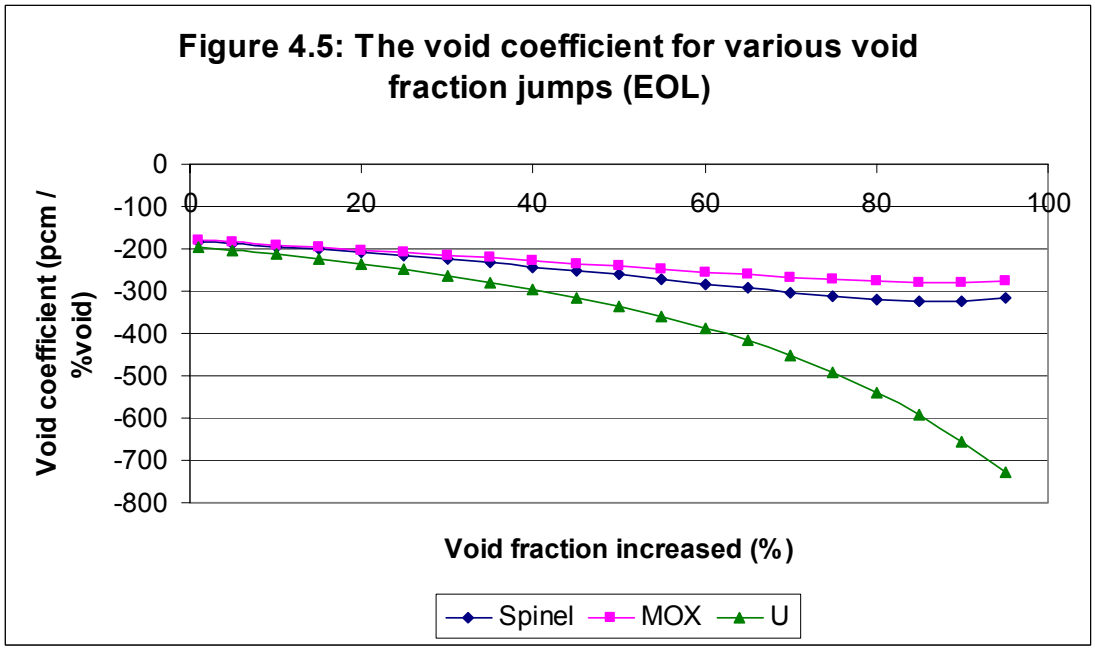

According to the results from Figures 4.1 to 4.5, the inert matrix fuel with 15% TRU loading yields reactivity increase at the beginning of life if a LOCA occurs since at all the different boron concentration cases, the void coefficient is positive when increasing the void fraction from 0 to a very high value. The most unsafe situation is with the highest boron

concentration (1500 ppm). In this case, changing the void fraction from 0 to 60 percent, the change in K_{inf} value turns positive thus the void coefficient would be calculated as positive.

However, using K_{inf}, neutron leakage is not considered, which gives conservatively high values of coolant void worth. At a high void fraction, leakage will be high and brings down the multiplication factor K, which in turn will cause a decrease in the void coefficient value. But will the void coefficient be just less positive after considering neutron leakage, or be in the much safer negative zone?

Although CASMO-4 doesn't calculate K_{eff} values directly if buckling is not specified, it does provide K_{inf} and migration area M^2 values. From these values and assuming certain leakage patterns, we can estimate K_{eff} and amend the void coefficient values. We can also specify an appropriate buckling value and direct CASMO-4 to calculate K_{eff}.

The leakage effect is considered using the following equation:

$$\rho_{eff} = \rho_{\inf} - \rho_L \qquad (4.6)$$

where ρ_{eff}, ρ_{inf} and ρ_L are effective, infinity and leakage reactivity, respectively. ρ is related to K as $\rho = (K-1)/K$. To apply Equation (4.6) to calculate ρ_{ef}, the ρ_L value must be known.

Depending on the power distribution, ρ_L has different relationships with the migration length M. If assuming a cosine power shape, ρ_L is proportional to M^2:

$$\rho_L \propto M^2 = CM^2 \qquad (4.7)$$

where C is a constant.

However, if assuming a flat power shape, ρ_L depends linearly on M, that is:

$$\rho_L \propto M = cM \qquad (4.8)$$

where c is also a constant. The C value in Equation (4.7) and the c value in Equation (4.8) are generally not the same.

Assuming a small leakage $\rho_L \approx 0.03$ at the reference operating condition, i.e., at a void fraction of 0, using the M value from CASMO-4, we can calculate the value of C in Equation (4.7) and c in Equation (4.8). After that, with different values of M at different void fractions, we can calculate ρ_L easily. Thus K_{eff} can be calculated for different void fractions. Using this K_{eff} value to calculate the void coefficient should be more accurate than using K_{inf}.

Because the power shape is unknown, both Equation (4.7) and Equation (4.8) are used in the estimation that follows. It is probably a good guess that the reality should stay somewhere in between the two results. (But as will be shown later, the reality is more close to the case assuming ρ_L is proportional to M.) This amendment is applied to boron concentration of 1500 ppm at BOL because it is the worst case. Again, the Spinel matrix fuel is used as a representative.

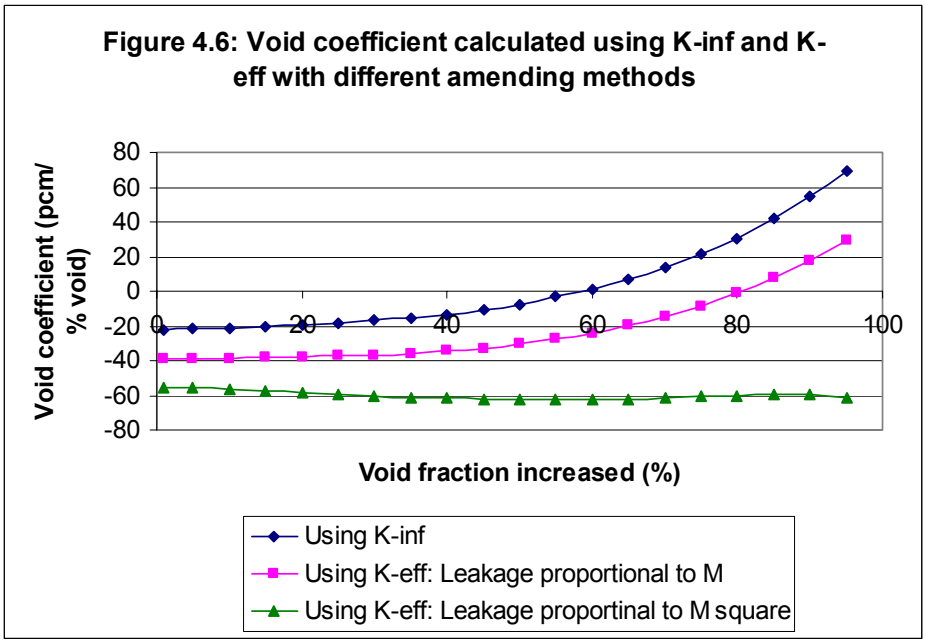

From Figure 4.6, the void coefficient will still be positive when increasing the void fraction from 0 to more than 80% when assuming that ρ_L is proportional to M. However, when assuming ρ_L is proportional to M^2, the curve is almost flat and always negative. Even if the reality lies in between these two curves, it is still possible that the void coefficient will become positive near the 100% void fraction, depending on whether the reality is closer to M or M^2 case. Under LOCA accident conditions when core water inventory decreases substantially, this would be a safety concern.

This situation deserves a closer look. Detailed investigation of the void coefficient should be calculated by using other methods such as the use of the Monte Carlo based MCNP or using some other code which can represent the leakage more accurately. A MCNP-4C whole core model has been developed for this purpose. This original model, assuming traditional UO_2 fuel, was developed by Dr. Zhiwen Xu and was given in a course lecture at MIT. Some modifications have been made to adapt it to the inert matrix fuel. The model is also used to calculate void coefficient of

traditional UO_2 fuel, for the sake of checking the correctness and consistency of the results.

The results are shown in Figures 4.7 through 4.14. Results for boron concentration of 0, 500, 1000, and 1500 ppm are calculated for both UO_2 and IMF fuel. The results calculated from amending the K_{inf} value from CASMO-4, as shown before, are also shown in the figures for better comparisons.

Figure 4.7 MCNP VC results for UO2 at BOL, BOR=0

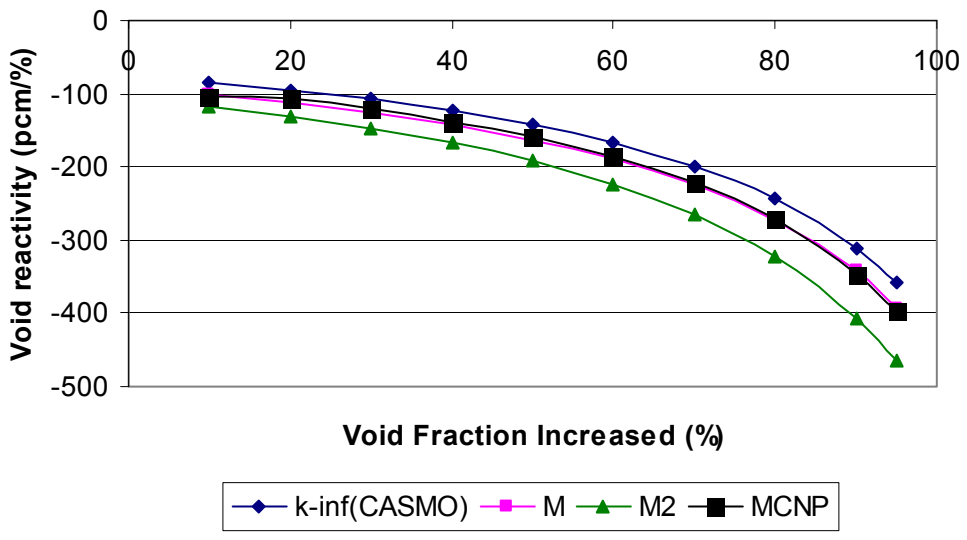

Figure 4.8: MCNP VC results for IMF at BOL, BOR=0

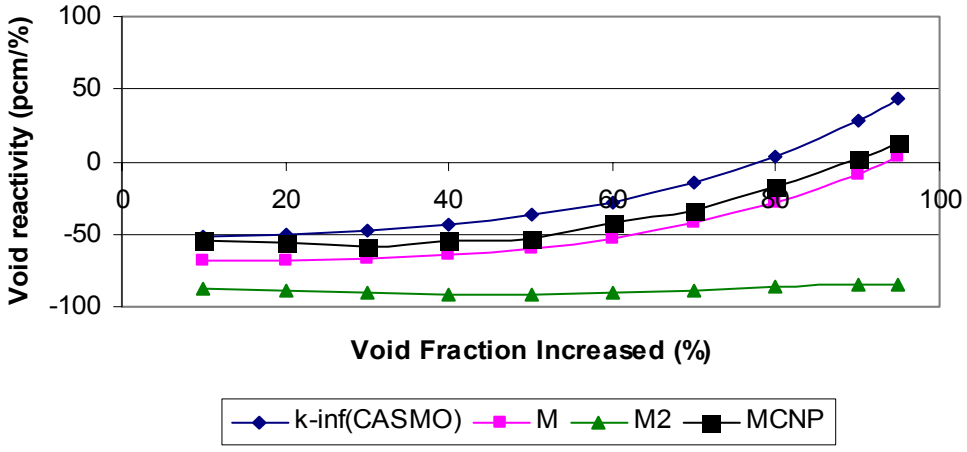

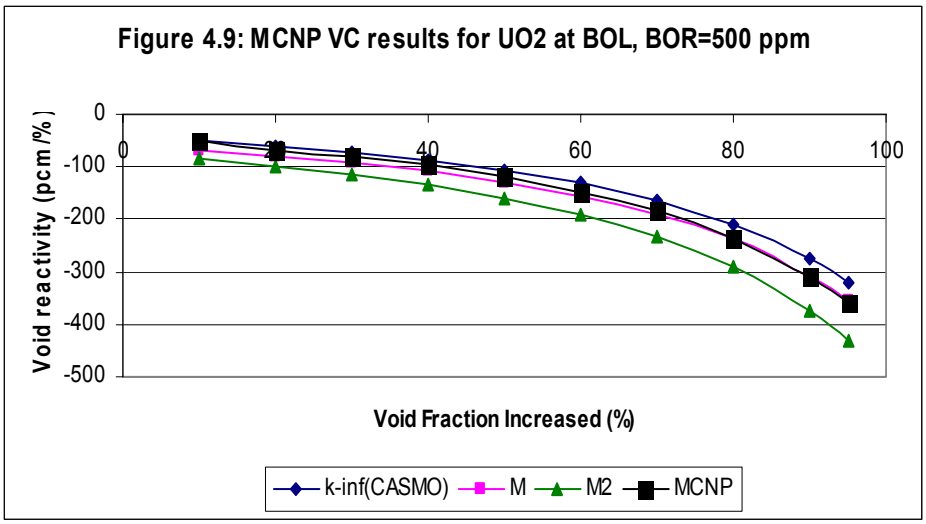
Figure 4.9: MCNP VC results for UO2 at BOL, BOR=500 ppm
Void reactivity (pcm/%)
0
-100
-200
-300
-400
-500
0
20
40
60
80
100
Void Fraction Increased (%)
k-inf(CASMO)
M
M2
MCNP

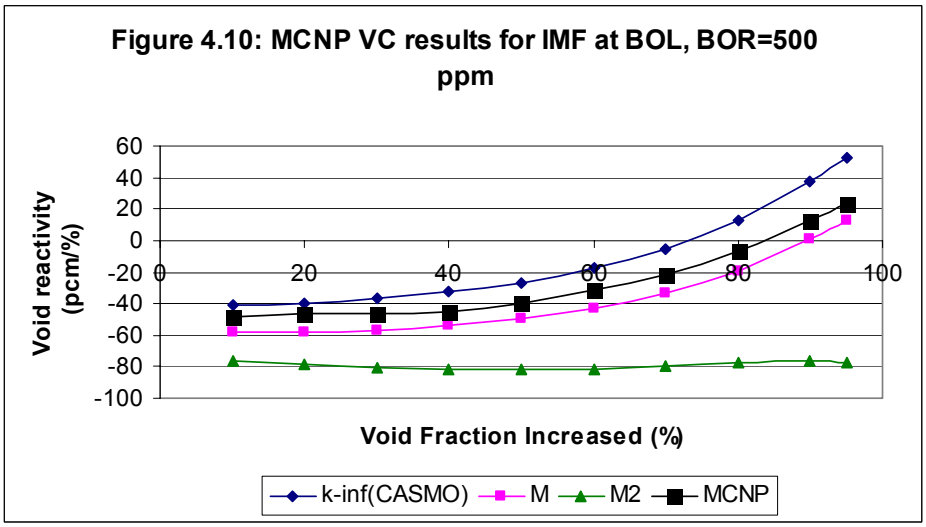
Figure 4.10: MCNP VC results for IMF at BOL, BOR=500 ppm
Void reactivity (pcm/%)
60
40
20
0
-20
-40
-60
-80
-100
0
20
40
60
80
100
Void Fraction Increased (%)
k-inf(CASMO)
M
M2
MCNP

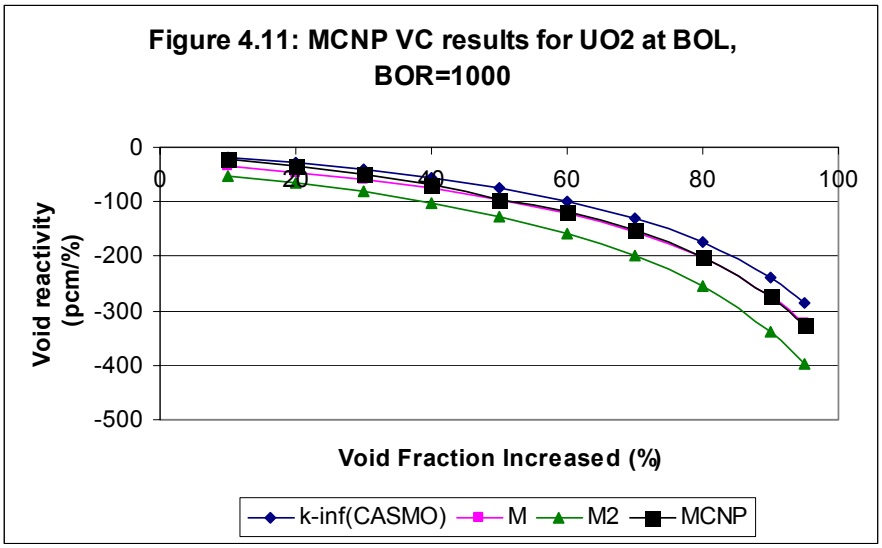
Figure 4.11: MCNP VC results for UO2 at BOL, BOR=1000
0
-100
-200
-300
-400
-500
0
20
40
60
80
100
Void reactivity (pcm/%)
Void Fraction Increased (%)
k-inf(CASMO)
M
M2
MCNP

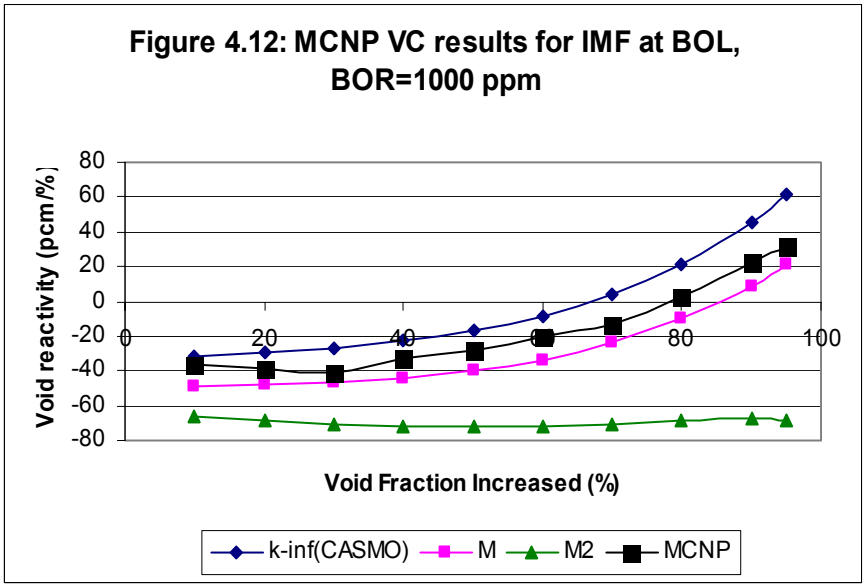
Figure 4.12: MCNP VC results for IMF at BOL, BOR=1000 ppm
80
60
40
20
0
-20
-40
-60
-80
0
20
40
60
80
100
Void reactivity (pcm/%)
Void Fraction Increased (%)
k-inf(CASMO)
M
M2
MCNP

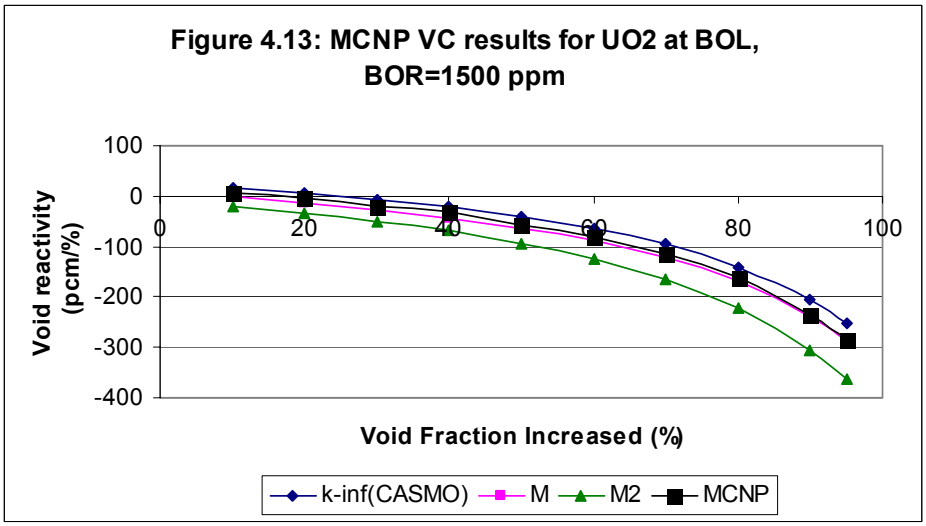

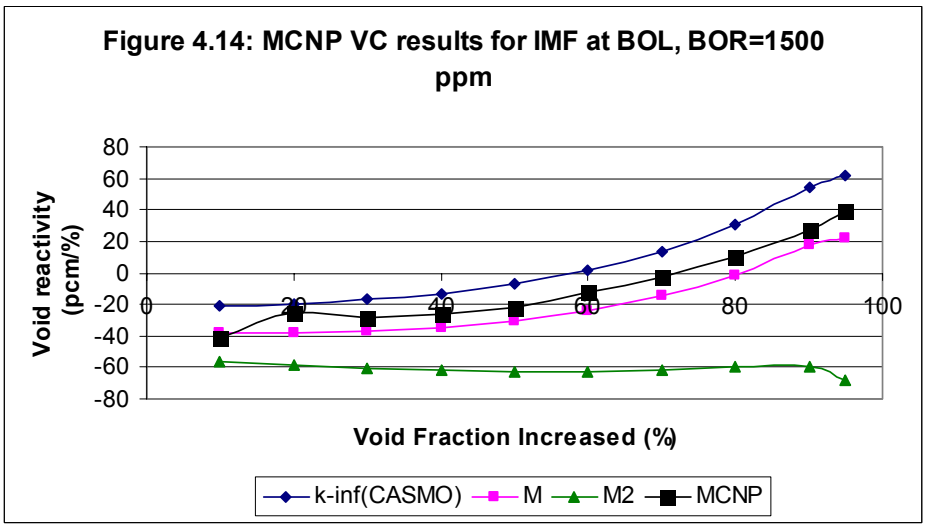

From Figures 4.7 to 4.14, it can be seen that at all boron concentration levels, and for both UO_2 and IMF fuel, the results calculated by MCNP-4C model are close to the results calculated using K_{eff} values amended from K_{inf} assuming ρ_L proportional to M. And it can be seen that the MCNP-4C result curves are not in the middle of M-proportional curves and M^2-proportional curves. In fact, they are above, although very close to, the M-proportional curves. Also, the void coefficients do turn positive when void fraction is large for IMF. For example, in Figure 4.14, when the void fraction increase is about 80%, the calculated void coefficient is positive.

It is strange that the MCNP-4C curve lies above the M-proportional

curve instead of between the M and M^2 curves. Efforts were made to explain this. It is noticed that in calculating the void coefficients, Equation 4.4, that is, $VC = \Delta K/(K_1*K_2*\Delta VF)$, is used. As discussed before, the difference of this from the alternative definition $VC = \Delta K/\Delta VF$ will be small if K_1 and K_2 are close to 1 (the difference is $1/(K_1*K_2)$). However, the K values used here are not close to one. For example, for IMF with 0 boron concentration, the BOL K infinity value is 1.234. If using the alternative definition, VC values should be multiplied by K_1*K_2. As the K values corresponding to M and M^2 curves are smaller than the MCNP-4C calculated K values, the multiplying factor for M and M^2 curves will be smaller. Multiplying a factor of more than 1 to an already negative value can be thought of as moving the three curves toward the (-y) direction. As we are multiplying a smaller factor by M and M^2 curves, these two curves are moved less than the MCNP-4C curve. This may bring the MCNP-4C curves to between M and M^2. However, when evaluated using the alternative definition of VC, the MCNP-4C curve is still above both M and M^2 curves for IMF fuel. We can also specify an appropriate geometry buckling value and direct CASMO-4 to calculate K_{eff} values and use these for the VC. The buckling can be chosen to make the K_{eff} value at 0 burnup approximately 1. However, the results show that the new VC curve lies below all the others and makes the situation less clear.

This issue stays unsolved and is a good candidate for future examination. The MCNP-4C model used is attached as an appendix for checking and future work.

4.3 Methods of improving the safety coefficients

As shown in Section 4.2, inert matrix fuels have problems of small

negative Doppler and void reactivity coefficients. In order to improve these safety coefficients, ThO_2 and UO_2 can be mixed in the fuel. The first approach is to add these additives directly into the fuel pin; the second is to keep the inert matrix fuel composition unchanged, but within each assembly replace some inert fuel pins with ThO_2 or UO_2 fuel pins; the third approach is to keep the same type of fuel pins within every assembly, but have different types of assemblies in the core: some assemblies contain only inert fuels, while others contain only ThO_2 or UO_2 pins.

Some or all of these approaches can be used at the same time to optimize the tradeoffs between the gains in safety coefficients and losses of plutonium and MA burning rates or burning fractions of initial loadings. In this study, the first two approaches are investigated. That is, the heterogeneity is introduced up to the assembly level.

As shown in Chapter 3 and previous sections of this chapter, the plutonium and minor actinides burning ability and safe characteristics of fertile free fuels using various inert materials as matrices are similar. It is reasonable to deduce that they will also be similar after introducing the safety characteristics improvement approaches mentioned above. Hence it suffices to only investigate one type of fuel to great detail. Again, fertile free fuel using Spinel as matrix acts as the representative here. CASMO-4 is the code used in the analysis. To prepare the input file for CASMO-4 in this situation, a similar process as presented in Section 3.1 will be used. The calculation process is not shown here.

The fuel is not exposed to the same burnup when comparing the burning percentages of plutonium and minor actinides before and after adding the fertile materials. Instead, the fuel is always burned to a burnup

BU_3, which is 1.5 times the reactivity limited burnup (Table 4.7). When adding the fertile material, either ThO_2 or UO_2, the burnup and cycle length of the fuel will change. More careful investigation of the effects of these additives could lead to changing the loading of TRU and additives proportionally to maintain the same cycle length.

Table 4.7: BU_3 burnup and total in-core time of fuel adding different amounts of ThO_2 and UO_2

Fertile material	BU_3 burnup (MWd/kg)	In-core time (EFPD)
0%, ThO_2	578.4	2373
5%, ThO_2	495.3	2307
10%, ThO_2	426.6	2235
15%, ThO_2	368.9	2158
20%, ThO_2	319.6	2077
25%, ThO_2	277.3	1991
30%, ThO_2	240.1	1897
0%, UO_2	578.4	2373
5%, UO_2	484.2	2261
10%, UO_2	411.4	2167
15%, UO_2	352.8	2082
20%, UO_2	304.5	2001
25%, UO_2	263.8	1921
30%, UO_2	228.8	1840

Tables 4.8 through 4.17 show the safety coefficients and burning ability of the new fuel when adding different amounts of ThO_2 or UO_2 into fuel pins. Some of the same information is also selected to be shown in Figures 4.15 through 4.19 for better viewing and comparison.

Table 4.8: Doppler coefficient, boron worth, and β_{eff} of Spinel inert matrix fuel containing different amounts of ThO_2.

ThO_2 weight percentage	DC(10^{-5}/K)		BW(10^{-5}/ppm)		β_{eff}(10^{-3})	
	BOL	EOL	BOL	EOL	BOL	EOL
0%	-0.73	-1.01	-1.80	-6.38	2.660	3.867
5%	-0.85	-1.20	-1.85	-5.94	2.657	3.707
10%	-1.02	-1.45	-1.91	-5.68	2.655	3.594
15%	-1.19	-1.69	-1.97	-5.50	2.653	3.501
20%	-1.35	-1.91	-2.03	-5.37	2.651	3.423
25%	-1.50	-2.09	-2.10	-5.30	2.649	3.357
30%	-1.65	-2.27	-2.17	-5.23	2.648	3.293
MOX	-2.90	-3.06	-3.00	-3.49	3.696	3.994
UO_2	-2.00	-3.34	-6.74	-10.89	7.199	4.524

Table 4.9: Moderator temperature coefficient (10^{-5}/K) of Spinel inert matrix fuel containing different amounts of ThO_2

ThO_2 weight percentage		BOL				EOL
	BOR(ppm)	0	500	1000	1500	0
0%		-19.90	-15.99	-12.14	-8.44	-49.97
5%		-22.97	-18.96	-15.07	-11.23	-50.14
10%		-25.38	-21.25	-17.33	-13.40	-49.92
15%		-27.62	-23.46	-19.42	-15.41	-49.33
20%		-29.54	-25.27	-21.15	-17.12	-48.70
25%		-31.47	-27.09	-22.86	-18.70	-48.38
30%		-33.72	-29.24	-24.89	-20.67	-48.15
MOX		-55.91	-50.18	-44.58	-39.04	-58.72
UO_2		-25.14	-15.34	-5.75	3.79	-49.57

Table 4.10: Void coefficient (10^{-5}/%) of Spinel inert matrix fuel containing different amounts of ThO_2

ThO_2 weight percentage		BOL				EOL
	BOR(ppm)	0	500	1000	1500	0
0%		-52.34	-42.02	-31.90	-21.89	-188.0
5%		-61.60	-51.02	-40.78	-30.50	-183.4
10%		-68.91	-58.11	-47.50	-37.12	-179.8
15%		-76.02	-65.17	-54.36	-43.92	-176.5
20%		-82.19	-71.01	-60.00	-49.34	-173.2
25%		-88.29	-76.95	-65.75	-54.74	-171.1
30%		-95.06	-83.42	-72.04	-60.83	-169.8
MOX		-164.9	-150.0	-135.6	-121.5	-184.8
UO_2		-79.25	-51.78	-24.70	1.74	-202.9

From Table 4.10, it can be seen that adding ThO_2 will worsen the void coefficient at EOL which contradicts the motive to add fertile material. However, the void coefficient at EOL is still about -170 after adding 30% weight percentage ThO_2 and the void coefficient at BOL improves from -52 to -95. Thus it is beneficial for improving the void coefficient to add Th to the inert fuel material.

Table 4.11: Percentage of initial loaded plutonium and minor actinides burned using Spinel inert matrix fuel containing different amounts of ThO_2

ThO_2 weight percentage	Pu burned	MA burned
0%	62.3%	42.6%
5%	60.8%	41.7%
10%	59.8%	40.9%
15%	58.8%	40.1%
20%	58.0%	39.3%
25%	57.1%	38.5%
30%	56.2%	37.7%
MOX	13.2%	19.0%

Table 4.12: Plutonium and minor actinides burning rate using Spinel inert matrix fuel containing different amounts of ThO_2

ThO_2 weight percentage	Burning rate, kg/(GWe-Year)	
	Pu	MA
0%	1029	109
5%	1007	107
10%	993	105
15%	981	103
20%	971	102
25%	962	100
30%	954	99
MOX	285	63

Table 4.13: Doppler coefficient, boron worth, and β_{eff} of Spinel inert matrix fuel containing different amounts of UO_2

UO_2 weight percentage	DC(10^{-5}/K)		BW(10^{-5}/ppm)		β_{eff}(10^{-3})	
	BOL	EOL	BOL	EOL	BOL	EOL
0%	-0.73	-1.01	-1.80	-6.38	2.660	3.867
5%	-1.20	-1.51	-1.86	-5.18	2.682	3.730
10%	-1.53	-1.95	-1.90	-4.72	2.709	3.670
15%	-1.76	-2.25	-1.95	-4.47	2.739	3.638
20%	-1.92	-2.16	-2.00	-2.85	2.771	3.286
25%	-2.05	-2.56	-2.05	-4.21	2.807	3.621
30%	-2.17	-2.68	-2.12	-4.13	2.845	3.624
MOX	-2.90	-3.06	-3.00	-3.49	3.696	3.994
UO_2	-2.00	-3.34	-6.74	-10.89	7.199	4.524

Table 4.14: Moderator temperature coefficient (10^{-5}/K) of Spinel inert matrix fuel containing different amounts of UO_2

UO_2 weight percentage		BOL				EOL
	BOR(ppm)	0	500	1000	1500	0
0%		-19.90	-15.99	-12.14	-8.44	-49.97
5%		-23.99	-19.95	-16.04	-12.19	-53.03
10%		-26.33	-22.24	-18.23	-14.31	-53.96
15%		-28.50	-24.33	-20.24	-16.24	-54.31
20%		-30.50	-26.26	-22.10	-18.08	-41.47
25%		-32.06	-27.75	-23.51	-19.30	-55.02
30%		-33.99	-29.52	-25.17	-20.99	-55.51
MOX		-55.91	-50.18	-44.58	-39.04	-58.72
UO_2		-25.14	-15.34	-5.75	3.79	-49.57

Table 4.15: Void coefficient (10^{-5}/%) of Spinel inert matrix fuel containing different amounts of UO_2

UO_2 weight percentage		BOL				EOL
	BOR(ppm)	0	500	1000	1500	0
0%		-52.34	-42.02	-31.90	-21.89	-188.0
5%		-64.53	-53.90	-43.34	-33.17	-186.5
10%		-71.45	-60.68	-49.97	-39.51	-185.0
15%		-78.22	-67.08	-56.44	-45.74	-183.5
20%		-84.35	-73.02	-62.01	-51.25	-128.4
25%		-89.44	-78.07	-66.87	-56.05	-183.1
30%		-95.10	-83.40	-72.00	-60.65	-183.6
MOX		-164.9	-150.0	-135.6	-121.5	-184.8
UO_2		-79.25	-51.78	-24.70	1.74	-202.9

Table 4.16: Percentage of initial loaded plutonium and minor actinides burned using Spinel inert matrix fuel containing different amounts of UO_2

UO_2 weight percentage	Pu burned	MA burned
0%	62.3%	42.6%
5%	56.2%	40.0%
10%	52.6%	38.5%
15%	49.8%	37.2%
20%	47.5%	36.1%
25%	45.5%	35.1%
30%	43.5%	34.1%
MOX	13.2%	19.0%

Table 4.17: Plutonium and minor actinides burning rate of Spinel inert matrix fuel containing different amounts of UO_2

UO_2 weight percentage	Burning rate, kg/(GWe-Year)	
	Pu	MA
0%	1029	109
5%	951	105
10%	905	102
15%	867	100
20%	834	98
25%	804	96
30%	774	94
MOX	285	63

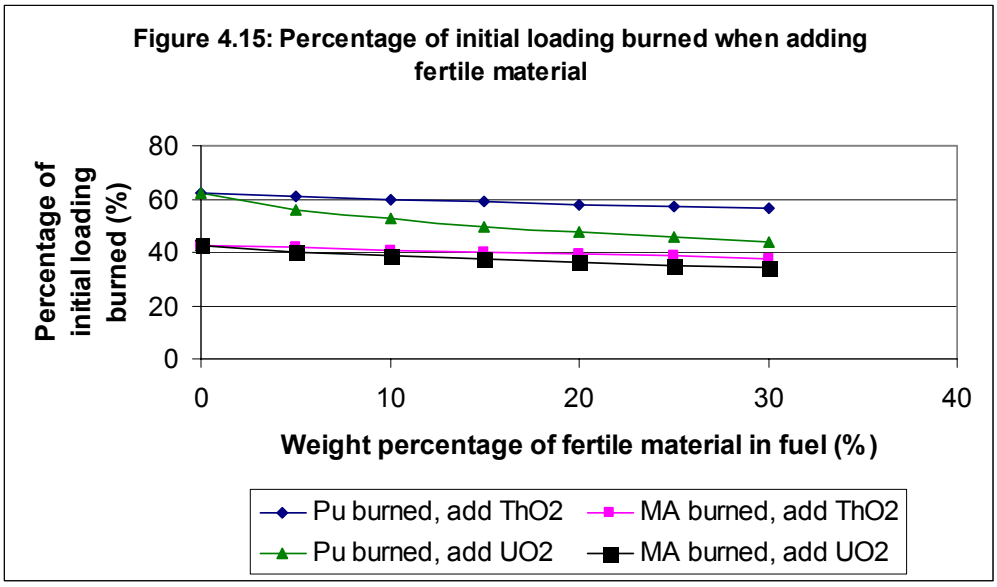
Figure 4.15: Percentage of initial loading burned when adding fertile material
Percentage of initial loading burned (%)
80
60
40
20
0
0
10
20
30
40
Weight percentage of fertile material in fuel (%)
Pu burned, add ThO2
MA burned, add ThO2
Pu burned, add UO2
MA burned, add UO2

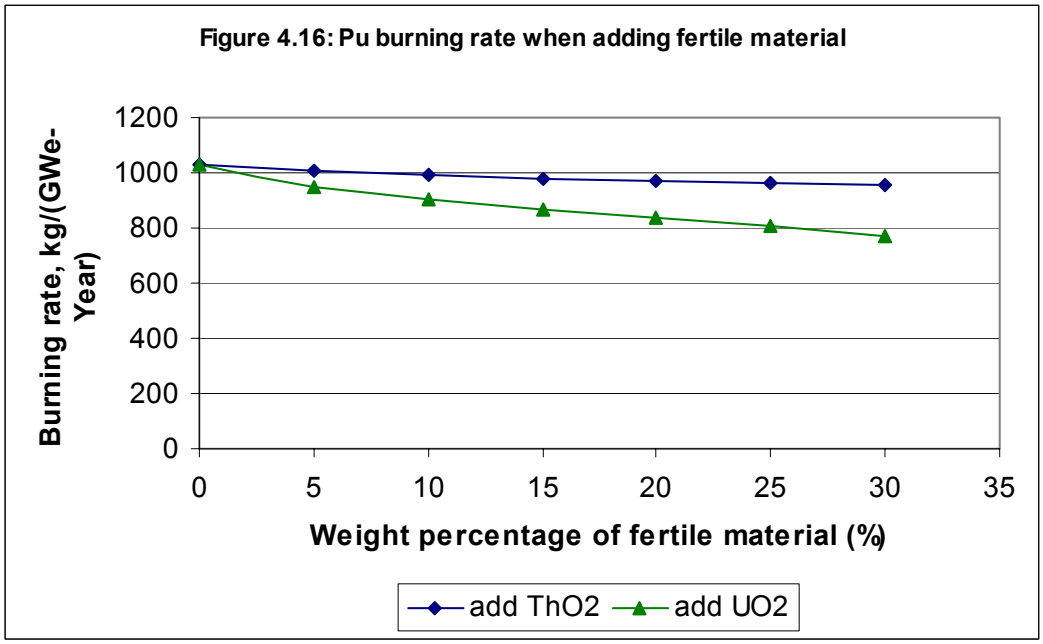
Figure 4.16: Pu burning rate when adding fertile material
Burning rate, kg/(GWe-Year)
1200
1000
800
600
400
200
0
0
5
10
15
20
25
30
35
Weight percentage of fertile material (%)
add ThO2
add UO2

Figure 4.17: MA burning rate when adding fertile material

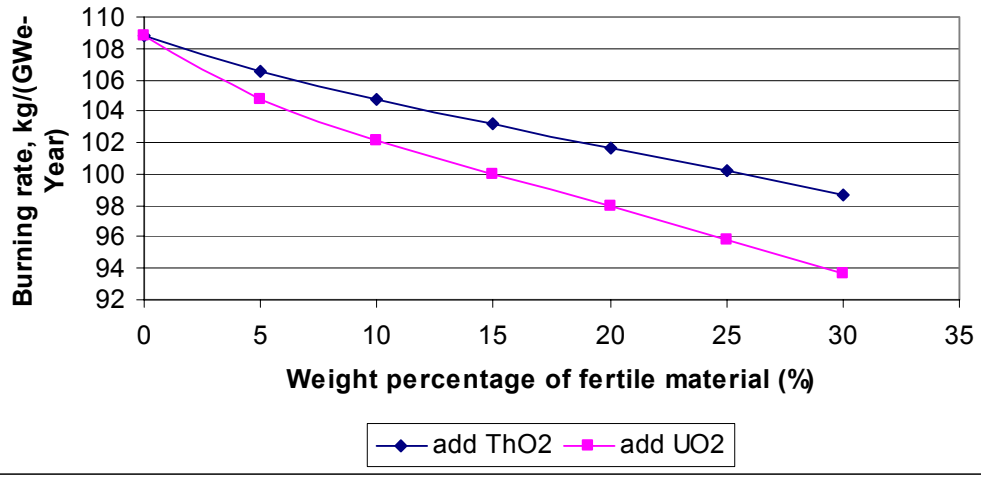

Figure 4.18: BOL Doppler coefficient when adding fertile material

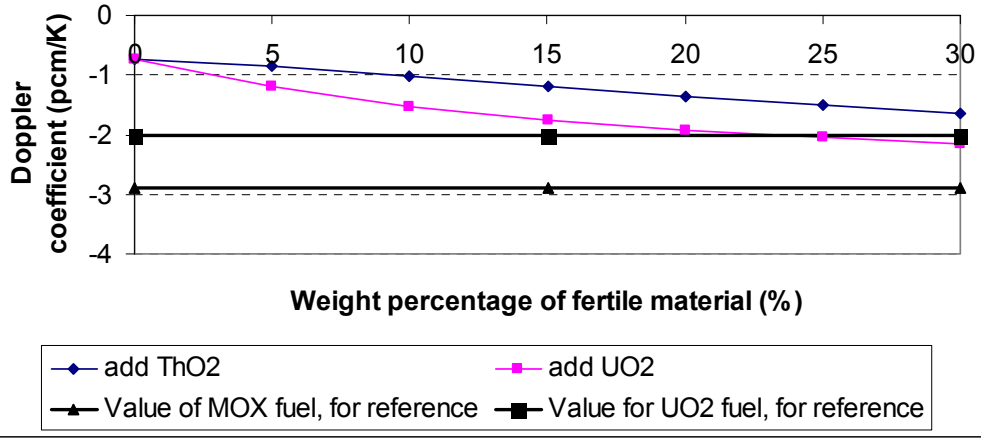

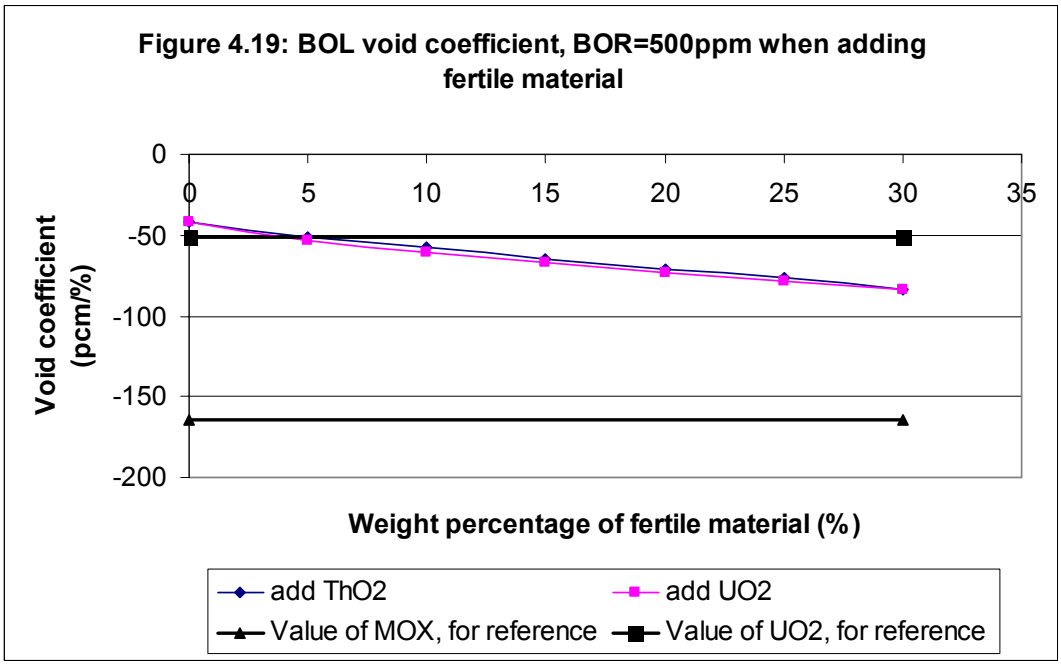

From Tables 4.8 through 4.17 and Figures 4.15 through 4.19, it is seen that as the percentage of fertile material increases, all the safety coefficients at BOL are improved, except for β_{eff} in the case of adding ThO_2. However, the burning abilities of both plutonium and minor actinides degrade. Adding UO_2 leads to a much better β_{eff} behavior. The safety coefficients at EOL do not change towards the safer side as expected. This is because the values for EOL are at different burnup, as shown in Table 4.7. If we compare the EOL safety coefficients at the same burnup, they will behave as expected, that is, adding more fertile material will generally provide better safety coefficients.

From Figures 4.15, 4.16 and 4.17, it is seen that adding UO_2 will result in a worse degradation of burning ability, in terms of either the burning percentage or the burning rate, than adding ThO_2. However, adding UO_2 will provide a better Doppler coefficient than adding ThO_2, as can be seen in Figure 4.18. Adding about 20% of UO_2 will arrive at a BOL Doppler coefficient and other safety coefficients comparable to the traditional UO_2

fuel. Yet, the fuel still has a much better burning percentage than MOX fuel for Pu (47.5% versus 13.2%) and for MA (36.1% versus 19.0%), and a much better burning rate for Pu (834 versus 285 kg/GWe-Year) and for MA (98 versus 63 kg/GWe-Year).

Adding fertile pins into the fuel assembly

Another approach to achieving better safety coefficients is to add fertile fuel pins into the fuel assembly. Before adding the fertile pins, every assembly has a layout as follows:

2
1 1
1 1 1
2 1 1 2
1 1 1 1 1
1 1 1 1 1 2
2 1 1 2 1 1 1
1 1 1 1 1 1 1 1
1 1 1 1 1 1 1 1 1

This shows 1/8 of one assembly, where 2 stands for guide tubes and 1 stands for fertile free fuel pins. We can replace some "1" with "3", which denotes fertile fuel pins. We need to decide the fuel composition for fuel "3", the positions where to put fuel "3", and how many "3" positions to use. In this study, 4% enriched UO_2 fuel is used as fertile fuel pins, and 13 UO_2 fuel pins are inserted into the 1/8 assembly which brings the assembly to this layout:

2

1 1

1 3 1

2 1 3 2

1 3 1 3 1

3 1 3 1 3 2

2 1 1 2 1 1 1

1 3 1 3 1 3 1 1

1 1 3 1 3 1 3 1 1

Adding 13 UO_2 fuel pins roughly corresponds to having 1/3 loading of fertile fuel pins. The resultant safety coefficients and plutonium and MA burning abilities are shown in Table 4.18 and Table 4.19, together with the corresponding values of adding fertile material into fuel pins, whole fertile free fuel assembly, MOX and traditional UO_2 fuel for comparison.

Table 4.18: The effects of heterogeneous assembly on safety coefficients

	Safety Coefficients[1]		
Fuel type	DC (pcm/K)	MTC (pcm/K)	VC (pcm / %void)
Heterogeneous assembly (1/3 UO_2 pins)	-1.34	-32.46	-92.13
Add 30w/o UO_2 in fuel pin	-2.17	-33.99	-95.10
All fertile-free	-0.73	-19.90	-52.35
MOX	-2.90	-55.91	-164.9
UO_2	-2.00	-25.14	-79.25

1: Safety coefficients are calculated at BOL with 0 soluble boron concentration

Table 4.19: The effects of heterogeneous assembly on plutonium and MA burning ability

	Fraction burned		Burning rate (kg/GWe-Year)	
Fuel type	Pu	MA	Pu	MA
Heterogeneous assembly (1/3 UO_2 pins)	52.8%	36.9%	637.0	68.7
Add 30w/o UO_2 in fuel pin	43.5%	34.1%	774.0	94.0
All fertile-free	62.3%	42.6%	1029.0	108.8
MOX	13.2%	19.0%	284.9	63.3

The burning rates shown in Table 4.19 may not be achievable due to large BOL power peaking as shown below.

0.000
1.166 1.192
1.291 0.569 1.378
0.000 1.396 0.640 0.000
1.375 0.586 1.394 0.647 1.467
0.594 1.284 0.578 1.425 0.630 0.000
0.000 1.256 1.278 0.000 1.335 1.239 1.095
1.238 0.548 1.263 0.594 1.262 0.533 1.095 1.009
1.090 1.183 0.575 1.307 0.573 1.241 0.539 1.070 1.023

In order to reduce power peaking, burnable poison can be used, but this will reduce the plutonium and MA burning rates.

From the results in Table 4.18, we can see the trade-off between improving safety coefficients and degradation of plutonium and minor actinides burning rates. However, in this case, unlike in the case of adding ThO_2 or UO_2 directly into the fertile free fuel pin cell, the burning rate of the

minor actinides becomes comparable to that of MOX: 68.7 versus 63.3 kg/GWe-Year. In the case of adding UO_2 into the fertile free fuel, similar safety coefficients improvements are achieved by containing 25 w/o of UO_2 in the fuel, yet the burning rate of minor actinides is still faster than MOX, about 95.8 kg/GWe-Year. Thus the option of adding fertile material into the fuel pins is preferable over a heterogeneous assembly option if fast burning of minor actinides is favored.

Chapter 5: Spent fuel characteristics

This chapter will investigate the spent fuel characteristics of inert matrix fuels. It is a requirement that the selected inert matrix fuels would not compromise the environment, should they be disposed of without any further reprocessing.

Compared to other nuclides, plutonium and minor actinides have the most lasting impact on environment due to their long half lives: this is why significant R&D efforts worldwide are devoted to either properly isolate them or transmute them. From the results and discussions in Chapter 3, it is found that using inert matrix fuel in a once-through scenario can roughly burn 60% of the initial plutonium and 40% of the initial minor actinides loading (Table 3.9). Thus, there is a benefit from employing this fuel. However, because of the large initial loading, the remaining Pu and MA in the spent fuel may still be more per assembly or per unit volume than those present in the spent UO_2 fuel thus result in a more radiotoxic fuel format in spite of the large fraction of plutonium and minor actinides destroyed. However, when calculated on the basis of amount disposed per unit electricity generation, there will be significant reduction.

5.1 Methodology

In Chapter 3, the burnup calculation is done by using CASMO-4. CASMO-4 also gives the fuel composition at the end of life, which can be used to calculate various spent fuel characteristics up to 1 million years after discharge. The calculated parameters are: Total radioactivity (Ci), thermal power (watts), neutron production from (alpha, n) reaction (neutrons/sec), spontaneous fission neutron production (neutron/sec), radioactive inhalation

hazard (m^3 air), and radioactive ingestion hazard (m^3 water).

The calculation is done by using the code ORIGEN2.2, a zero dimension, one-group code for calculating buildup, decay, and processing of radioactive materials [Croff 1980]. ORIGEN2.2 was developed at Oak Ridge National Laborotory (ORNL) and distributed by the Radiation Safety Information Computational Center (RSICC).

Various spent fuel characteristics are compared normalized to the derived energy, i.e., per GWe-Year base. From the burnup value B ($MW_{th}D/kg$), Equation 5.1 is used to transfer it to the unit of (GWe-Year/cm^3). Why change to this unit will be apparent shortly.

$$B\frac{MW_{th}d}{kg} = \frac{B(MW_{th}d)}{kg} * \frac{Year}{365.25D} * \frac{0.33MWe}{1MW_{th}} * \frac{GWe}{1000MWe} * \frac{kg}{1000g} * \frac{\rho(g)}{cm^3}$$

$$= \frac{B*0.33*\rho}{365.25*1000*1000}\left(\frac{GWeYear}{cm^3}\right)$$

$$\Rightarrow B\left({}^{MW_{th}d}\!/\!_{kg}\right) = (9.035\text{E}-10)*\text{B}*\rho\left({}^{\text{GWe - Year}}\!/\!_{\text{cm}^3}\right) \qquad (5.1)$$

Note that the density ρ is not the initial fuel density but is the value of initial Heavy Metal/cm^3 because the burnup is in the unit of MWd/(kg initial heavy metal). This value is not difficult to calculate. In Chapter 3, in the process of preparing the input file for CASMO-4, we have calculated the density of the fuel and the isotope weight percentages. Summing up all the weight percentages of heavy metal nuclides we can get the weight percentage of the heavy metal in the fuel. Multiplying the fuel density by this percentage is the value for ρ in Equation 5.1.

For example, the density for 15% volume percent initial TRU loading

Spinel inert matrix fuel is 5.09 g/cm^3, the initial heavy metal percentage in the fuel is 28.0%, and the discharge burnup is 578.357 MWd/kg, which will result in:

$$(9.035E\text{-}10)*578.357*5.09*0.28 = 7.447E\text{-}7 \text{ (GWe-Year/cm}^3\text{)}$$

The reason we convert the burnup to this value is because CASMO-4 gives the spent fuel composition in units of #/cm^3 for each nuclides. From this value and the (GWe-Year/cm^3) value calculated by Equation 5.1, it is easy to get a value in units of (#/GWe-Year). Divide this by the Avogadro number and multiply it by the atom weight, the unit is converted to g/GWe-Year. Then the value for gram can be readily used as input into ORIGEN2.2 and we can get the spent fuel characteristics normalized to GWe-Year.

The details of this step for preparing the input file for ORIGEN2.2 is not shown here because of the large amount of nuclides involved. The information extracted from ORIGEN2.2 output file is quite straightforward by consulting the code manual.

5.2 Results

The total reactivities for different inert matrix spent fuels are shown in Figure 5.1:

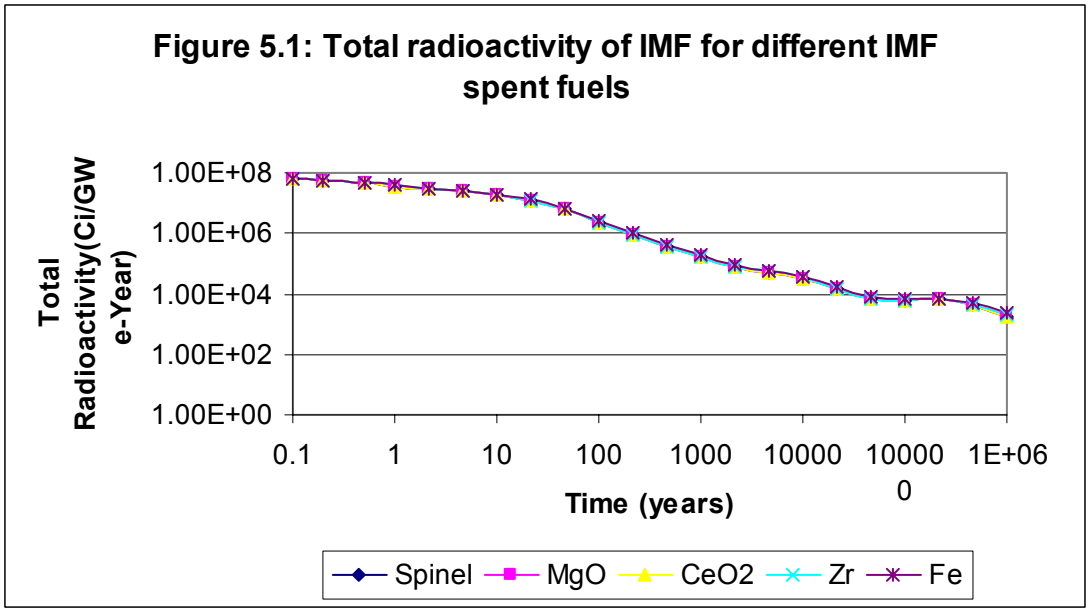

There are actually five curves in Figure 5.1: one for each matrix. However, there is hardly any difference among them. Recall the results from Chapter 3 and Chapter 4, all the matrices have similar behavior in terms of either burning percentage, burning ability, or safety coefficients. It is not surprising that the similarities carry over to their spent fuel characteristics.

Therefore we don't need to compute the spent fuel characteristics for every matrix. In this regard, Spinel and Zr matrices are used as representatives for CERCER and CERMET fuels, respectively. Their spent fuel characteristics are to be compared to those of MOX and UO_2. In some figures, you only see three curves instead of four, because the curves for Spinel and Zr inert matrix fuels overlap.

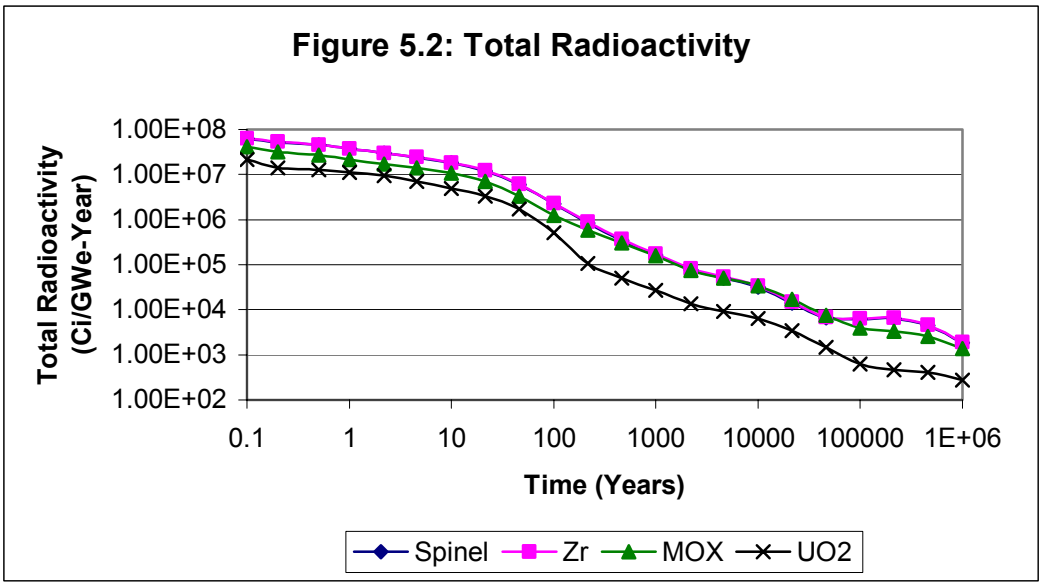
Figure 5.2: Total Radioactivity
Total Radioactivity (Ci/GWe-Year)
1.00E+08
1.00E+07
1.00E+06
1.00E+05
1.00E+04
1.00E+03
1.00E+02
0.1
1
10
100
1000
10000
100000
1E+06
Time (Years)
Spinel
Zr
MOX
UO2

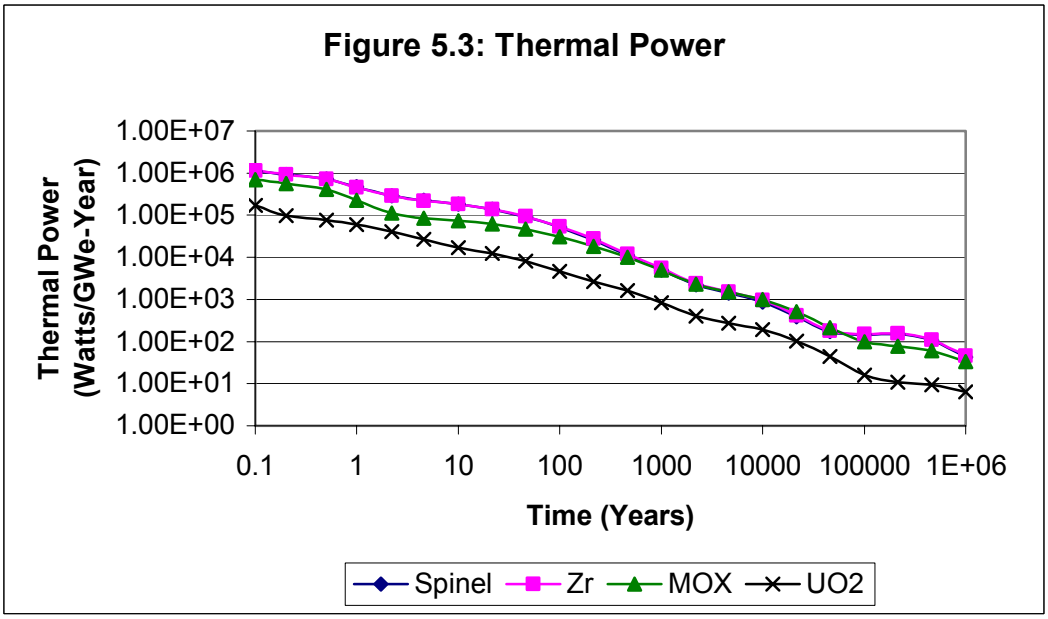
Figure 5.3: Thermal Power
Thermal Power (Watts/GWe-Year)
1.00E+07
1.00E+06
1.00E+05
1.00E+04
1.00E+03
1.00E+02
1.00E+01
1.00E+00
0.1
1
10
100
1000
10000
100000
1E+06
Time (Years)
Spinel
Zr
MOX
UO2

Figure 5.4: (alpha,n) neutron source

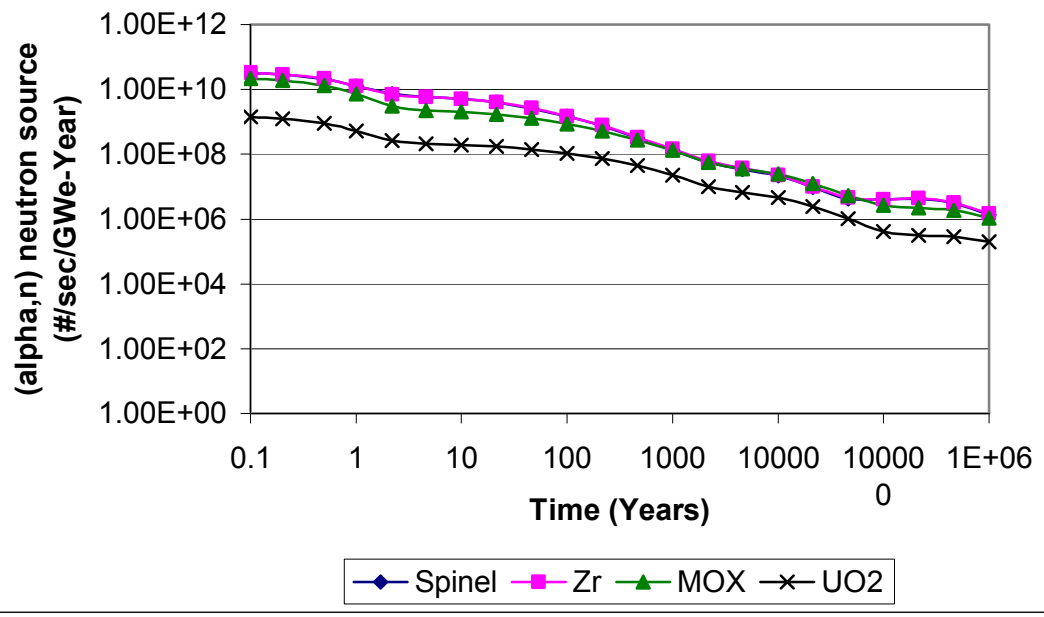

Figure 5.5: Spontaneous Fission Neutron Source

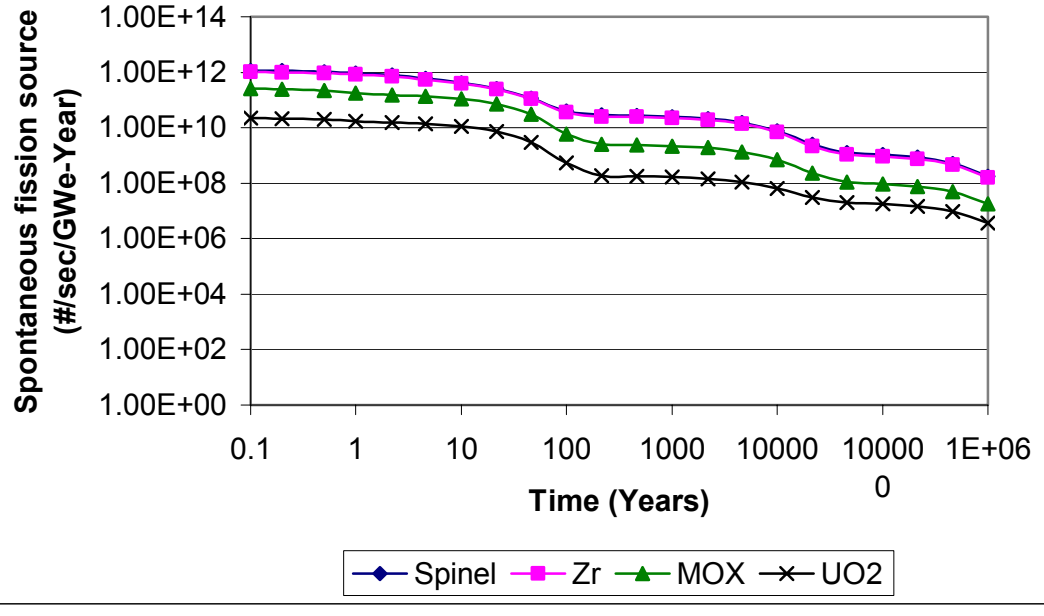

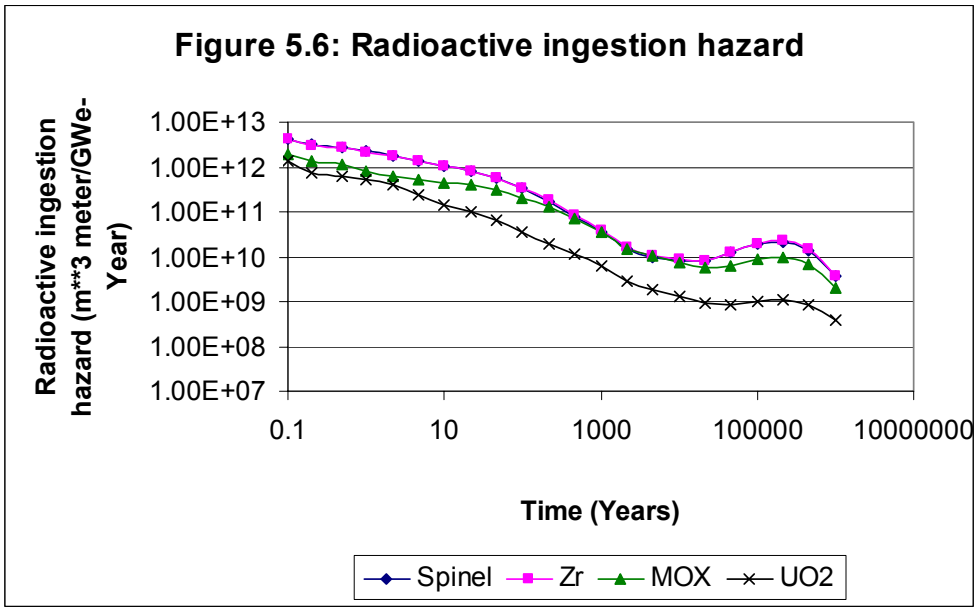

From the results in Figures 5.2 through 5.6, it is confirmed that the fertile free fuels with different matrices have similar behavior, since the curves for Spinel and Zr almost fall on only one curve. It is also apparent that the inert material spent fuels are more radiotoxic than MOX and traditional UO_2 spent fuels. The values of different characteristics, radioactivity, thermal power, spontaneous fission neutron, (alpha, n) fission, and radioactive ingestion hazard, are 5 to 10 times larger than those of UO_2 spent fuels. Note that in normalizing these parameters against produced energy, only the energy produced by IMF is used. Because TRU is reprocessed from the spent fuel of UO_2 fuels, if the energy produced by these UO_2 fuels is also included, there will be smaller difference between UO_2 and IMF results.

Table 5.1 shows the fuel composition of important heavy metal elements upon discharge, in terms of number density (#/cm^3). It can be seen that spinel inert matrix fuel has more plutonium and minor actinides in the spent fuel upon discharge than MOX and UO_2 fuels. The relative amounts of plutonium and minor actinides upon discharge of these three types of

fuels are in correspondence with the spent fuel characteristics shown in Figures 5.2 through 5.6 (IMF > MOX > UO_2).

Table 5.1: Heavy metal number density upon discharge of different type of fuels

	Spinel inert fuel	MOX	UO_2
U-234(#/cm^3)	5.84E+18	1.18E+18	3.03E+18
U-235(#/cm^3)	2.52E+18	9.62E+19	1.15E+20
U-236(#/cm^3)	7.08E+17	1.35E+19	1.19E+20
U-237(#/cm^3)	2.43E+15	2.08E+17	6.50E+17
U-238(#/cm^3)	6.62E+18	2.13E+22	2.03E+22
U-239(#/cm^3)	4.62E+13	1.17E+16	1.56E+16
Np-236(#/cm^3)	4.21E+15	1.03E+15	1.22E+14
Np-237(#/cm^3)	5.16E+19	7.01E+19	1.56E+19
Np-238(#/cm^3)	1.56E+17	1.34E+17	5.80E+16
Np-239(#/cm^3)	8.10E+15	1.69E+18	2.25E+18
Pu-238(#/cm^3)	2.26E+20	9.77E+19	7.75E+18
Pu-239(#/cm^3)	1.03E+20	5.26E+20	1.19E+20
Pu-240(#/cm^3)	3.37E+20	3.58E+20	6.04E+19
Pu-241(#/cm^3)	2.14E+20	1.93E+20	3.72E+19
Pu-242(#/cm^3)	2.60E+20	9.91E+19	2.30E+19
Pu-243(#/cm^3)	3.02E+16	1.21E+16	5.67E+15
Am-241(#/cm^3)	2.60E+19	3.72E+19	1.14E+18
Am-242(#/cm^3)	5.71E+16	4.33E+16	3.71E+15
Am-243(#/cm^3)	6.53E+19	3.19E+19	5.20E+18
Am-244(#/cm^3)	5.81E+16	2.09E+16	5.68E+15
Am-242m(#/cm^3)	5.59E+17	9.55E+17	1.62E+16
Cm-242(#/cm^3)	1.27E+19	9.52E+18	5.89E+17
Cm-243(#/cm^3)	8.64E+17	4.77E+17	1.88E+16
Cm-244(#/cm^3)	8.50E+19	2.64E+19	2.68E+18
Cm-245(#/cm^3)	1.74E+19	4.11E+18	1.67E+17
Cm-246(#/cm^3)	5.68E+18	4.58E+17	2.73E+16
Cm-247(#/cm^3)	2.57E+17	1.21E+16	3.78E+14
Cm-248(#/cm^3)	4.45E+16	9.95E+14	3.24E+13
Cm-249(#/cm^3)	7.65E+11	1.16E+10	4.69E+08

Chapter 6: Conclusions and recommendations for further work

Inert matrix fuels are considered for use in current LWRs to reduce the large stockpile of plutonium and minor actinides worldwide. The inert matrix fuel design should be done carefully because the absence of uranium in the fuel significantly influences the burnup reactivity swing, the reactivity coefficients and the kinetic parameters of the fuel.

Two major categories of inert matrix fuels are studied: CERCER (CERamic-in-CERamic), a composite ceramic fuel particles dispersed in another ceramic which acts as a matrix for filling the fuel rod; and CERMET (CERamic-in-METal), in the form of ceramic fuel particles dispersed into a metallic matrix. In the category of CERCER, the current world wide research effort has been focused on three matrix candidates: (1) Spinel ($MgAl_2O_4$); (2) CeO_2, and (3) MgO. In contrast, there are still no emerging commonly accepted matrix candidates for a CERMET. Zr and Fe are used in this study.

Different inert matrix fuels have similar burning abilities in terms of how much and how fast the plutonium, minor actinides or the entire trans-uranium elements can be burned, and they are all superior to MOX fuel. Generally large deviation from the reference operating conditions by changing H/HM ratio or initial TRU loading or changing power densities for the sake of improving the burning ability does not pay off. Only small improvements are achievable.

The lack of U-238 and the neutronic characteristics of plutonium lead

to degradation of safety related kinetic parameters. Various inert matrix fuels have similar safety parameter values for the Doppler coefficient, moderate temperature coefficient, void coefficient, boron worth and effective delayed neutron fraction β_{eff}. Their Doppler coefficients, void coefficients and effective delayed neutron fractions are much worse than UO_2 fuels. The coolant void reactivity worth becomes positive if the void fraction changes from 0 to more than 80 percent, at BOL for boron concentration 1500 ppm case. It will also turn positive for other boron concentration cases. This result is calculated using the K_{eff} value amended from CASMO-4 output K_{inf}, and is confirmed by MCNP-4C calculations.

In order to improve these safety coefficients, fertile materials such as ThO_2 and UO_2 can be mixed in the fuel. The first approach is to add these additives directly into the fuel pin; the second is to keep the inert matrix fuel composition unchanged, but within each assembly replace some inert fuel pins with ThO_2 or UO_2 fuel pins; the third approach is to keep the same type of fuel pins within every assembly, but have different types of assemblies in the core: some assemblies contain only inert fuels, while others contain only ThO_2 or UO_2 pins. The third approach is not investigated in this study.

Adding UO_2 will result in a faster degradation of burning ability, in terms of either the burning percentage or the burning rate, than adding ThO_2. However, adding UO_2 will provide a better Doppler coefficient than adding ThO_2. Adding fertile fuel pins into IMF assembly, in order to get to the same level of safety coefficients, result in a burning rate of the minor actinides comparable to that of MOX. Thus the option of adding fertile material into the fuel pins is preferable over a heterogeneous assembly option if fast burning of minor actinides is favored.

The different inert matrix fuels have similar spent fuel characteristics, and their spent fuels are more radioactive than the UO_2 fuel.

This study is mainly based on a once-through scenario. For future work on the neutronics of actinide burning, the recycling option is a natural extension. Also, the void coefficient discussion in Chapter 4 deserves more careful investigation, as the MCNP-4C curve doesn't lie between M and M^2 curves as expected. The third approach to improve safety coefficients is to have different types of assemblies in the core so that some assemblies contain only inert fuels, while others contain only ThO_2 or UO_2 pins. This was not studied in this paper and could be a topic for future work. On related topics, both the inert materials behavior in core, and the ability to process the fuel into the desired manufacture state are worthy of examination.

Appendix: MCNP PWR Core Model input file

The input file shown here is based on the work of Dr. Zhiwen Xu as part of a lecture of MIT course 22.351. The overall concept and geometry structure are set up by him. The model is changed to a modeling of PWR core using inert matrix fuel and operating under different void fraction. Shown here is the input file for 0 void fraction case. For other void fraction, density of the water is changed accordingly.

```
STANDARD WESTINGHOUSE 4-LOOP PWR CORE MODEL
c
c --------------------------------------------------------------------
c  Typical Westinghouse 4-loop PWR core
c --------------------------------------------------------------------
c  CORE
c    Number of primary loops             4
c    Total thermal power rating        3411 MW(thermal)
c    Total electricity output          1150 MW(electrical)
c    Number of assemblies               193
c    Core dimensions                  15X15 assemblies
c    Core barrel ID/OD               3.76/3.87 m
c --------------------------------------------------------------------
c  PRIMARY COOLANT
c    System pressure                  15.5 MPa
c    Inlet water temperature          565.85 K
c    Average water temperature         583.1 K
c    Average water density             0.705 g/cc
c --------------------------------------------------------------------
c  FUEL ASSEMBLY DESIGN
c    Assembly lattice                 17X17 square lattice
c    Number of fuel rods                264
c    Number of guide tubes               25
c    Pin-to-pin pitch                  1.26 cm
c    Assembly pitch                    21.5 cm
c    Fuel pellet (UO2) density          10.4 g/cc
c    Average fuel temperature            900 K
c    Fuel pellet radius               0.4096 cm
c    Gap thickness                      82 um
c    Fuel rod diameter                  0.95 cm
c    Guide tube inner radius           0.5690 cm
c    Guide tube outer radius           0.6147 cm
c    Clad/can material               Zircolay-4
c    Active fuel height                 3.66 m
c --------------------------------------------------------------------
c  ASSUMPTIONS
c    (1) The fuel reload differences are ignored, and all UO2 pellet use
```

```
c       3 w/o enrichment.
c    (2) Axial blanket designs in a fuel assembly are not considered.
c    (3) Axial vairations of coolant density are ignored. All the fuel
c       and coolant are modeled at their average conditions.
c    (4) All control rods are not modeled.
c -------------------------------------------------------------------
c
c
c -------------------------------------------------------------------
c  INERT MATRIX FUEL
c    15%TRU-15%YSZ-70%SPINEL (Volume percentage)
c    Fuel density:  5.0906 g/cc
c    Void fraction 0 ---> Water coolant density: 0.705 g/cc
c -------------------------------------------------------------------
c
c
c
c
c  Cell Cards
c  fuel rod
  1  1 -5.0906     -1  u=1  imp:n=1  tmp=7.7553e-8   $ UO2 pellet
  2  2 -0.001  (1 -2)  u=1  imp:n=1                 $ gap
  3  3 -6.550  (2 -3)  u=1  imp:n=1  tmp=5.3520e-8   $ Zr-4 clad
  4  4 -0.705      +3  u=1  imp:n=1  tmp=5.0246e-8   $ coolant, 583.1K
c
c  guide tube
  5  4 -0.705      -4  u=2  imp:n=1  tmp=5.0246e-8   $ coolant inside
  6  3 -6.550  (4 -5)  u=2  imp:n=1  tmp=5.3520e-8   $ guide tube (GT)
  7  4 -0.705      +5  u=2  imp:n=1  tmp=5.0246e-8   $ coolant outside
c
c  17X17 lattice
  8  0  -6 7 -8 9  u=3  imp:n=1  lat=1  fill=-8:8 -8:8 0:0
     1  1  1  1  1  1  1  1  1  1  1  1  1  1  1  1  1
     1  1  1  1  1  1  1  1  1  1  1  1  1  1  1  1  1
     1  1  1  1  1  2  1  1  2  1  1  2  1  1  1  1  1
     1  1  1  2  1  1  1  1  1  1  1  1  1  2  1  1  1
     1  1  1  1  1  1  1  1  1  1  1  1  1  1  1  1  1
     1  1  2  1  1  2  1  1  2  1  1  2  1  1  2  1  1
     1  1  1  1  1  1  1  1  1  1  1  1  1  1  1  1  1
     1  1  1  1  1  1  1  1  1  1  1  1  1  1  1  1  1
     1  1  2  1  1  2  1  1  2  1  1  2  1  1  2  1  1
     1  1  1  1  1  1  1  1  1  1  1  1  1  1  1  1  1
     1  1  1  1  1  1  1  1  1  1  1  1  1  1  1  1  1
     1  1  2  1  1  2  1  1  2  1  1  2  1  1  2  1  1
     1  1  1  1  1  1  1  1  1  1  1  1  1  1  1  1  1
     1  1  1  2  1  1  1  1  1  1  1  1  1  2  1  1  1
     1  1  1  1  1  2  1  1  2  1  1  2  1  1  1  1  1
     1  1  1  1  1  1  1  1  1  1  1  1  1  1  1  1  1
     1  1  1  1  1  1  1  1  1  1  1  1  1  1  1  1  1
c
c  assembly
  9  0        (-10 11 -12 13)  u=4  imp:n=1  fill=3
 10  4 -0.705  (10:-11:12:-13)  u=4  imp:n=1  tmp=5.0246e-8
c
c  core configuration
```

```
  11  4 -0.705  -14 15 -16 17  u=5  imp:n=1  lat=1  fill=-8:8 -8:8 0:0
c       R  P  N  M  L  K  J  H  G  F  E  D  C  B  A
     5  5  5  5  5  5  5  5  5  5  5  5  5  5  5  5  5
     5  5  5  5  5  4  4  4  4  4  4  4  5  5  5  5  5   $ 1
     5  5  5  4  4  4  4  4  4  4  4  4  4  4  5  5  5   $ 2
     5  5  4  4  4  4  4  4  4  4  4  4  4  4  4  5  5   $ 3
     5  5  4  4  4  4  4  4  4  4  4  4  4  4  4  5  5   $ 4
     5  4  4  4  4  4  4  4  4  4  4  4  4  4  4  4  5   $ 5
     5  4  4  4  4  4  4  4  4  4  4  4  4  4  4  4  5   $ 6
     5  4  4  4  4  4  4  4  4  4  4  4  4  4  4  4  5   $ 7
     5  4  4  4  4  4  4  4  4  4  4  4  4  4  4  4  5   $ 8
     5  4  4  4  4  4  4  4  4  4  4  4  4  4  4  4  5   $ 9
     5  4  4  4  4  4  4  4  4  4  4  4  4  4  4  4  5   $ 10
     5  4  4  4  4  4  4  4  4  4  4  4  4  4  4  4  5   $ 11
     5  5  4  4  4  4  4  4  4  4  4  4  4  4  4  5  5   $ 12
     5  5  4  4  4  4  4  4  4  4  4  4  4  4  4  5  5   $ 13
     5  5  5  4  4  4  4  4  4  4  4  4  4  4  5  5  5   $ 14
     5  5  5  5  5  4  4  4  4  4  4  4  5  5  5  5  5   $ 15
     5  5  5  5  5  5  5  5  5  5  5  5  5  5  5  5  5
c
c  one-eighth core cut
  12  0  (18 19 -20 (-21:-22) -23 24 -25) imp:n=1 fill=5  $ 1/8th core
  13  4 -0.705  (18 19 -26 (20:23:(21 22)) 24 -25)   $ radial reflector
      imp:n=1  tmp=5.0246e-8
  14  5 -7.90 (18 19 26 -27 24 -25) imp:n=1   $ stainless steel baffle
  15  4 -0.705  (18 19  -20 (-21:-22) -23 28 -24)  $ bottom reflector
      imp:n=1  tmp=5.0246e-8
  16  4 -0.705  (18 19  -20 (-21:-22) -23 25 -29)  $ top reflector
      imp:n=1  tmp=5.0246e-8
  17  0  #12 #13 #14 #15 #16  imp:n=0

c  Surface Cards
c  fuel rod
   1  cz  0.4096     $ pellet radius
   2  cz  0.4178     $ inner-clad radius
   3  cz  0.4750     $ outer-clad radius
c
c  guide tube
   4  cz  0.5690     $ inner-GT radius
   5  cz  0.6147     $ outer-GT radius
c
c  square lattice (pin)
   6  px  0.63       $ east pitch edge
   7  px -0.63       $ west pitch edge
   8  py  0.63       $ north pitch edge
   9  py -0.63       $ south pitch edge
c
c  17X17 lattice
  10  px  10.71      $ east lattice boundary
  11  px -10.71      $ west lattice boundary
  12  py  10.71      $ north lattice boundary
  13  py -10.71      $ south lattice boundary
c
c  square assembly
  14  px  10.75      $ east assm. edge
```

```
  15  px -10.75      $ west assm. edge
  16  py  10.75      $ north assm. edge
  17  py -10.75      $ south assm. edge
c
c  1/8th core cut
 *18  py   0.0              $ y=0, symmetry
 *19  p    1.0 -1.0 0.0 0.0   $ x-y=0, symmetry
  20  px 161.25       $ core boundary
  21  py  75.25       $ core boundary
  22  px 139.75       $ core boundary
  23  py 118.25       $ core boundary
c
c  axial dimensions
  24  pz -183.0
  25  pz  183.0
c
c  core barrels
  26  cz  188.0       $ inside radius of core barrel
  27  cz  193.5       $ outside radius of core barrel
c
c  axial core reflectors
  28  pz -193.0       $ bottom reflector boundary
  29  pz  193.0       $ top reflector boundary

c  Data cards
c  Inert Matrix Fuel
m1      &
       92234.86c   -1.84221E-05   &
       92235.16c   -0.000645694   &
       92236.86c   -0.000538846   &
       92238.16c   -0.09090746    &
       93237.82c   -1.859286668   &
       94238.86c   -0.769639971   &
       94239.16c   -13.62114365   &
       94240.86c   -6.433731008   &
       94241.86c   -1.939078371   &
       94242.86c   -1.40909348    &
       95241.82c   -1.302984513   &
       95242.82c   -0.005319447   &
       95243.78c   -0.412117147   &
       96243.98c   -0.001399854   &
       96244.82c   -0.13886556    &
       96245.98c   -0.010638894   &
       96246.98c   -0.001679825   &
       39089.42c   -1.881608147   &
       40000.58c   -11.10134394   &
       12000.42c   -8.694343631   &
       13027.78c   -19.30471608   &
       8016.54c    -31.02089939
c
c  AIR gap
m2     8016.53c -1.0
c
c  Zr-4 clad
m3     8016.53c -0.00125
```

```
      24000.50c -0.0010
      26000.55c -0.0021
      40000.58c -0.98115
      50000.40c -0.0145
c
c  H2O, thermal scattering allowed
m4     1001.53c 2
       8016.53c 1
mt4    lwtr.04t
c
c  Stainless steel
m5    14000.60c -0.0051
      24000.50c -0.1740
      25055.60c -0.0199
      26000.55c -0.6835
      28000.50c -0.1170
c
c  ksrc   10 5 0
kcode  10000 1.3 10 1010
prdmp  110 110 110
```

References

Akie, H., Takano, H., Anoda, Y., & Muromura, T. Proc. Int. Conf. on Future Nuclear Systems (GLOBAL97), October 5-10, 1997, Yokohama, Japan, Vo1.2, (1997) 1129.

Baldi, S., & Porta J. Elements of comparison between different inert matrix fuels as regards plutonium utilization and safety coefficients. Progress in Nuclear Energy, Vol. 38, No. 3-4, pp. 375-378, 2001.

Bulletin of the Atomic Scientists, September/October 1999.

Burakov, B. E., Anderson, E. B., Zamoryanskaya, M. V., Nikolaeva, E. V., Strykanova, E. E., Yagovkina, M. A., & Khlopin, V. G. Investigation of zircon/zirconia ceramics doped with 239Pu and 238Pu. Proceedings of Global 2001 international conference on "Back-end of the fuel cycle, from research to solutions", Paris, France, September 9-13, 2001.

Burghartz, M., Ledergerber, G., Ingold, F., Xie, T., Botta, F., & Idemitsu, K. Concepts and first fabrication studies of inert matrix fuel for the incineration of plutonium, Proceedings of OECD/NEA Workshop on Advanced Reactors with Innovative Fuels, Villigen, Switzerland, October 21-23, 1998.

Chauvin, N., Konings, R.J.M., & Matzke, Hj. Optimisation of inert matrix fuel concepts for americium transmutation. Journal of Nuclear Materials, Vol. 274, pp.105-111, 1999.

Chodak, P., Driscoll, M.J., Miller, M.M., & Todreas, N.E. Destruction of plutonium using non-uranium fuels in pressurized water reactor peripheral assemblies. (Report MIT-MFC-TR-001). Department of Nuclear Engineering, Massachusetts Institute of Technology, January 1997.

Cocuaud, N. Picard, E., Konings, R. Conti, A., & Matzke, H. U-free Pu fuels and U-free-Am targets studies. Fourth CAPRA Seminar, June 16-18, 1997.

Croff, A. G. "A User's Manual For The ORIGEN2 Computer Code," ORNL/TM-7175 (CCC-371), Oak Ridge National Laboratory, July 1980.

Degueldre, C., & Paratte, J.M. Concepts for an inert matrix fuel: An overview. Journal of Nuclear Materials, Vol. 274, pp.1-6, 1999.

Driscoll, M. J., Downar, T. J., & Pilat, E. E. The Linear Reactivity Model for Nuclear Fuel Management, American Nuclear Society, LaGrange Park, 1990.

Edenius, M., Ekberg, K., Forssén, B. H., & Knott, D. "CASMO-4, A Fuel Assembly Burnup Program, User's Manual," STUDSVIK/SOA-95/1, Studsvik of America, Inc., 1995.

Hejzlar, P., Driscoll, M.J., and Kazimi, M.S. High Performance Annular Fuel For Pressurized Water Reactors, Transactions of the American Nuclear Society, Vol. 84, Milwaukee, June 17-21, 2001.

Kasemeyer, U., Paratte, J-M., Grimm, P., & Chawla, R. Comparison of pressurized water reactor core characteristics for 100% plutonium-containing loadings. Nuclear Technology, Vol. 122, April, 1998.

Kloosterman, J.L. & Konings, R.J.M. Investigation of the fuel temperature coefficient of innovative fuel types. Proceedings of OECD/NEA Workshop on Advanced Reactors with Innovative Fuels, Villigen, Switzerland, October 21-23, 1998.

Long, Y., Zhang, Y., & Kazimi, M.S. Inert Matrix Materials as Hosts of Actinide Nuclear Fuels. (Report MIT-NFC-TR-055). Department of Nuclear Engineering, Massachusetts Institute of Technology, March, 2003.

Matzke, Hj. Radiation stability of inert matrix fuels. Proceedings of OECD/NEA Workshop on Advanced Reactors with Innovative Fuels, Villigen, Switzerland, October 21-23, 1998.

Matzke, Hj., Rondinella, V. V., & Wiss, T. Materials research on inert matrices: a screening study. Journal of Nuclear Materials, Vol. 274, pp.47-53, 1999.

Micholas, N. J., Coop, K. L. & Estep, R. J. Capability and Limitation Study of DDT Passive-Active Neutron Waste Assay Instrument (Los Alamos National Laboratory, LA-12237-MS, 1992).

Pillon, S., Delpech, M., Tommasi, J., Beaumont, H. & Newton, T. Plutonium utilisation in PWR and FR. Proceedings of OECD/NEA Workshop on Advanced Reactors with Innovative Fuels, Villigen, Switzerland, October 21-23, 1998.

Porta, J., & Puill, A. U-free Pu fuels for LWRs: The CEA/DRN strategy.

Proceedings of OECD/NEA Workshop on Advanced Reactors with Innovative Fuels, Villigen, Switzerland, October 21-23, 1998.

Porta, J., & Doriath, J-Y. Toward very high burnups: A strategy for plutonium utilization in pressurized water reactors. Journal of Nuclear Materials, Vol. 274, pp.153-159, 1999.

Porta, J., Aillaud, C., & Baldi, S. Core severe accidents with CERMET fuels: A specific study for pressurized water reactors. Journal of Nuclear Materials, Vol. 274, pp.174-180, 1999.

Puill, A., & Bergeron, J. Advanced Plutonium Fuel Assembly: an Advanced Concept for Using Plutonium in Pressurized Water Reactors", Nuclear Technology, Vol. 119, August 1997.

Shwageraus, E., Hejzlar, P., & Kazimi, M. S. An Evaluation of Feasibility of Light Water Reactor (LWR) Based Actinide Transmutation Concepts, MIT report, MIT-NFC-PR-049, October 2002.

Stanculescu, A., Kasemeyer, U., Paratte, J-M., & Chawla, R. Conceptual studies for pressurized water reactor cores employing plutonium-erbium-zirconium oxide inert matrix fuel assemblies. Journal of Nuclear Materials, Vol. 274, pp.146-152, 1999.

Tommasi, J., Beaumont, H.M. & Newton, T.D. A fast spectrum Pu burner reactor with nitride fuel. Proceedings of OECD/NEA Workshop on Advanced Reactors with Innovative Fuels, Villigen, Switzerland, October 21-23, 1998.

Verrall, R.A., Vlajic, M.D. & Krstic, V.D. Silicon carbide as an inert matrix fuel for CANDU reactors. Proceedings of OECD/NEA Workshop on Advanced Reactors with Innovative Fuels, Villigen, Switzerland, October 21-23, 1998.

Yamashita, T., Akie, H., Nakano, Y., Kuramoto, K., Nitani, N., & Nakamura, T. Current status of researches on the plutonium rock-like oxide fuel and its burning in light water reactors, Progress in Nuclear Energy, Vol. 38. No. 3-4, PP. 327-330, 2001.

Yuan, Y., No, H. C., & Kazimi, M. S. A preliminary investigation of performance of rock-like fuel for high burnup in LWRs. (Report MIT-NFC-TR-037). Department of Nuclear Engineering, Massachusetts Institute of Technology, December, 2001.